LASER INTERFEROMETER GRAVITATIONAL WAVE OBSERVATORY
- LIGO -
CALIFORNIA INSTITUTE OF TECHNOLOGY
MASSACHUSETTS INSTITUTE OF TECHNOLOGY

Technical Note	**LIGO-T2300439–v1**	2024/01/14

Quantum Noise Modeling of LIGO Livingston Detector in O4

Wenxuan Jia

California Institute of Technology
LIGO Project, MS 18-34
Pasadena, CA 91125
Phone (626) 395-2129
Fax (626) 304-9834
E-mail: info@ligo.caltech.edu

Massachusetts Institute of Technology
LIGO Project, Room NW22-295
Cambridge, MA 02139
Phone (617) 253-4824
Fax (617) 253-7014
E-mail: info@ligo.mit.edu

LIGO Hanford Observatory
Route 10, Mile Marker 2
Richland, WA 99352
Phone (509) 372-8106
Fax (509) 372-8137
E-mail: info@ligo.caltech.edu

LIGO Livingston Observatory
19100 LIGO Lane
Livingston, LA 70754
Phone (225) 686-3100
Fax (225) 686-7189
E-mail: info@ligo.caltech.edu

http://www.ligo.caltech.edu/

This report is generated from git.ligo.org/wenxuan.jia/qnd/-/blob/main/qnd.ipynb

Main result of this report:

L1 IFO parameters	
Arm power	$257^{+3.9}_{-1.6}$ kW
Arm to SEC mismatch	2.7%
Arm to SEC mismatch phase	0°
SEC detuning (round-trip phase)	0.14°
SEC Gouy phase	$43.0^{+4.5}_{-5.2}$ °
Readout angle	-11°
Total readout loss	$8.0^{+1.2}_{-0.5}$ %
IFO to OMC mismatch	$3.6^{+0.5}_{-0.5}$ %
IFO to OMC mismatch phase	-51 °
Squeezing parameters	
Generated squeezing	17.4 dB
Squeezing angle	10.5 °
Injection loss	7.1%
SQZ to OMC mismatch	$1.1^{+1.3}_{-0.2}$ %
SQZ to OMC mismatch phase	-45°
Phase noise (RMS)	27 mrad
Filter cavity parameters	
Length	300 m
Detuning	−25.6 Hz
Finesse	7000
Full-linewidth	71 Hz
Input coupler transmission	797 ppm
Derived round-trip loss	100 ppm
Squeezer to FC mismatch	0.2%
Squeezer to FC mismatch phase	−65°
Length noise (RMS)	0.2 pm

1 Introduction

Quantum noise is one of the major contributions to the total noise measured by Advanced LIGO detector. It's important to understand the quantum noise accurately to estimate the total noise budget and contributions from other sources of noises. In addition, the parameters estimated by quantum noise model also tell us the decoherence and degradation of the optical system of LIGO. Knowing the locations of degradations such as loss and mode-mismatches, we can optimize the optical design to aim for better squeezing at all frequencies. However, it's difficult to measure quantum noise directly, since LIGO only measures the total noise. Thus, we need an accurate model to infer the quantum noise from the total noise.

The model we use is Gravitational-Wave Interferometer Noise Calculator (GWINC). In the latest release, it incorporates the novel type of degradations known as mode-mismatch. The mismatch between two wavefronts is organized into a mismatch of the second-order spatial mode of two cavities. This can be used to explain and model the frequency-dependent loss observed previously (PRD 104, 062006).

Squeezing is a technique that has been used to reduce the quantum noise of LIGO. It also provides a way to probe the optical system of LIGO, since it's very sensitive to degradations along the optical path. Therefore, we purposely change one of the squeezing parameters known as the squeezing angle to constrain and infer the parameters from the model. In the end, we can infer the measured quantum noise from total noise with a trustworthy interferometer model.

During the Engineering Run 15 (ER15), we took many DARM measurements with various configurations of the squeezing system (LLO64872).

The full interferometer model with frequency-dependent squeezing has around 25 parameters. It's not possible to attempt to fit all of them in a single fit. Therefore, we isolate partial parameters and fit them in a simpler system. Then we can use these parameters to infer new parameters introduced in the full system. We would be able to find all parameters in a stepwise fashion.

The first measurement we fit first is the sensing function measured by photon calibrator (Pcal).

2 Analysis of Sensing Function

The sensing function is an optical gain that converts the measured optical power fluctuation in Watt to the change of the length difference between two arms of LIGO, known as differential arm lengths (DARM). The sensing function depends only on the unsqueezed interometer's response to the arm length perturbations, mostly including degradations of the output path and responses of the signal-recycling cavity (SRC, sometimes also called as sideband-extraction cavity, SEC).

In **conventional SRC response formalism**, the SRC length (SRCL) detuning is related to the optical spring frequency and Q factor of the detuned SRC. They can be found in the calibration report (05/02 report and 05/19 report). The derivation can be found in T1600278 and CQG 36, 205006. However, the conventional analytical formalism is known to have issues. Instead, numerical simulation like gwinc can handle all parameters that may affect SRC responses. Its sensing function is more accurate than the single-pole approximation.

The calibration sweep measures the sensing function, which includes coupled-cavity pole (f_{cc}) and SRC spring information at low frequencies. The f_{cc} is not an accurate description of the sensing function if we have mode-mismatches. Therefore, we infer SRC parameters from sensing functions produced by gwinc.

The sensing function C depends on these paramters:

- Arm power P_{arm}
- Readout loss Λ_{RO}
- Interferometer (IFO) to output mode cleaner (OMC) mode-mismatch Υ_{OMC}
- IFO to OMC mode-mismatch phase Υ_{OMC} phase
- SRC loss Λ_{SR}
- Arm cavity to SRC mode-mismatch Υ_{SR}
- Arm to SRC mode-mismatch phase Υ_{SR} phase
- SRC Gouy phase ψ_{SR}
- SRC detuning $\Delta\phi_{SR}$

2.1 Parametric study

We perform a parametric study to understand how each of the gwinc parameters affect the sensing function. We first find canonical set of parameters that closely represents the truth, and then perturb each dimension from that point. The change of the modeled sensing function is plotted with respect to each dimension that is perturbed.

There are two scenarios with the arm to SRC mismatch Υ_{SR}, controlled by the parameter is_OPD. When is_OPD is true, the thermal lensing is more dominant than quadratic mode-mismatch, creating the optical path distortion and thus the name of the parameter. We analyze both case separately:

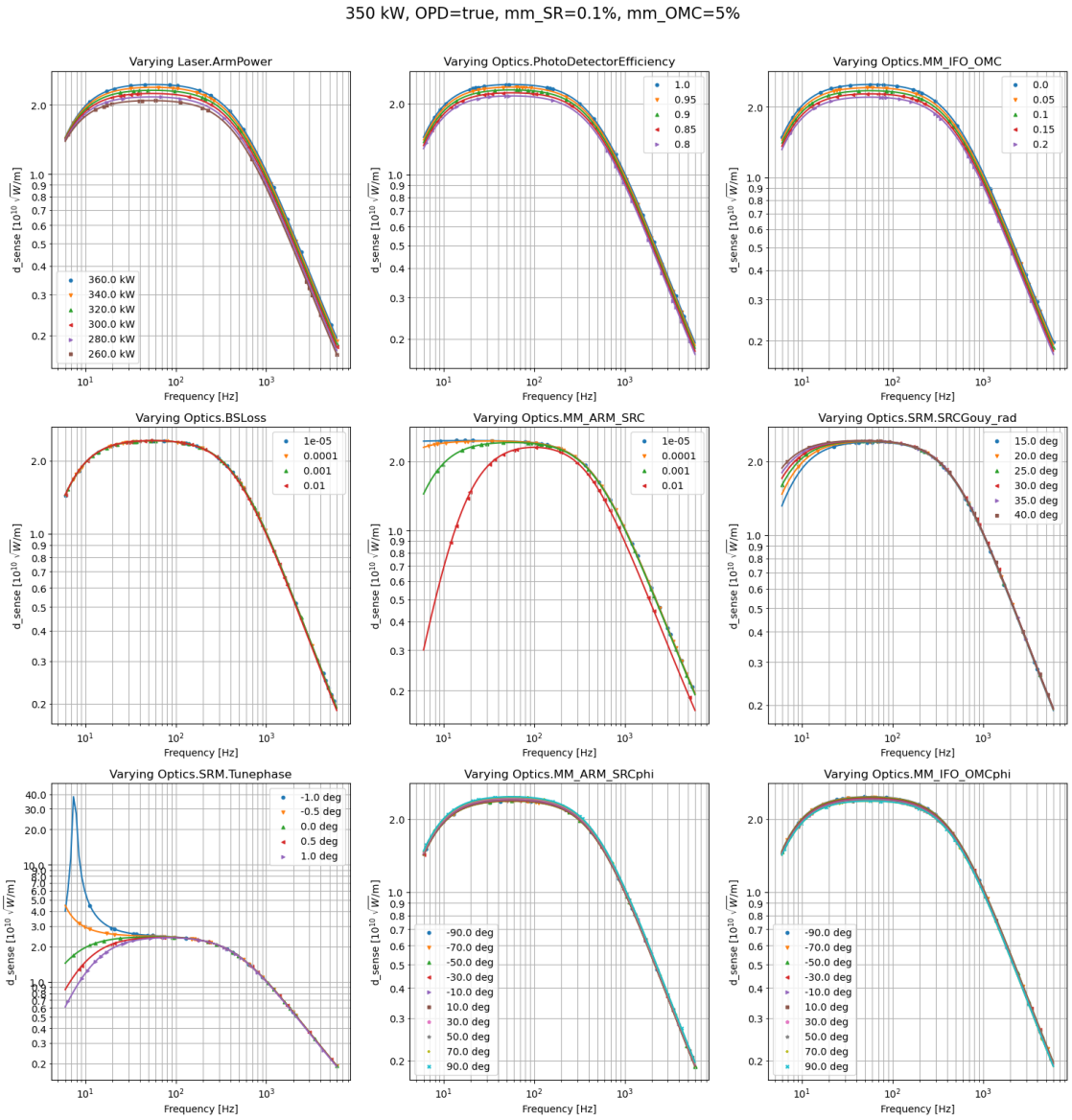

These plots show how the sensing function from gwinc is affected by ifo parameters. The title shows the canonical parameter set where we perturb from. For each subplot, the title says the perturbed parameter. The various values of such parameters are labeled in the legend. The sensing function is therefore very sensitive to Υ_{SR}.

The top row represents degeneracy between arm power and readout loss/mode-mismatches. With only 0.1% of Υ_{SR} and 5% of Υ_{OMC}, Υ_{OMC} is quite degenerate with readout loss, and

both of them affect the sensing function in the similar way as arm power. Note that it is with small Υ_{SR} .

The center row represents loss/mismatches in SRC. The simple SRC loss changes the coupled cavity pole by a tiny bit, as the high frequency of C changes but not low frequency. Υ_{SR} don't change the cavity pole by much, but they affect the SRC spring heavily due to the extra mismatch phasing. At low Υ_{SR}, it affects C like SRCL detuning. When it's large, it also reduces high frequency optical gain.

The SRC Gouy phase is kind of a hidden parameter that can change over thermalizing. Higher Gouy phase actually damps the spring by changing the mismatch phasing that reduces the misroation when coherently summed with 00 modes.

The bottom row represents other phasing due to cavity detuning and mismatches. The SRCL detuning affects the spring heavily as expected. Note that it could counteract the effect due to Υ_{SR} so they form a degenerate pair. The other mismatch phasings contribute relatively less than other phasings. Given the low-frequency shape of the measured Pcal sweep, the Υ_{SR} couldn't be too high and therefore the mismatch phasing don't matter much. They would definitely matter with squeezing.

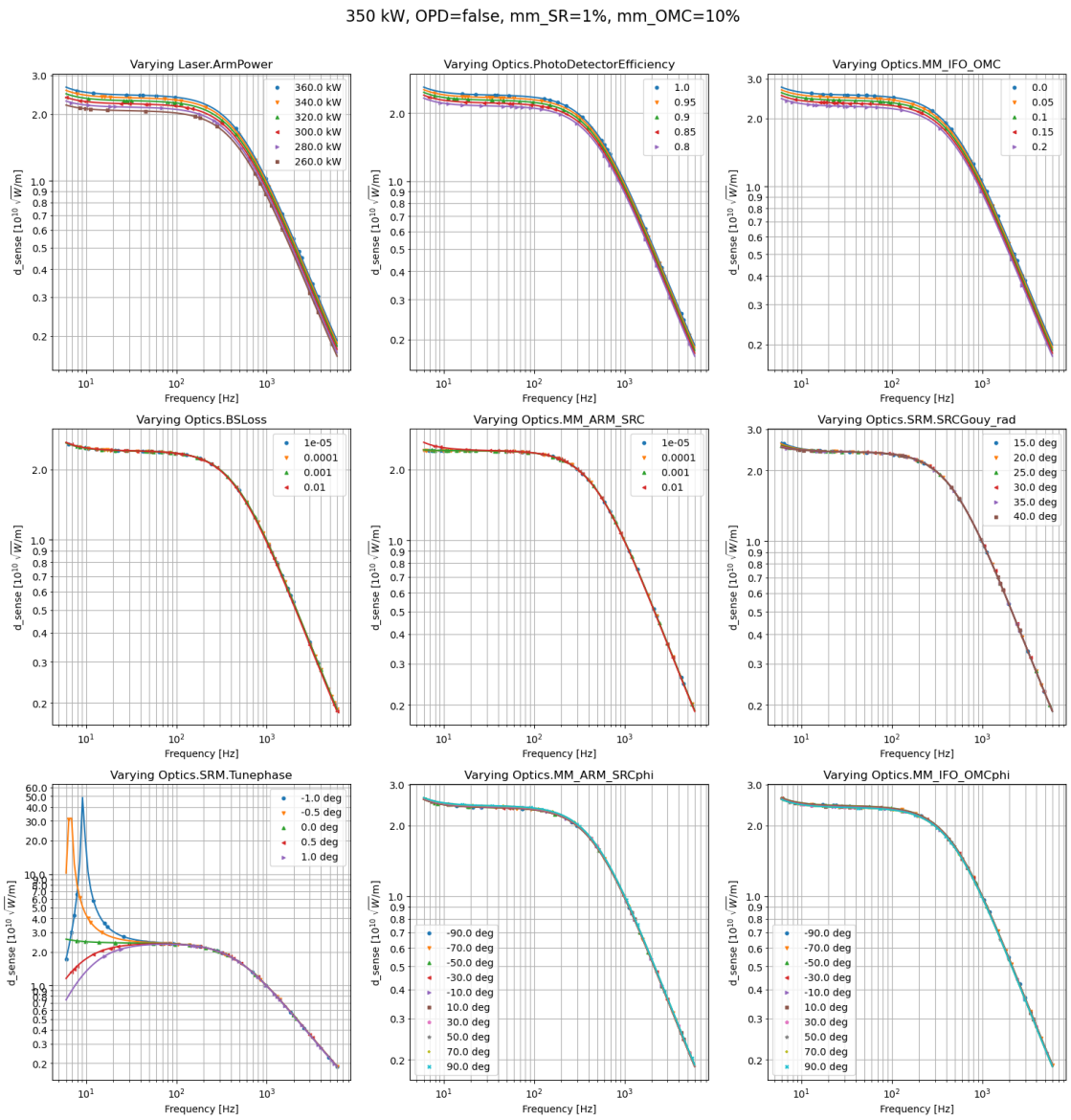

This is the case where is_OPD is false so the thermal lensing is less dominant than quadratic mode-mismatch. The sensing function is not super sensitive to Υ_{SR}. We need at least 1% of arm to SRC mismatch to see any effect.

Without thermal lensing, Υ_{SR} affects the SRC spring in the opposite way, making it more pro-spring. Everything else is pretty much the same as the OPD=true case. The mismatch phasings are not significant here.

2.2 MCMC on Pcal sweep

The Pcal sweep data is measured in DARM ERR cts/m. To get W/m, we go back from DARM_ERR to the OMC-DCPD_SUM which has a fairly flat response of 23.974 dB, to

where photodiode counts are expressed in mAmps. The filter bank, eg OMC- DCPD_A, includes an unused A2mW bank which comes from the specs of the photodiode (flat gain of 1403). Therefore, the calibration factor is 10**(24/20)/1000*1403/1000.

The diaggui plot is here. The calibration factor is 10**(24/20)/1000*1403/1000. This transfer function is not measured with actuation sweep so the high frequency part is not accurate.

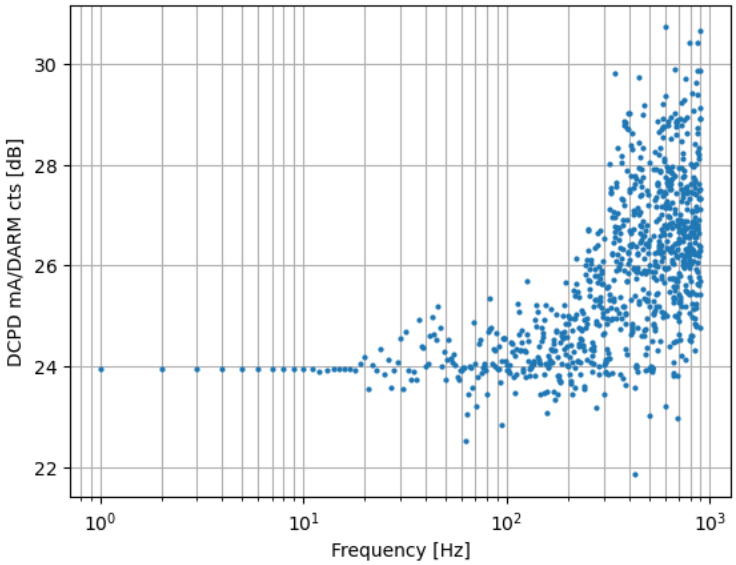

The sensing function from gwinc (d_sense) is in the unit of $\sqrt{\mathrm{W}}/\mathrm{m}$. To convert it to W/m, we need to multiply it with the sqrt of the LO power on DCPD. We manually fit the pcal data first with both OPD scenarios.

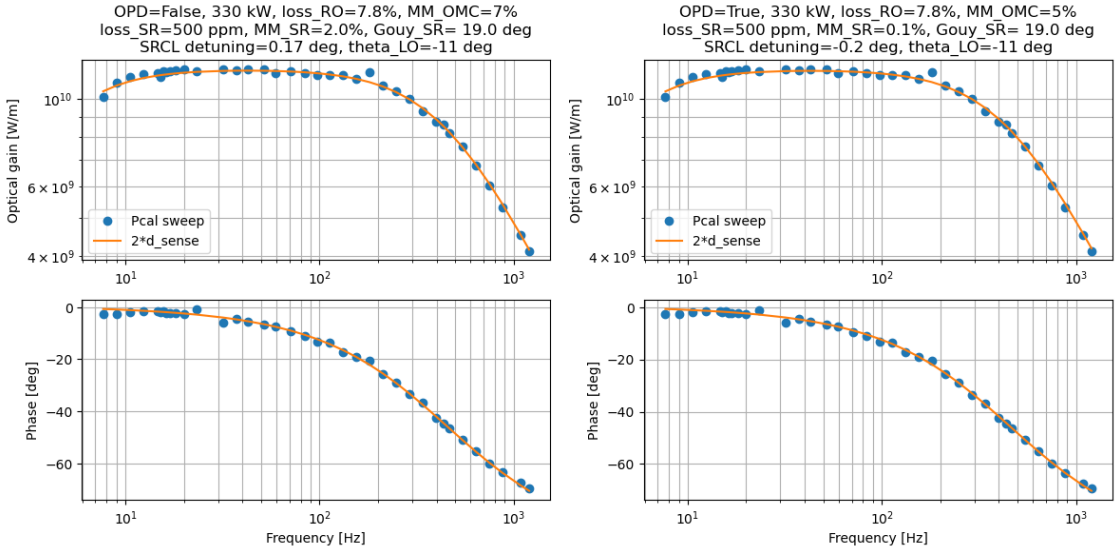

There's a factor of 2 difference between the gwinc model and measured optical gain. We've compared the optical gain with another simulation tool o_O and they match relatively well. We will still fit the offset difference anyway.

Knowing one set of parameters that's close to truth, we can perform a Monte-Carlo-Markov-Chain (MCMC) method to infer those parameters that could significantly affect the sensing function. We have 5 degrees of freedom in the MCMC run: scale factor, SRC loss, SRCL offset, ARM2SRC mismatch, and IFO2OMC mismatch. The arm power and readout loss are absorbed in the scale factor. The initial walkers are distributed perturbatively around the optimal point found manually. The MCMC result is shown in the corner plot.

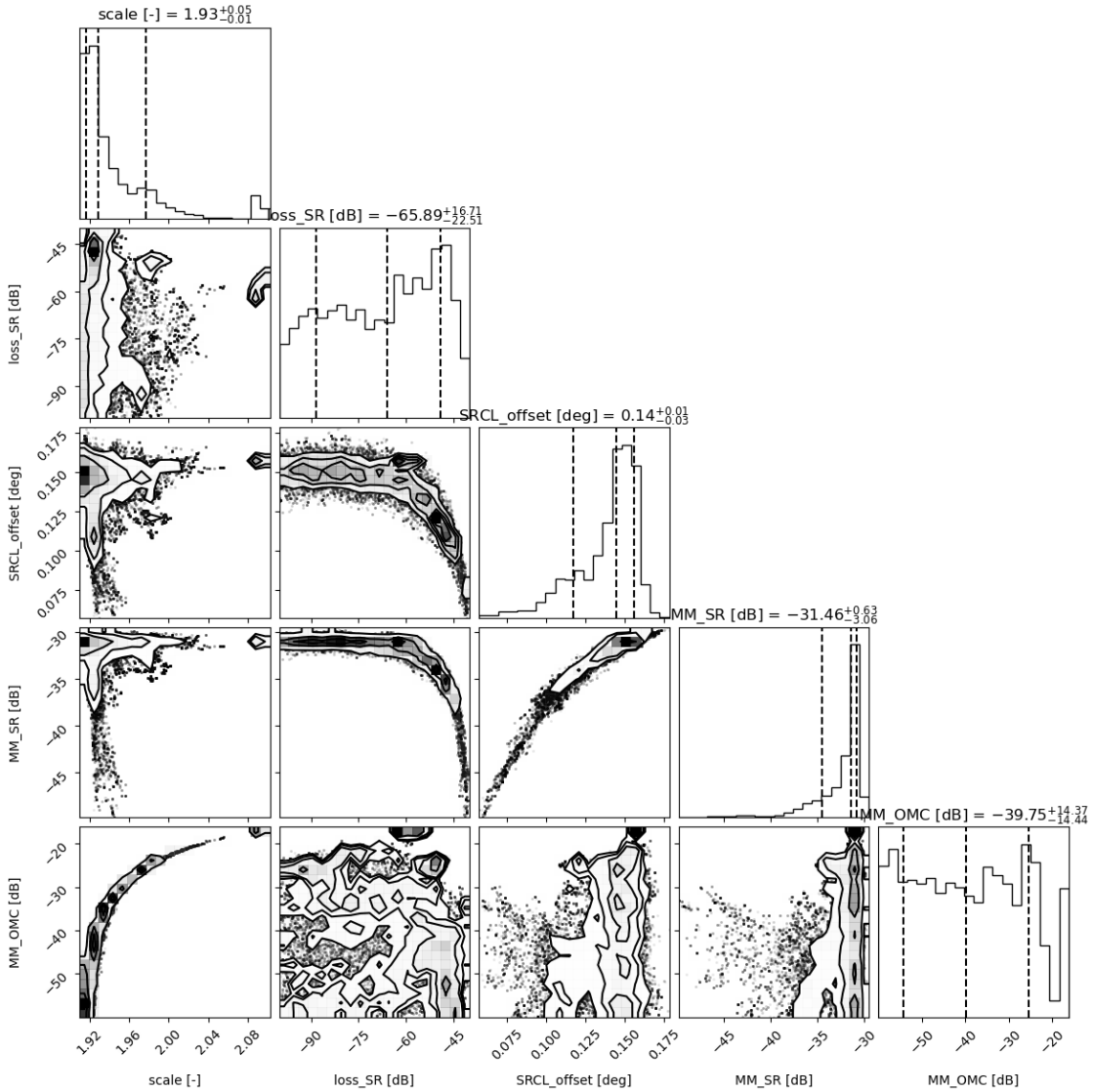

In the case where thermal lensing is negligible, the MCMC constrains the scale and SRCL detuning pretty well. Other parameters like losses and mismatches are not well constrained

as they could be anything. The Υ_{SR} already has upper bound to be more than -30 dB (3%), which is a reasonable non-ideality. Note that these degrees of freedom are not orthogonal with each other; we can see a strong correlation between scale factor and Υ_{OMC}, SRCL detuning and Υ_{SR}, etc.

For the case of OPD=true where thermal lensing is dominant, the result is shown here

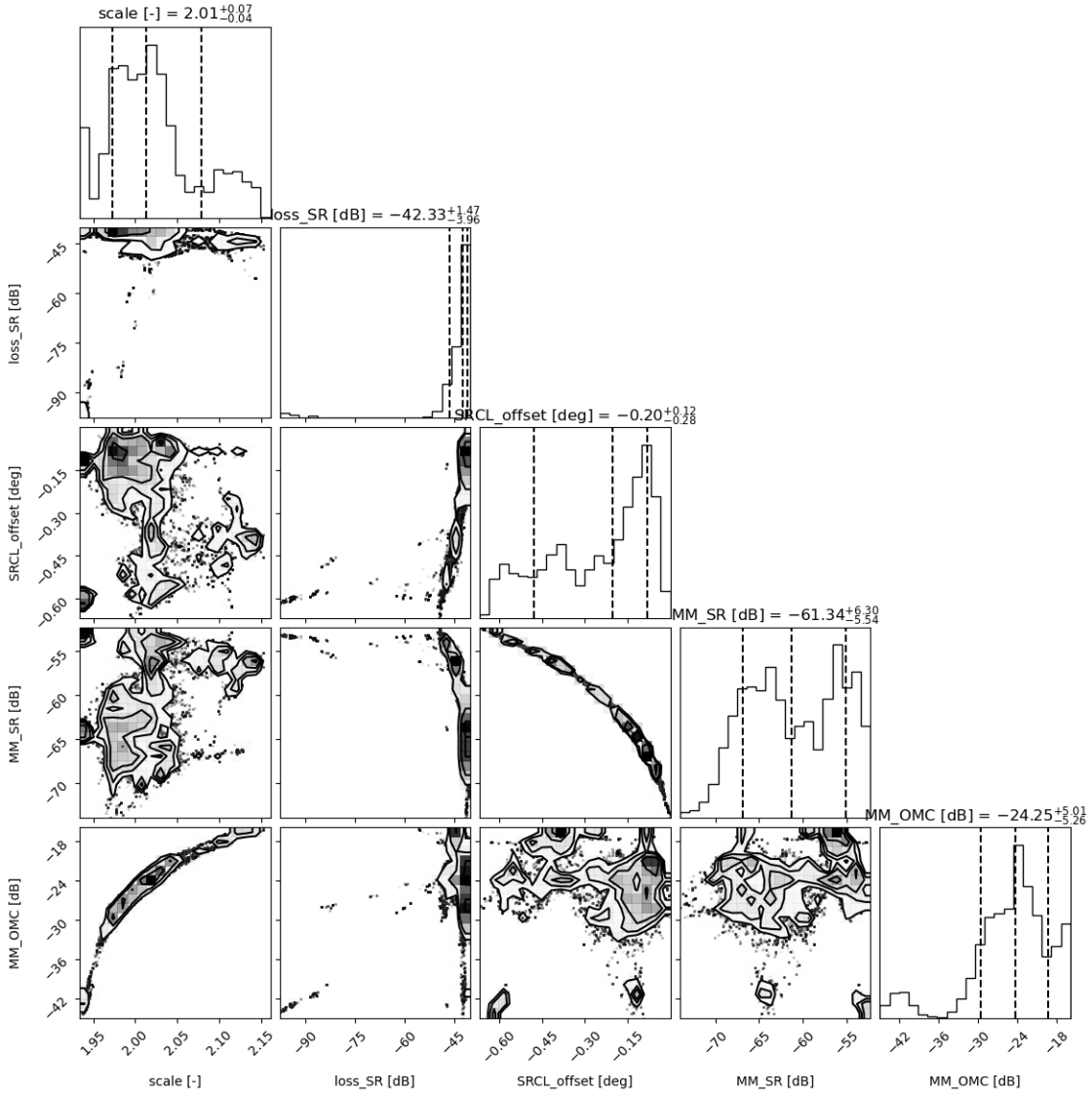

For the strong thermal lensing case, we've set the upper bound of Υ_{SR} to be -60 dB (0.1%). The distribution of the Υ_{SR} also shows that the likelihood of it being above -60 dB is very small. The scale factor and SRCL detuning is also constrained well. The SRCL detuning is estimated to be less than OPD=False case and it makes sense. The mismatches are still difficult to estimate because the contribution is likely to be the sum of quadratic mismatch and thermal lensing effect. In conclusion, we choose the default case where quadratic mismatch dominates and gives the most reasonable SRC parameters for later on analysis.

The SRC parameters inferred from sensing functions are

Parameter	**MCMC result**
Arm to SRC mode-mismatch	2.8%
SRCL detuning	0.14 degree

3 Analysis of Unsqueezed DARM

The quantum noise of the unsqeezed DARM can be directly modeled with gwinc. However, it can't be directly observed since we can only measure the total noise of unsqueezed interferometer. Nonetheless, we still have methods to estimate the quantum noise directly or indirectly at some frequency band, for example, using the NULL DARM power spectral density.

See Appendix A for the study of properly estimating of DARM power spectral density.

3.1 Quantum shot noise & radiation pressure noise

Quantum noise can be sub-divided to quantum shot noise and quantum radiation pressure noise (QRPN). Without squeezing, they are represented in equations below:

$$S_{QN} = S_{shot} + S_{QRPN}$$

$$S_{shot} = \frac{\hbar\gamma}{4kLP}\left(1 + \frac{\Omega^2}{\gamma^2}\right)$$

$$S_{QRPN} = \frac{64\hbar kP}{m^2 L^3 \gamma}\frac{1}{\Omega^4}\left(1 + \frac{\Omega^2}{\gamma^2}\right)^{-1}$$

where γ is the signal bandwidth of 450 Hz. The sub-budget of quantum noise is shown below.

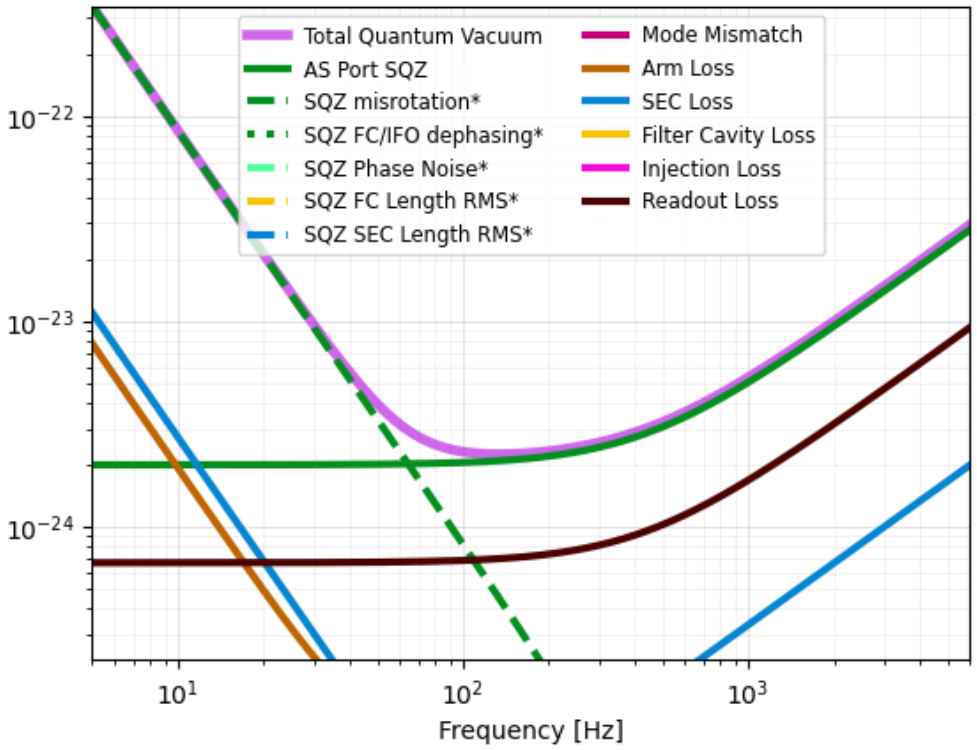

The shot noise is the sum of "AS Port SQZ", "Readout Loss", and "Mode Mismatch". The QRPN is "SQZ misrotation". In fact, the quantum noise can be understood as a single quantum mode that experiences frequency-dependent ponderomotive squeezing from interferometer, which is how gwinc models it.

The shot noise is essentially a flat shot noise divided by the sensing function. So it only gives one more physical information about the scaling factor in addition to the sensing function. The QRPN is very important to estiamte how much of the ponderomotive squeezing we have, but it's difficult to infer QRPN directly.

3.2 NULL & Cross-correlation

The unsqueezed DARM is the sum of classical and quantum noises. Both are assumed and verified to be quite stationary, so we can subtract classical from DARM to get pure quantum noise, which is something we can model. One way to measure classical noise is the cross-correlation (xcorr). See Appendix B for the sanity check on cross PSD estimation methods.

$$S_{xcorr} = 2\hbar\omega_0 B^\dagger(\langle bb^\dagger\rangle - \langle dd^\dagger\rangle)B + S_c$$

where B is the carrier, b is the quantum mode from OMC TRANS, d is the vacuum from the empty port of the DCPD beam splitter. S_c is the classical noise that is common to two PDs (so excluding dark noise). At high frequency where quantum noise is shot noise, $\langle bb^\dagger\rangle = \langle dd^\dagger\rangle$ and the xcorr is the common classical noise (useful). At low frequency where quantum radiation pressure noise dominates, xcorr can't separate common classical noise from total noise.

If we subtract xcorr from DCPD sum

$$S_{SUM} = 2\hbar\omega_0 B^\dagger\langle bb^\dagger\rangle B + S_c + S_{dark1} + S_{dark2}$$

we get NULL

$$S_{NULL} = S_{SUM} - S_{xcorr} = 2\hbar\omega_0 B^\dagger\langle dd^\dagger\rangle B + S_{dark}$$

The shot noise is

$$S_{shot} = S_{NULL} - S_{dark}$$

After calibration (dividing DCPD current shot noise with sensing function), the spectrum is pure quantum shot noise, which can be used to infer arm power, readout loss, etc. The low-frequency estimation of the DARM can be difficult, so we mostly rely on the Pcal measurement to infer SRC info.

Note that the shot noise is only a part of total quantum noise. We can't infer the QRPN that is correlated between two DCPD. Above 4 kHz, there are excessive laser noise, which still leads to 5% change of quantum noise after subtraction. So our interested frequency band is 20 - 4 kHz.

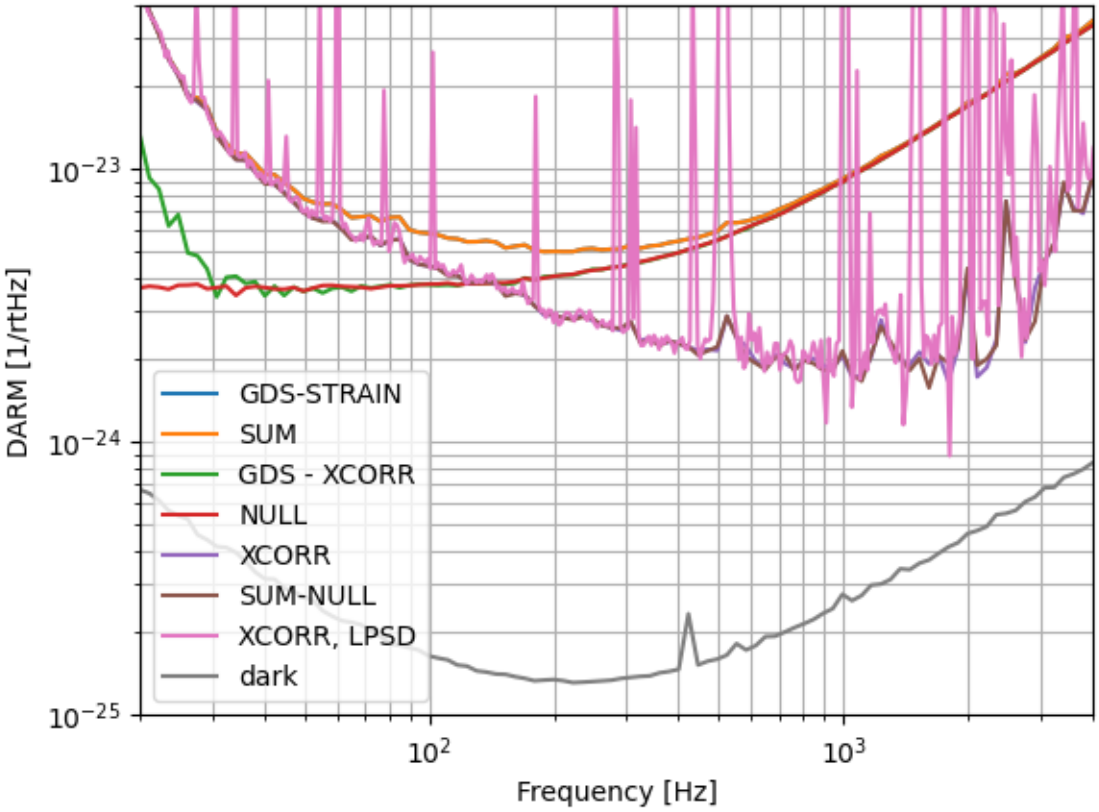

In fact, we could obtain the NULL spectrum either by subtracting cross-correlation from the total (SUM), or just directly calculating the PSD of the difference of two DCPD time series. The results are verified to be approximately the same. In this plot, the blue 'GDS' curve is the PSD calculated from GDS-STRAIN channel. The orange 'SUM' curve is calculated from the DCPD SUM channel CAL-DELTAL_EXTERNAL. A frequency-dependent correction function is applied to make sure the GDS and SUM are identical. This correction will also be applied to individual PD signals from CAL-DELTAL. The red 'NULL' curve is calculated from the difference of raw time series of two PD (CAL-DELTAL_A and CAL-DELTAL_B), and the purple 'XCORR' is the cross-spectral density of two raw time series. The SUM - NULL curve is verified to overlap with XCORR. The GDS - XCORR curve, however, deviates from the NULL at low frequencies. This is because the difference between GDS and XCORR is small and has a large uncertainty after subtraction. The NULL channel is best to estimate the calibrated shot noise (after subtracting gray DARK trace). The pink 'XORR, LPSD' uses a different algorithm (LPSD method, see Appendix B) to obtain cross-PSD as a sanity check; it is equal to the XCORR curve.

The calibration difference between GDS and PD time series are fixed by multiplying PD spectrum with the ratio. The null PSD is cleaner at low frequencies compared with subtraction. We will use null noise - dark noise as the shot noise from now on. The dark noise is a factor of 30 smaller at high frequency and a factor of 7 smaller at low frequency, in ASD.

3.3 Get all shot noises

These DARM were taken with FC misaligned but diverter open. The OPO is dither-locked on CLF with no pump light (no NLG). The CLF ISS was on and the LO was locked with the single-sideband CLF. They are

- 0514_1, 5, 9, 13
- 0514_17, 20, 23, 25, 27, 29
- 0515_5, during FDS taking
- 0516 all
- 0522_4, 5

4 DARM were taken with FC aligned and locked on single-sideband RLFCLF. The goal is to assert that they are all the same, and aligned FC doesn't introduce extra classical noise.

- 0515_2, 4, during FDS taking, loop not retuned
- 0522_1, 2, 3. Trace #1 is not retuned but #2 and #3 are well tuned (see LLO64982)
- 0523_8, 9, PRX paper. FC loop was well tuned

The shot noises contain these info:

1. Null systematic error
2. dark systematic error
3. delta N, G, D

3.4 Uncertainty propagation

We need unsqueezed DARM taken at different times to estimate if the system's stationarity. There are total 30 unsqueezed DARM taken at 6 different locks. The classical noise should be stationary locally within each lock.

The uncertainty of shot noise PSD S_{shot} is

$$\Delta S_{shot} = S_{shot}\sqrt{\delta G_{cal}^2 + \delta D^2 + \delta N^2}$$

where

- δG_{cal} is the quoted combined calibration error and uncertainty estimate ($|R^{(\mathrm{sample})}/R^{(\mathrm{MAP})}|-1$).
- δD is the statistical uncertainty due to PSD estimation of measured DARM ($1/\sqrt{\Delta T \Delta f}$). Note that it's not $2\delta D^2$ that double-counts uncertainties of both SUM and XCORR from the same data-series.
- δN is the non-stationary changes in the classical noise contributions $\delta N^2 = \delta N_t^2 + \delta N_m^2$, where δN_t is time-stationarity and δN_m is the operating mode stationarity between unsqueezed and squeezed interferometer. Note that it's over-estimated by a factor of $S_{shot}(\Omega)/S_{clas}(\Omega)$

The uncertainty of dark noise is not propagated because it only contributes to an additional $\sqrt{1+(S_{dark}/S_{shot})^2}-1 = \sqrt{1+(1/7)^4}-1 = 0.02\%$.

The stationarity error is estimated from the same method as Nature 583, 43, but we only have unsqueezed DARM taken at various times.

$$\delta N_t^2 \approx \frac{\mathcal{N}_\Sigma^2}{n}$$

where n is the number of observed unsqueezed DARM at various times and

$$\mathcal{N}_\Sigma^2 = \frac{2}{n(n-1)} \sum_{i \neq j}^{n} \mathcal{N}_{ij}^2$$

where $\mathcal{N}_{ij}^2$ is the pairwise relative non-stationarity between two such discontiguous segments with PSD D_i and D_j

$$\mathcal{N}_{ij} = 2\frac{D_i - D_j}{D_i + D_j}$$

In reality, the statistical error of each DARM D_i should also contribute to δN_t, especially at high frequencies with linear FFT. It's difficult to isolate the non-stationary error from the statistical error.

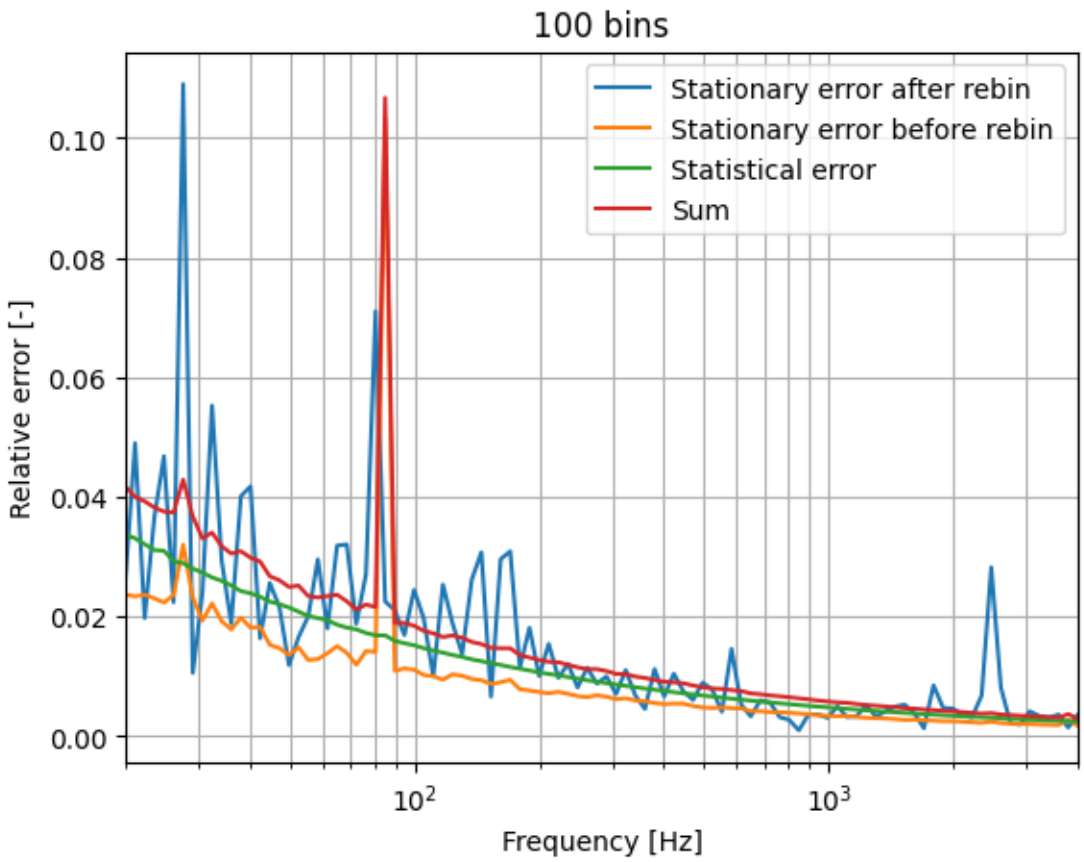

If we rebin DARM first, the statistical uncertainty would be suppressed at high frequencies while the stationary error shouldn't change, assuming the stationary error has enough bandwidth to not be averaged out by rebinning. This is the blue trace, which still resembles the statistical error. We only know that the 80 Hz peak is scatter noise and non-stationary, the rest is hard to tell if its stationary or not.

If we get δN_t first and rebin the error, we have the yellow curve. Note that it's less than the blue curve and also the statistical error (green curve). The sum of yellow and green gives the sum curve. Since the blue curve includes statistical error, it should be very close to the Sum curve. They agree quite well.

The stationarity of the two locks on 05/14 are compared here:

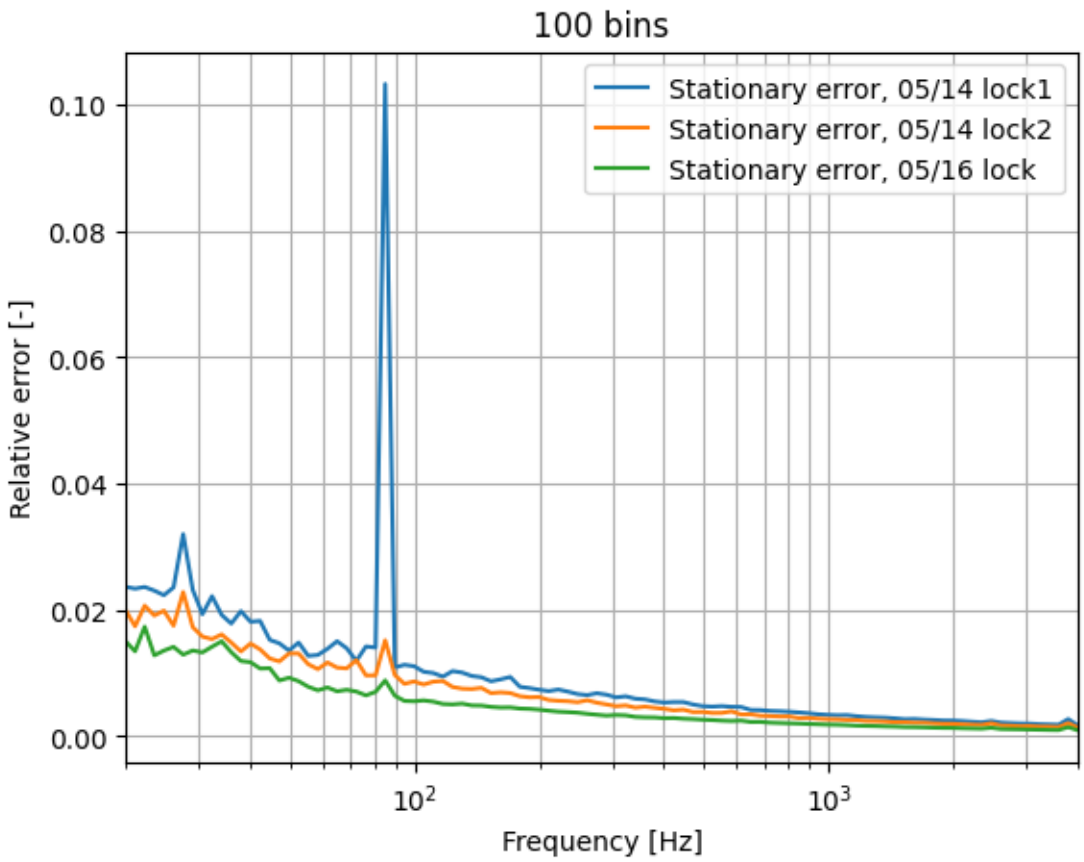

The stationary error in lock2 is lower because it has 50% more unsqueezed DARMs than lock1. Same story with 05/16 lock. Note the scatter noise at 80 Hz is less in the second case. It is because the scatter noise is stationary, not because we had lower scatter noise.

For δN_m, we can verify that there's small difference between unsqueezed DARM measured at two operating modes: diverter closed and FC locked on RLFCLF.

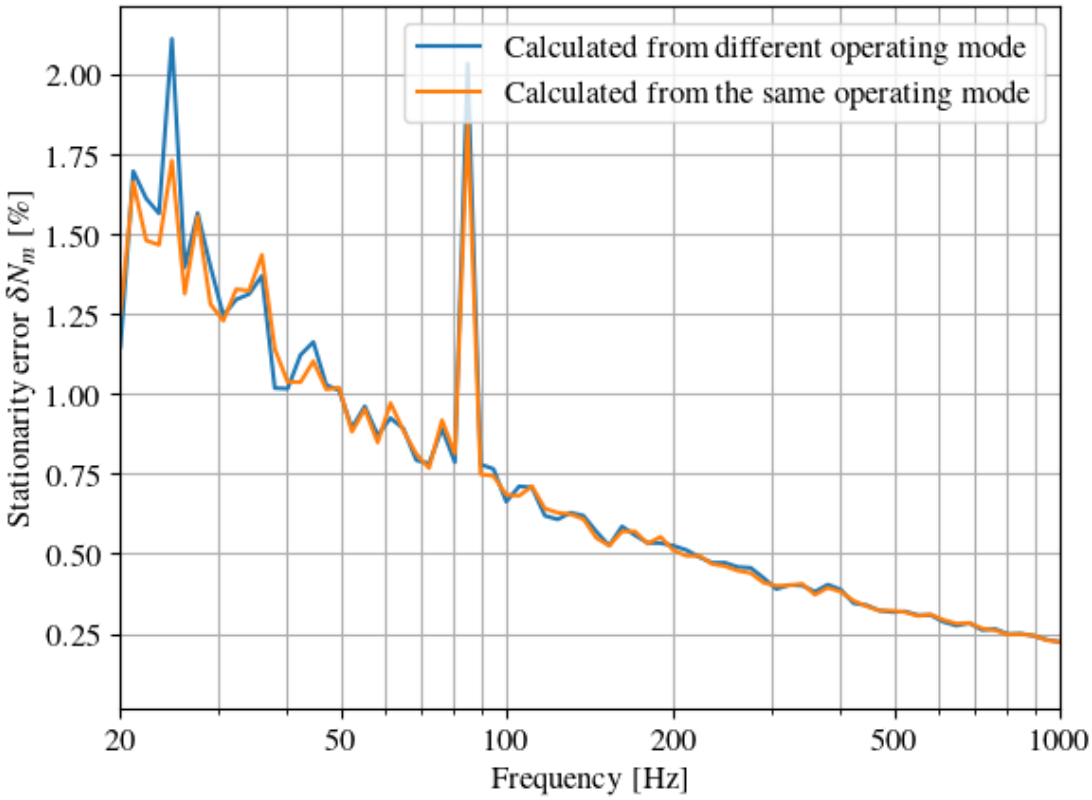

The non-stationary error due to switching operating mode (from FC misaligned to FC aligned) doesn't introduce any more error than the time-stationary error. The cross curve means the pairwise N_{ij} is always taken with one FC-misaligned DARM and one FC-aligned DARM. The shuffle curve uses N_{ij} always computed using the same operating mode DARM. There is no significant difference between these two curves besides some peaks known to be scatter noise. The nominal FDS doesn't introduce extra noises to the system (also indicated by measuring backscatter noise in FDS DARM LLO65120).

$$\delta N_m(\Omega) \approx 0$$

3.5 Thermalization

The interferometer is known to have a thermalization period once it reaches ~350 kW arm power. The 10 traces taken on 05/16 are chronologically ordered 20-min traces starting 45 minutes after reaching final arm power. The FC was misaligned and LO loop was still locked on single-side CLF.

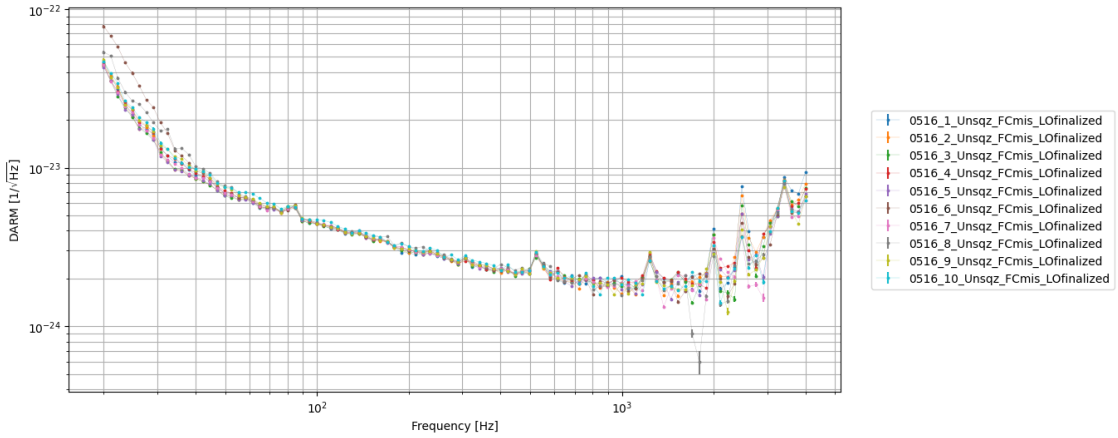

The xcorr spectra show some breathing at around 40 Hz. It's hard to see the change at high frequencies on the spectra. They are plotted here:

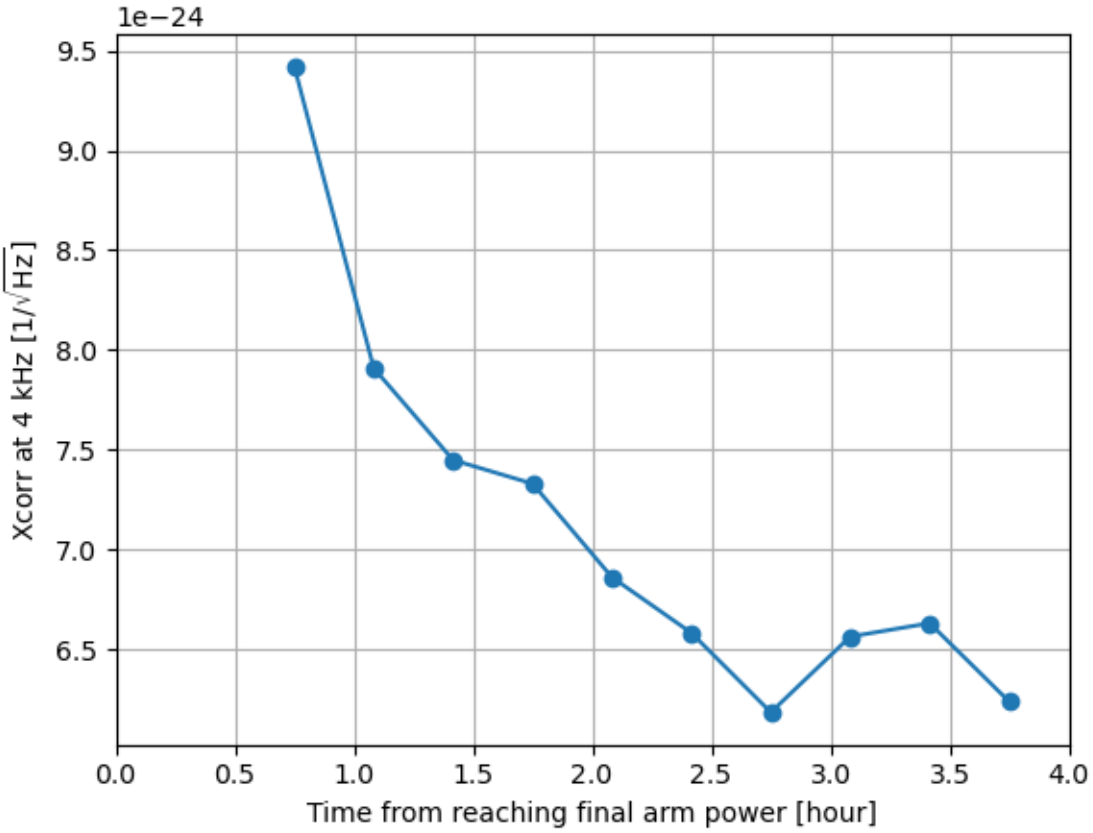

There is a clear trend of thermalizing until 2.5 hours from reaching high power. The difference

is around 2%, which would be attributed to arm power or loss uncertainty. Therefore, we only pick those above 2.5 hours as the shot noises for fully thermalized interferometer.

3.6 Cross-check sensing function

The NULL is essentially the flat shot noise divided by optical gain, so it doesn't give more information than the sensing function except that its DC level is very trustworthy. It gives very tight bounds on the loss/arm power. We can divide the flat shot noise of 50 mA with the calibrated NULL noise to get sensing function again.

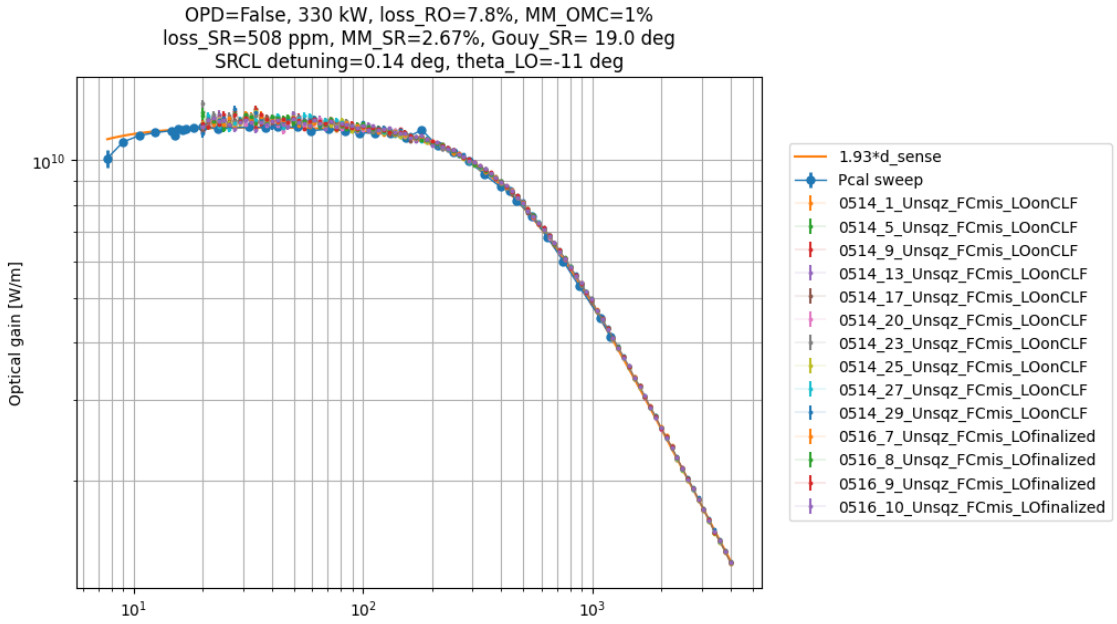

Both sensing functions measured in two different ways agree pretty well, along with the model curves. The DC level is still questionable, as the scale factor 1.93 can't be easily absorbed into the arm power of 330 kW.

Similar to Pcal scan, there isn't much interesting at high frequency. At low frequency, the anti-spring acts on the shape together with mode-mismatch. The unsqueezed DARM is also not very sensitive to mismatch phasing.

3.7 Parametric study

There are 9 parameters to that affects the quantum noise of unsqueezed interferometer:

- Arm power P_{arm}
- Readout loss Λ_{RO}

- Interferometer (IFO) to output mode cleaner (OMC) mode-mismatch Υ_{OMC}
- IFO to OMC mode-mismatch phase Υ_{OMC} phase
- SRC loss Λ_{SR}
- Arm cavity to SRC mode-mismatch Υ_{SR}
- Arm to SRC mode-mismatch phase Υ_{SR} phase (known from MCMC on sensing function)
- SRC Gouy phase ψ_{SR}
- SRC detuning $\Delta\phi_{SR}$ (known from MCMC on sensing function)

in addition to parameters that don't contribute much

- SRC length total RMS motion (not important for the current ifo)
- Arm cavity Gouy phase (only change 0.3 deg for change of 5-m ITMRoC. Negligible)

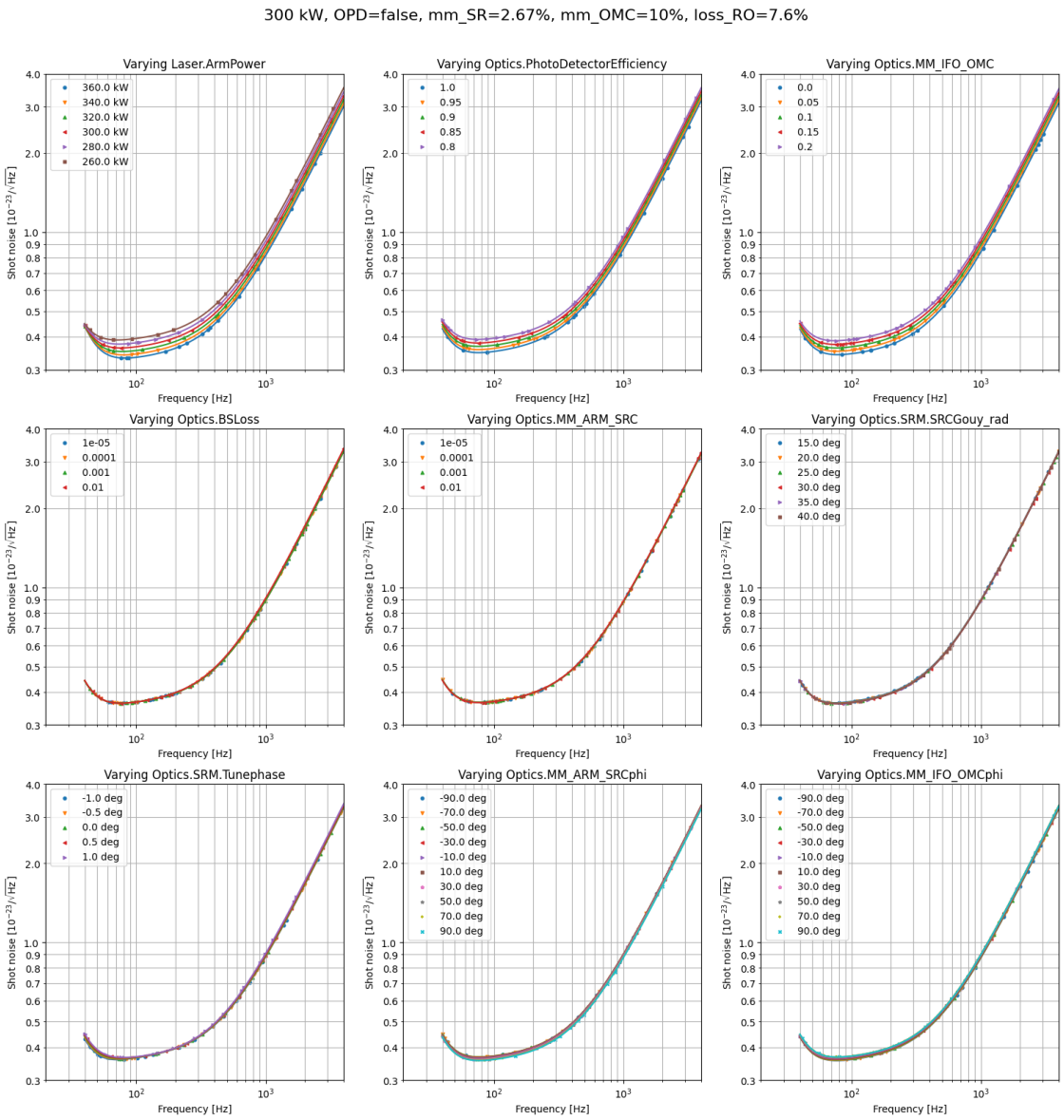

The unsqueezed DARM will not be very sensitive to the bottom row of three phasing parameters because the SRC mode-mismatch is -30 dB (~3%). There will also be a strong degeneracy among the three loss parameters in the mid-row of the plot. Overall, the parameters don't affect model significantly across different dimensions.

3.8 MCMC on unsqueezed QN

We can estimate the QRPN if we know the classical noise at low frequency. One of the dominant classical noise there is coating Brownian noise at 100-200 Hz. We could infer a certain level of QRPN, and thus total quantum noise, by subtracting modeled classical noises at low frequency (see Appendix C for a study on modeling coating Brownian noise). It turns

out that the uncertainty of inferred QRPN is relatively high, and the inferred unsqueezed total quantum noise doesn't costrain the parameter very well.

The Λ_{RO} and Υ_{OMC} are not strictly degenerate even with unsqueezed case, when the SRC is mode-mismatched to the interferometer.

For the current gwinc release (superQK, not superQKwieldSS), we don't need to find these parameters:

- DARM offset (from Pcal lines)
- Input-mode cleaner to power-recycling cavity mode-mismatch (from REFL PD)
- X-arm to Y-arm mode-mismatch or assymetrical loss (from contrast defect light)
- Spatial mode scattering matrix inside arm cavity

and these parameters can be independently measured:

- Power incident on Input Mirror 4 (IM4) = 63.73*0.97
- Readout angle = -11 degree (llo65447)

So the rest parameters to fit are:

- Arm power P_{arm}
- Readout loss Λ_{RO}
- Interferometer (IFO) to output mode cleaner (OMC) mode-mismatch Υ_{OMC}
- IFO to OMC mode-mismatch phase Υ_{OMC} phase
- Arm to SRC mode-mismatch phase Υ_{SR} phase
- SRC Gouy phase ψ_{SR}

As mentioned above, the mode-mismatch doesn't affect the unsqz quantum noise in a significant way. We can still do a MCMC and see the posterior distribution.

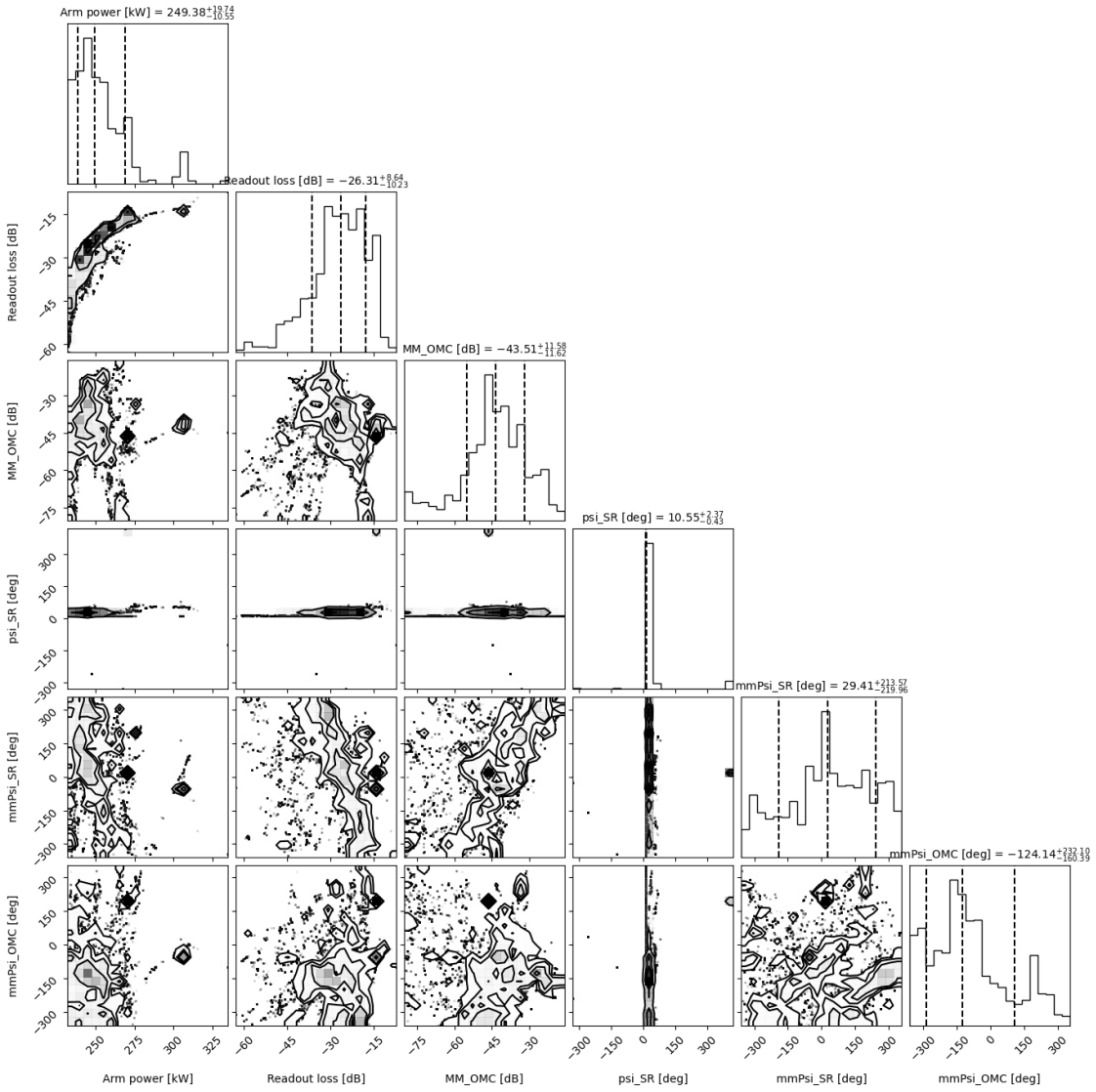
Arm power [kW] = 249.38$^{+19.74}_{-10.55}$
Readout loss [dB] = −26.31$^{+8.64}_{-10.23}$
MM_OMC [dB] = −43.51$^{+11.98}_{-11.62}$
psi_SR [deg] = 10.55$^{+2.37}_{-0.43}$
mmPsi_SR [deg] = 29.41$^{+213.57}_{-219.96}$
mmPsi_OMC [deg] = −124.14$^{+232.10}_{-160.39}$
Arm power [kW]
Readout loss [dB]
MM_OMC [dB]
psi_SR [deg]
mmPsi_SR [deg]
mmPsi_OMC [deg]

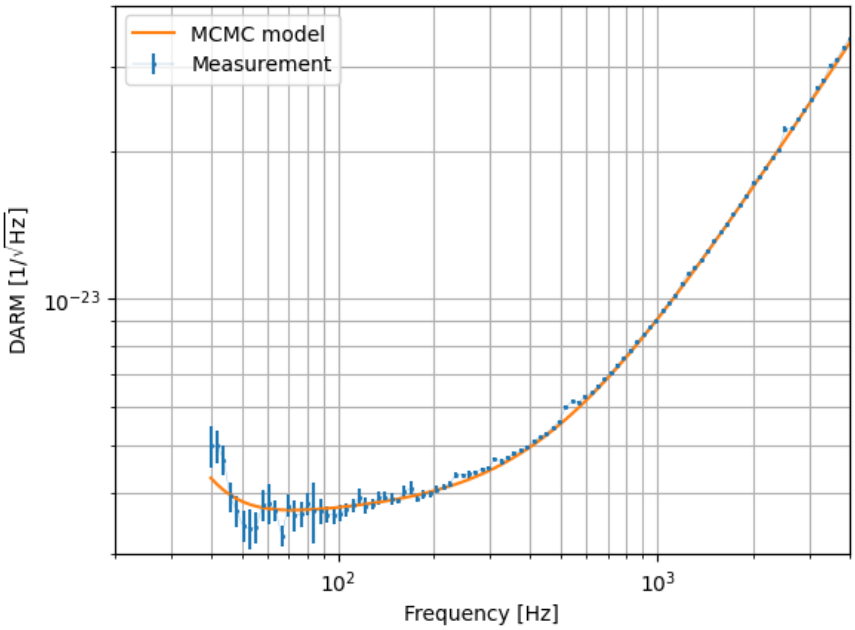

The MCMC on unsqz quantum noise only constrains the SRC Gouy phase. All other parameters are not well localized. This is because both the measurement doesn't have the sharp feature that MCMC can extract and the uncertainties are large. The model is plotted here with the data.

4 Analysis of Frequency-Independent Squeezing

Frequency-independent squeezing (FIS) represents the DARM spectra with squeezing input. There is no filter cavity in this case to produce the frequency-dependent squeezing angle.

4.1 Getting all FIS DARM difference

These FIS spectra were taken with FC misaligned. The OPO is locked on co-resonance with 532-nm transmission power to 0.13 mW. Based on our OPO characterization LLO64250, the threshold power is 0.224 mW. Therefore, we got nonlinear interaction strength of

$$x = \sqrt{P/P_{th}} = 0.762$$

and NLG of $1/(1-x)^2 = 17.65$. The generated squeezing is $10\log_{10}((1-x)^2/(1+x)^2) = -17.4$ dB. This assumes that the OPO had not degraded since the characterization (a period of 1.5 month).

We took 20 measurements with various squeezing angles:

- 0514_2, FIS 5.6 dB
- 0514_3, FIAS 15.8 dB
- 0514_4, 0514_8, CLF -140 a.u.
- 0514_6, CLF -150 a.u.
- 0514_7, CLF -170 a.u.
- 0514_10, QND, CLF -30 a.u.
- 0514_11, QND, CLF -50 a.u.
- 0514_12, QND, CLF +100 a.u.
- 0514_14, QND, CLF +143 a.u.
- 0514_15, 0514_16, QND, CLF +140 a.u.
- 0514_18, QND, CLF +200 a.u.
- 0514_19, QND, CLF +250 a.u.
- 0514_24, QND, CLF +40 a.u.
- 0514_26, QND, CLF +70 a.u.
- 0514_28, QND, CLF +140 a.u.
- 0514_30, QND, CLF +170 a.u.

- 0523_2, FIS 5.7-5.8 dB
- 0523_3, FIAS ~16 dB

We will only focus on the data taken on 05/14 first, since the ifo is stationary over these two locks. All the uncertainties of each spectra can be estimated except for that of modeling

Since the classical noise is common to both squeezing and unsqueezed DARM, we can simply subtract these two and model the PSD difference. All the additional noises introduced between squeezing and unsqueezed DARM that is not quantum noise have been included in the stationarity uncertainty. **The nice thing about DARM difference is that it excludes classical noise, so it's a direct measurement of the quantum noise difference that is model-able by gwinc.**

As mentioned above, the total error of inferred quantum noise $Q = D_r - (D_s - M_s)$ is

$$\Delta Q^2 = Q^2 \delta G_{cal}^2 + \Delta D_s^2 + \Delta D_r^2 + \Delta M_r^2 + C^2(\delta N_t^2 + \delta N_m^2)$$

where D_r, D_s, C are reference, squeezed DARM PSD, and classical noises. We will explain more in the later sections.

Since we are interested in the difference between two data sets $S = D_s - D_r$, the uncertainty should be

$$\Delta S^2 = S^2 \delta G^2 + \Delta D_s^2 + \Delta D_r^2 + C^2(\delta N_t^2 + \delta N_m^2)$$

Since we don't have the model M_r, we don't know C, but we can replace it with D_r which would only overestimate the uncertainty at high frequencies where the error is already small. It won't underestimate the error.

4.2 Cross-check NULL

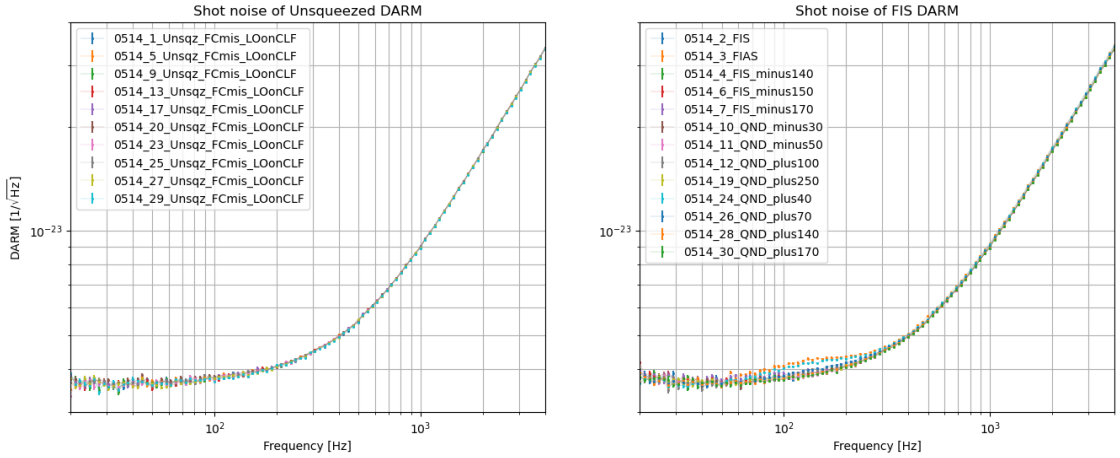

The shot noise of FIAS and near anti-squeezing have weird bump around 150 Hz. This is perhaps because the increasing of quantum noise that reduces SNR of calibration lines. Luckily, the anti-squeezing spectra are not very sensitive to many parameters, which will be shown later.

4.3 Preliminary fitting

These 16 parameters that affect FIS are ranked by impact:

- Squeezing angle θ_{SQZ} (inferred from high-f squeezing on QN)
- Generated squeezing (inferred from OPO green transmission LLO64250)
- Phase noise ϕ_{rms} (inferred from DARM NLG scan and phase noise budget LLO63517)
- Injection loss Λ_{inj} (in-chamber measurements LLO62872 $\times$ escape efficiency LLO60851 $\times$ OFI LLO55716)
- IFO to OMC mismatch Υ_{OMC}
- SQZ to OMC mismatch Υ_{SQZ}
- Readout loss Λ_{RO}
- Arm power P_{arm}
- SQZ to OMC mismatch Υ_{SQZ} phase
- IFO to OMC mismatch Υ_{OMC} phase
- LO angle θ_{LO} (from contrast defect LLO65447)
- Arm to SRC mismatch Υ_{SR}, is_OPD (from coupled cavity pole of sensing function in previous section)
- SRC Gouy phase ψ_{SR} (from ifo thermalized situation)
- SRCL_detuning $\Delta\phi_{SR}$ (from sensing function in previous section)
- Arm to SRC mismatch Υ_{SR} phase
- loss_SR Λ_{SR}

in addition to parameters that don't contribute much

- SRC residual RMS motion $L_{SR,rms}$ (not important for the current ifo)
- Arm cavity Gouy phase ψ_{arm} (only change 0.3 deg for change of 5-m ITMRoC. Negligible)

We can manually find a set of preliminary paramters that is not too far away from the truth.

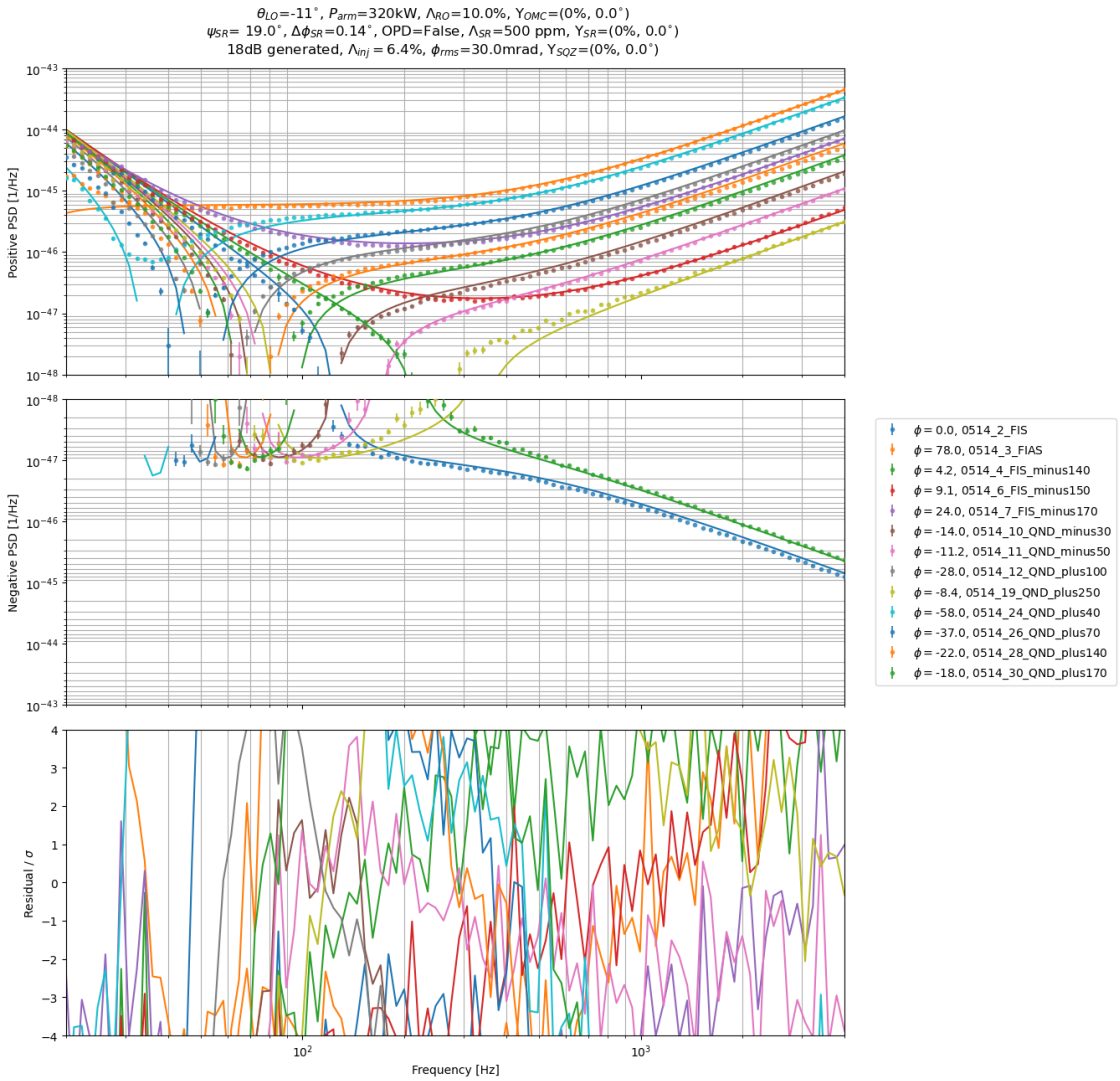

This plot shows a model without MM that fits the DARM difference at high frequencies. It fits positive (non-QND) squeezing angles quite well. However, it is quite far away from the low-frequency part of the negative (QND) squeezing angles while fitting the high frequency part. This is especially problematic for -58 deg case where the low frequency dip at around 35 Hz was totally missing. Mode-mismatch can perhaps accomplish the broadband fitting.

Some measurements are redundant, for example, measurement No. 8, 14, 15, 16, 18. This leaves us with 13 unique relative squeezing angles.

The θ_{SQZ} =**-58** and **78** spectra are the most problematic. They both show a low-frequency feature that is very different from what the quantum noise model predicts. For -58 deg one, the DARM difference doesn't show any squeezing at low frequencies, which is physically possible even at 20 Hz. It could be the calibration problem like we saw in the null spectra,

where anti-squeezed quantum noise biases the estimation of pcal line heights. It will distort the kappa parameters. It could also be the case when the backscatter noise gets amplified by anti-squeezing, which is unique in the anti-sqz mode and won't be seen in the stationarity noise.

The squeezing angles away from squeezing are not very interesting. For example, $\theta_{SQZ} =$ **9.7** and **24** degrees. The DARM difference is very smooth and doesn't have any features useful for extracting model parameters.

Similarly, the spectra are also not super useful for QND angles that squeezes QRPN at too low frequencies, for example, **-37** and **-28** degrees. The DARM difference is quite large and pretty much all anti-squeezing above 100 Hz. The anti-squeezing is less sensitive to parameters.

Although we have very precise and constraining measurement of the total DARM at high frequencies up to 4 kHz, we probably don't want to weigh too much over there where mode-mismatch doesn't affect much. We could cut the high frequency up to 1-2 kHz. We can play with it to find the best inferrence.

We can also do a manual fit with non-zero mode-mismatch. For example, we can attribute to all unknown readout loss to OMC mode-mismatch.

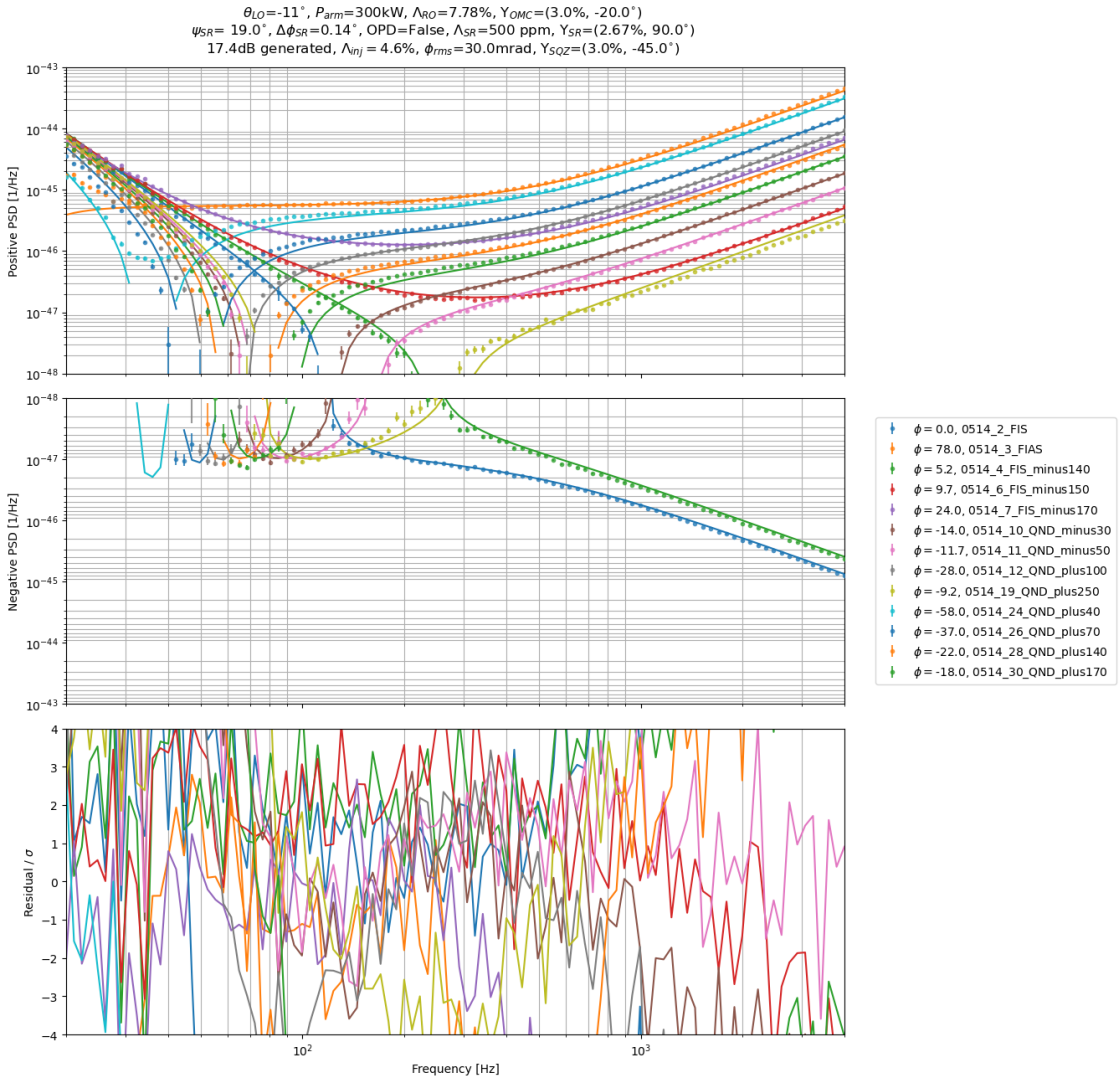

It's hard to tell whether the introduction of additional mismatch parameters help or not. We will compare MCMC of both cases shortly.

4.4 Absolute SQZ angle reference

The actual SQZ angle that maximizes high-frequency squeezing depends on the homodyne angle, detunings of core optics cavity, and mismatch phasing. It will also depend on the mismatch, loss, etc. We want to know if we can find an absolute angular reference so we don't have to feed squeezing angle as a free parameter for each FIS trace. It would be too many free parameters for MCMC analysis.

We can first sweep the phasings and see if the DARM difference maintains the shape

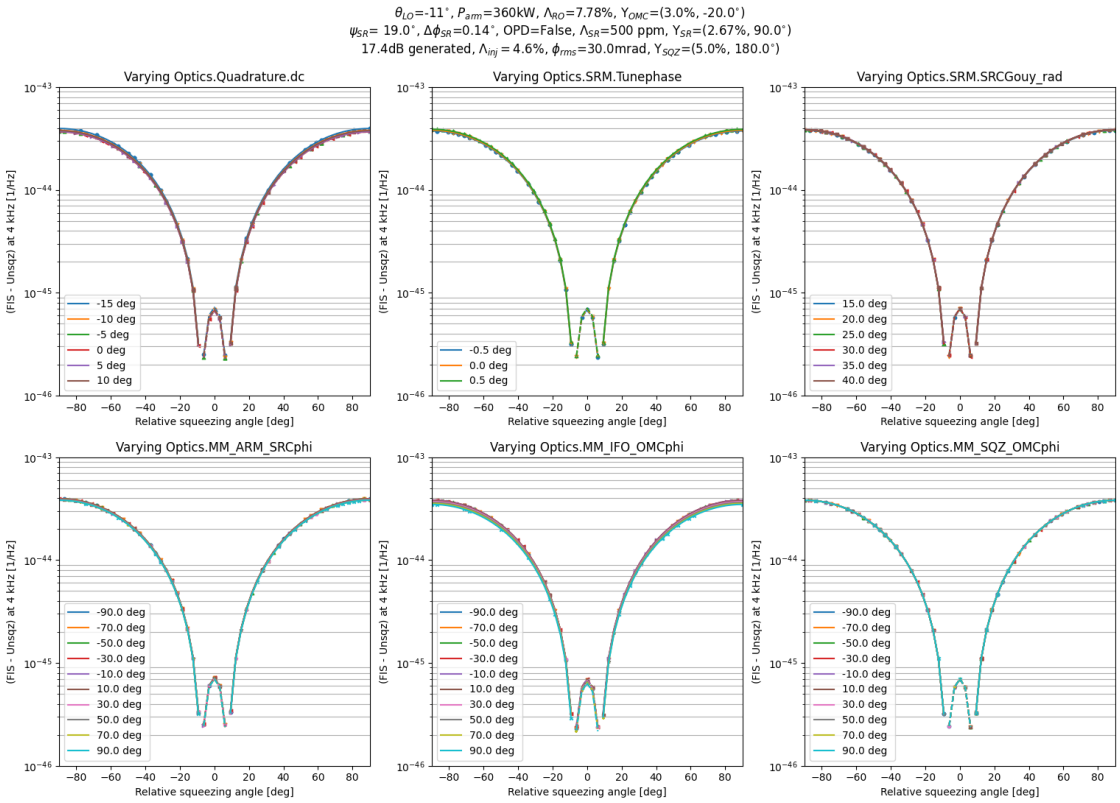

The free phasing parameters doesn't change the shape nor the magnitude of the DARM difference. The Υ_{OMC} phase will change the magnitude by more than 10% near anti-squeezing, but it doesn't change much between -40 to 40 degree.

However, finding the squeezing angle that minimizes high-freq QN takes a lot more time than each gwinc run, because it runs gwinc multiple times to search for minumum. We will see if it saves time by finding relative squeezing angle each time or set each squeezing angle as a free parameter.

4.5 Parametric study

We perturb parameters around the canonical setting and see how each one affects the DARM differences. We will do the max squeezing of shot noise first.

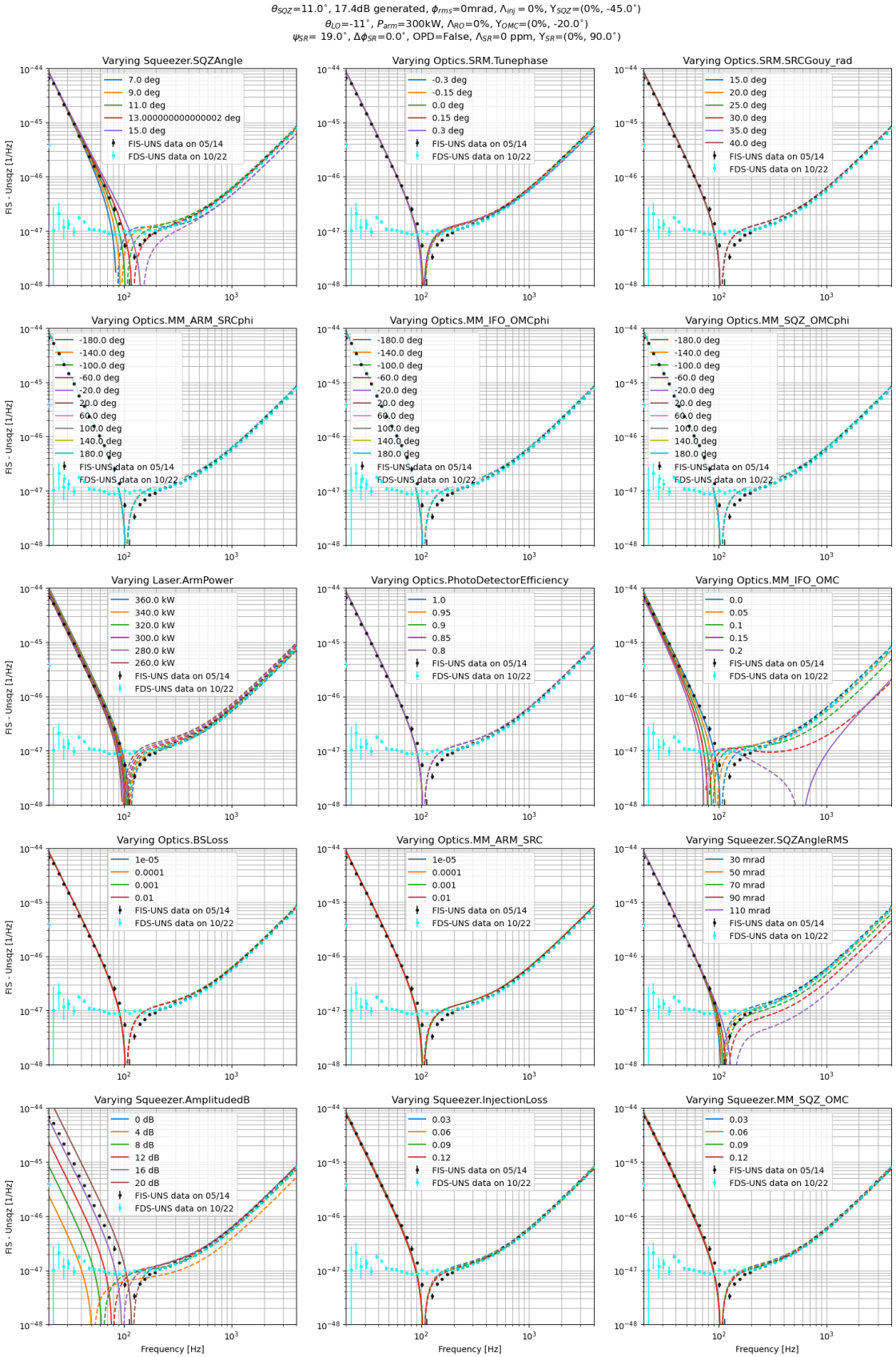
θ_{SQZ}=11.0°, 17.4dB generated, ϕ_{rms}=0mrad, Λ_{inj} = 0%, Y_{SQZ}=(0%, -45.0°)
θ_{LO}=-11°, P_{arm}=300kW, Λ_{RO}=0%, Y_{OMC}=(0%, -20.0°)
ψ_{SR}= 19.0°, $\Delta\phi_{SR}$=0.0°, OPD=False, Λ_{SR}=0 ppm, Y_{SR}=(0%, 90.0°)
Varying Squeezer.SQZAngle
7.0 deg
9.0 deg
11.0 deg
13.000000000000002 deg
15.0 deg
Varying Optics.SRM.Tunephase
-0.3 deg
-0.15 deg
0.0 deg
0.15 deg
0.3 deg
Varying Optics.SRM.SRCGouy_rad
15.0 deg
20.0 deg
25.0 deg
30.0 deg
35.0 deg
40.0 deg
Varying Optics.MM_ARM_SRCphi
Varying Optics.MM_IFO_OMCphi
Varying Optics.MM_SQZ_OMCphi
-180.0 deg
-140.0 deg
-100.0 deg
-60.0 deg
-20.0 deg
20.0 deg
60.0 deg
100.0 deg
140.0 deg
180.0 deg
Varying Laser.ArmPower
360.0 kW
340.0 kW
320.0 kW
300.0 kW
280.0 kW
260.0 kW
Varying Optics.PhotoDetectorEfficiency
1.0
0.95
0.9
0.85
0.8
Varying Optics.MM_IFO_OMC
0.0
0.05
0.1
0.15
0.2
Varying Optics.BSLoss
1e-05
0.0001
0.001
0.01
Varying Optics.MM_ARM_SRC
Varying Squeezer.SQZAngleRMS
30 mrad
50 mrad
70 mrad
90 mrad
110 mrad
Varying Squeezer.AmplitudedB
0 dB
4 dB
8 dB
12 dB
16 dB
20 dB
Varying Squeezer.InjectionLoss
0.03
0.06
0.09
0.12
Varying Squeezer.MM_SQZ_OMC
FIS-UNS data on 05/14
FDS-UNS data on 10/22
FIS - Unsqz [1/Hz]
Frequency [Hz]

We manually find a canonical set of parameters that are pretty close to the truth, We perturb parameters around the canonical setting and see how each one affects the DARM differences. We will do the max squeezing of shot noise first. The plot is shown here. The title shows the canonical parameter set where we perturb from. For each subplot, the title says the perturbed parameter. The various values of such parameters and the two measured DARM difference data are labeled in the legend. The solid curve is the positive of FIS - Unsqz, and the dashed curve is the negative part of the difference that is flipped to positive side. The figures for each squeezing angles are saved in ./fig/FIS/.

We can possibly observe some constraints from the squeezed spactra: - At high frequency, the DARM difference sets a bound on the arm power. The higher the power, the lower the absolute DARM difference is. This is because the shot noise scales inversely with arm power, so the difference is less for higher power. The phase parameters only reduces the difference as the squeezing angle is not optimized. Similarly, loss and phase noise also reduces difference in one way. More generated squeezing increases the difference, but it will plateau as the optical losses prevents more squeezing from being observed. This gives an upper bound of the arm power, in this case is **280 - 300 kW**. - At low frequency, the arm power and squeezing are degenerate. The loss will affect the QRPN, but it's small for small loss around 10%. This can set a lower bound of injected squeezing using the upper bound of arm power. - At mid frequency, we have a point where the difference crosses zero at the squeezing angle where the quantum noise ellipse is exactly 1. This angle depends on the arm power, ponderomotive squeezing, and injected squeezing. Both losses and phase degredations will change this angle in different ways.

To give some margin for certain degrees of freedom to alter DARM differece, the arm power needs to be lower than the upper bound.

Similarly, the anti-squeezing (on shot noise) spectra also gives useful information. However, we have trouble observing squeezing on QRPN at low frequency (below 40 Hz). Therefore, we could only use QRPN-squeezing above 40 Hz:

θ_{SQZ}=-13.7°, 17.4dB generated, ϕ_{rms}=30.0mrad, Λ_{inj} = 6.4%, Y_{SQZ}=(5.0%, -45.0°)
θ_{LO}=-11°, P_{arm}=300kW, Λ_{RO}=7.78%, Y_{OMC}=(3.0%, -20.0°)
ψ_{SR}= 19.0°, $\Delta\phi_{SR}$=0.14°, OPD=False, Λ_{SR}=500 ppm, Y_{SR}=(2.67%, 90.0°)

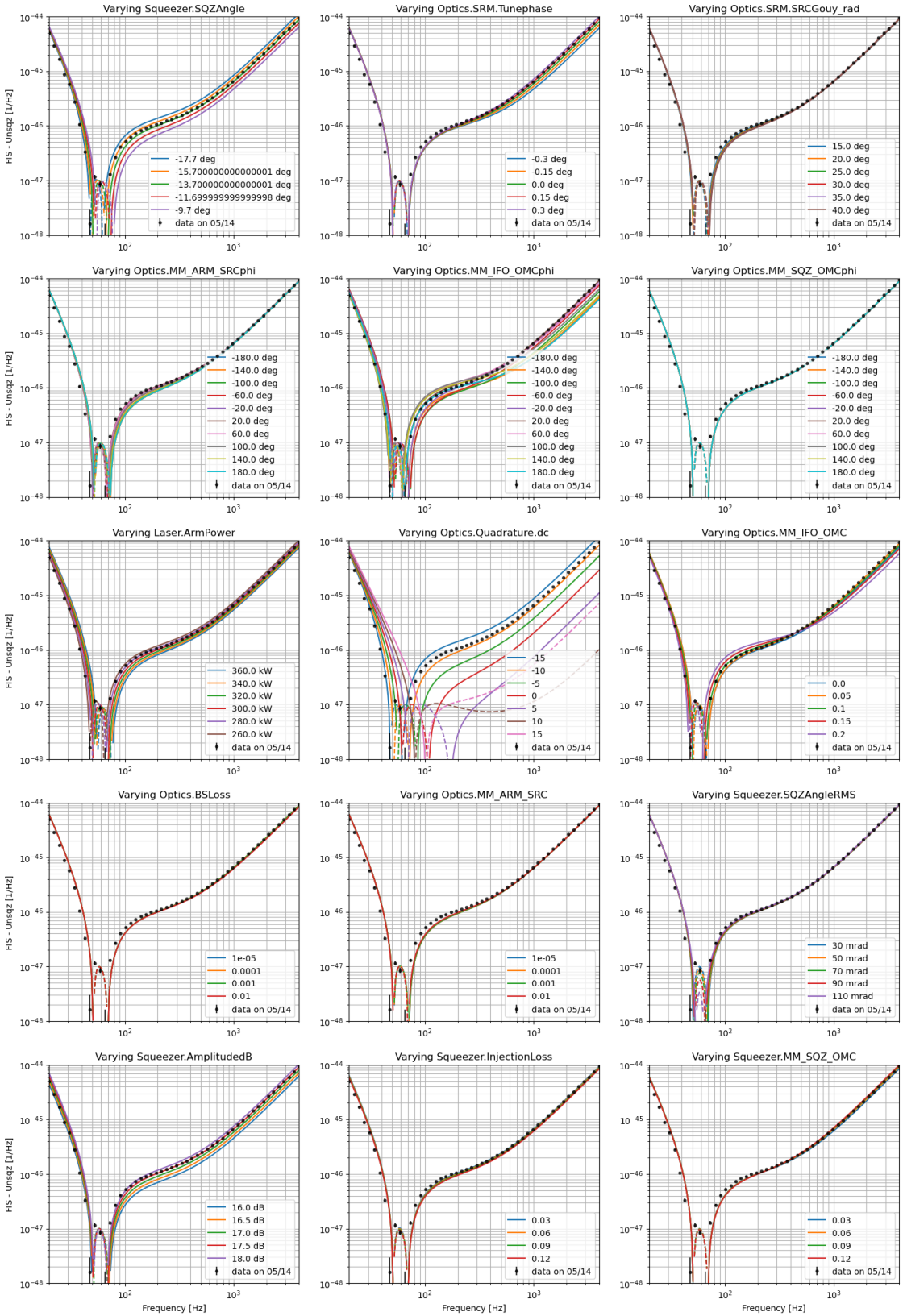

The first thing to notice from these subplots is that the **readout loss** doesn't affect the DARM difference at all frequencies. To explain this, we can define the readout loss as an effective beam splitter with amplitude reflectivity $r = \sqrt{1 - \text{loss}}$. The quantum noise in current is

$$S_I = 2\hbar\omega_0 r B^\dagger (r^2 \langle a a^\dagger \rangle + t^2 \langle v v^\dagger \rangle) r B$$

where a is the quantum field from interferometer and v is the vacuum fluctuations introduced by readout loss. The LO power B is also reduced by readout loss. Without squeezing, a is identical to v at high frequency and larger than v at low frequency.

$$S_I \propto r^2(r^2(1+\mathcal{K}^2) + t^2) \propto r^2(1+\mathcal{K}^2 r^2)$$

where $\mathcal{K}$ is the optomechanical coefficient. Note that the sensing function also depends on the loss:

$$g^2 \propto r^4$$

Therefore, increasing loss would decrease the DARM sensitivity S_I/g^2 at high frequency $(1/r^2)$, but doesn't change anything at low frequency limit (r cancels).

When we inject squeezing and take the DARM difference, the difference PSD is

$$\Delta S_I = 2\hbar\omega_0 r B^\dagger (r^2 \langle a_{(FIS)} {a_{(FIS)}}^\dagger \rangle - r^2 \langle a_{(UNS)} {a_{(UNS)}}^\dagger \rangle) r B \propto r^4$$

The vacuum are the same between the two $v_{FIS} = v_{UNS}$ and get subtracted out completely.

Therefore the difference DARM is $\Delta S_h = \Delta S_I / |g|^2$; so no more dependence on r broadbandly.

Besides readout loss, the DARM difference is also less sensitive to Λ_{RO} and Λ_{INJ}. These losses are mostly adjusting how much squeezing we can observe, which is removed when we take the difference of two DARM. We will infer them from a different observable.

Υ_{SR} slightly changes the observable at around 100 - 1000 Hz, below 2e-47 (so near squeezing). Υ_{SQZ} only changes spectra above 100 Hz near squeezing (-12 to 12 degree of relative squeezing angle). Υ_{OMC} heavily affects broadbandly and creates a interesting twist at 500-700 Hz when its around 20%.

The generated squeezing and P_{arm} pretty much serves as a scaling factor, except that the arm power flips scaling sign at SQL frequency. Phase noise is also effectively a loss that only impacts on the squeezing instead of anti-squeezing.

The mismatch phase between SQZ and OMC, Υ_{SQZ} phase also affects the DARM difference negligibly. It's probably because the amount of scattered squeezed fields are too small, and the scattered back squeezed fields are even less so their actual phase doesn't matter. The

scattered back fields scales with the product of all mismatches along the path. Even 10% mismatches along the path would contribute to 1%.

On the contrary, the Υ_{SR} phase and Υ_{OMC} phase change the DARM difference heavily because they affect the phase of the main laser and therefore LO angle. In addition, Υ_{SR} phase and ψ_{SR} are pretty much the same, where they only affect at the band of ~60 - 1000 Hz.

The SQZ angle θ_{SQZ} determines the squeezing level. The SRCL detuning $\Delta\phi_{SR}$ also changes the squeezing level, but it only affects frequency above 100 Hz.

We can also categorize the parameters based on the bandwidth it affects:

- Broadband: SQZ_dB > P_{arm} > Υ_{OMC} + phase
- Above 100 Hz: Υ_{SQZ} ~ ϕ_{rms} ~ θ_{SQZ} ~ $\Delta\phi_{SR}$
- 100 - 1000 Hz: ψ_{SR} ~ Υ_{SR} + phase
- Negligible: $\Lambda_{INJ} > \Lambda_{SR} > \Upsilon_{SQZ}$ phase ~ Λ_{RO}

The three parameters affecting 100-1000 Hz have very similar impacts on the observable shape. Therefore, we can reduce them to one for simplicity, and we pick Υ_{SR} phase as the representative because it gives the largest dynamic range. We can downselect it along with the top two types as the most influential parameters and plot them.

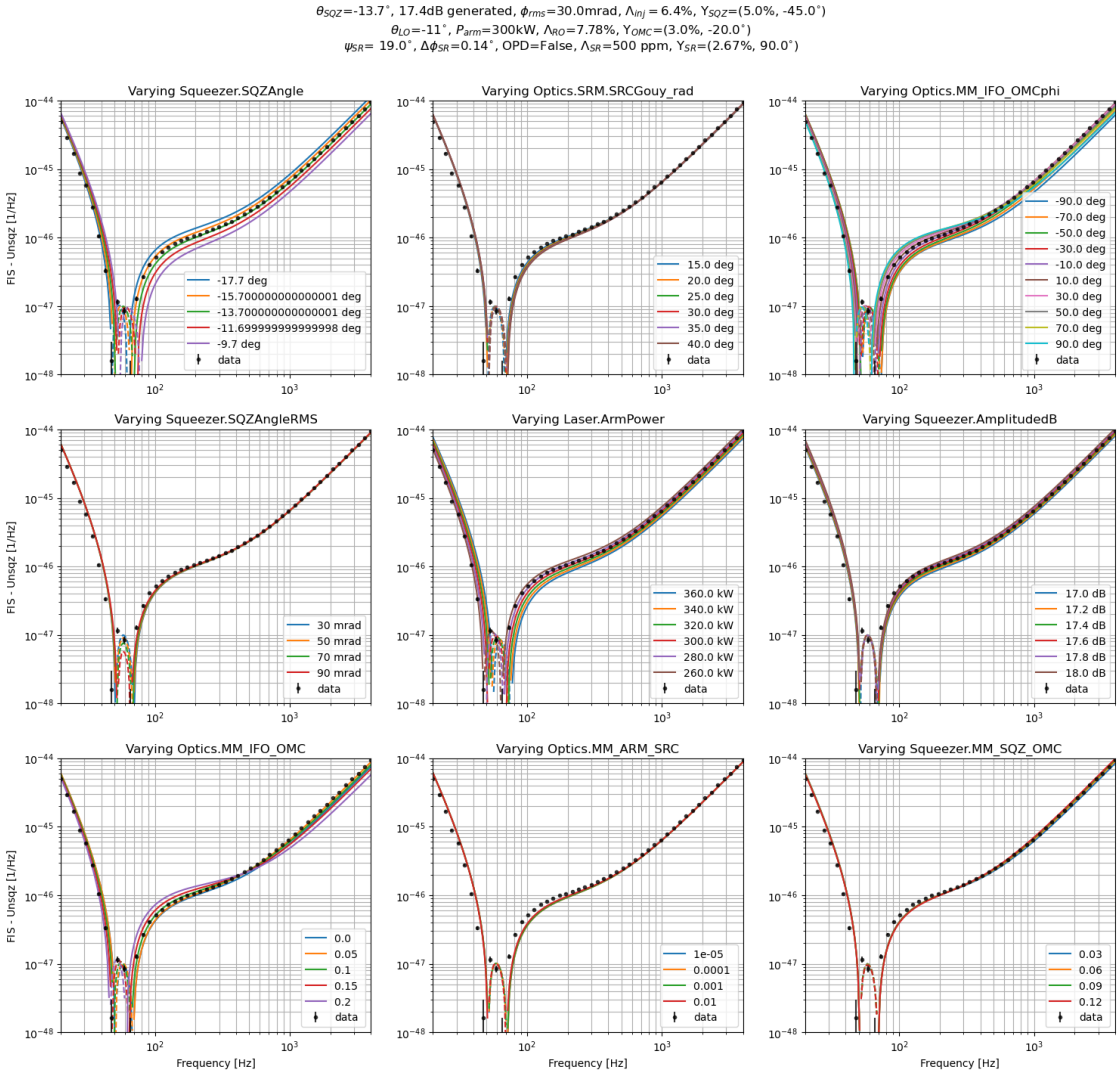

Only these 5 parameters are able to move the frequency of the dip, aka where the squeezed quadrature gets read out.

- θ_{SQZ}
- ψ_{SR} (or equivalently other SR phasing parameters)
- Υ_{OMC}
- Υ_{OMC} phase
- P_{arm}

There is no single parameter from them that can move the dip without messing with other things. Therefore, we need to tweak all of them to find a set that fits the data.

Another interesting case is the squeezing of QRPN at a higher frequency (at 100 Hz).

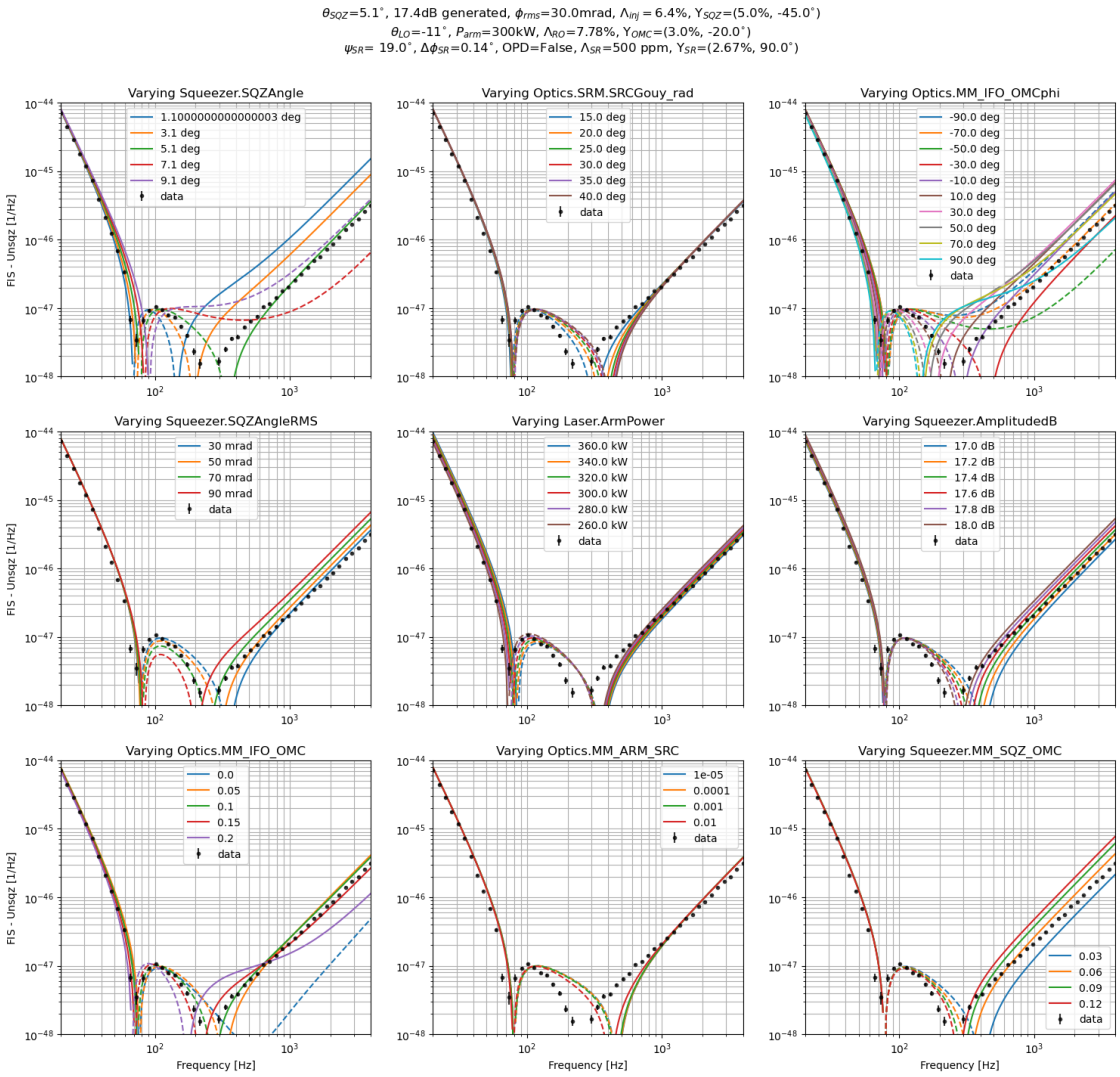

It can be seen that it is the same 5 parameters that can move the dip around 100 Hz.

Ranking of measurements based on "sensitivity" to various model parameters (or fitting priority): **-9.2°** > **-11.7°** > **5.2°** > **-14°** > **-18°** > **0°** > **-22°** > **-28°** > **-37°** > **9.7°** > **24°** > **78°** > **-58°**

4.6 MCMC on individual FIS

As discussed in previous section, we want to find a set of parameters that fits all of the FIS spectra. These parameters not only include those 15 (16 if including θ_{LO}) plotted before, but also the squeezing angle for each of the useful 13 measurements. These are almost 30 degrees of freedom, too much for MCMC.

We can start simple by fitting individual FIS separately. To reduce the number of parameters, we use the measured θ_{LO}, SQZ_dB, and inferred $\Delta\phi_{SR}$. These leave us with 7 parameters

affecting different frequency bands:

- Broadband: θ_{SQZ}, P_{arm}, Υ_{OMC} + phase
- Above 100 Hz: Υ_{SQZ}, ϕ_{rms}
- 100 - 1000 Hz: ψ_{SR}

Besides the DARM difference, we also fit the shot noise from NULL to make sure the DC level is correct. This requires another parameter

- Broadband: Λ_{RO}

So total 8 degrees of freedom for each individual FIS. Since each parameter is free to change for each FIS. they are "over-fitting" in some sense because some of them are common to each FIS measurements. For example, the readout loss Λ_{RO} is not expected to change in a single lock. Still, we are trying to see if it is even possible to fit these DARM PSD difference + NULL PSD.

4.6.1 MCMC set up

Flat prior isn't a good practice for Bayesian analysis, especially when we have certain knowledge about the parameters. Even the truth is outside a few sigmas of the standard deviation of the prior, it will still have enough likelihood to counter prior reduction and increase the posterior overall.

We choose a Gaussian likelihood despite that one of the uncertainties, the calibration uncertainty, is assymetrical. The reason is that the log likelihood of Gaussian is a closed form, whereas the skewed Gaussian is numerical and give -inf when we have a small log likelihood. This limits us of the space the walkers can explore. We average the positive and negative error bars for Gaussian likelihood.

On cluster or MATLAB computers, each gwinc run takes about $210*60/128/2000/2 = 0.025$ sec. To model one FIS case, we need to run it twice to model DARM difference. Therefore, running one MCMC with 256 walkers and 3000 steps takes $0.025*2*256*3000/3600 = 10.6$ hours

4.6.2 MCMC result on individual FIS

We first fit each **individual** DARM difference and NULL spectra measured at various FIS squeezing angle. This doesn't require the IFO parameters to be common, aka they are allowed to change for different FIS measurement. This assumption is not realistic because IFO parameters like arm power shouldn't change in a single thermalized lock, but it allows us to see if it's even possible to fit all FIS DARM difference. In this case, we also allow generated squeezing and SRCL detuning to change to "over-fit" all measurements.

Each parameter of the model is classified as:

- Fixed: the parameter is fixed for all individual FIS. They are summarized in the title of the plot below.
- Independent: MCMC will change independent parameters to optimize individual FIS.

The initial parameters are summarized in the table below:

TABLE I. MCMC on **individual** L1 05/14 data.

	PRX	MCMC			
			Set-up		Inferred
		Fixed/	Prior	Initial walker	Common/
		Chosen	Gaussian $(-\sigma, \sigma)$	Flat probability	Independent
Interferometer parameters					
Arm power	300 kW		(280, 320) kW	270-310 kW	Independent
SEC detuning (round-trip phase)	0.1°		(0.1, 0.2) °	0-0.2 °	Independent
Arm to SEC mismatch	N/A	2.7%			
Arm to SEC mismatch phase	N/A	0°			
SEC Gouy round-trip phase	N/A		(40, 50) °	30-70 °	Independent
Readout angle	-14°	-11°			
Total readout loss	6%		(6, 10) %	4-10 %	Independent
IFO to OMC mismatch	N/A		(6, 10) %	4-10 %	Independent
IFO to OMC mismatch phase	N/A		(-60, 20) °	-60-20 °	Independent
Squeezing parameters					
Generated squeezing	17 dB		(16.5-17.5)	(15.5, 17.5)	Independent
Squeezing angle	0°		$(\phi - 1, \phi + 1)°$	$(\phi - 2) - (\phi + 2)°$	Independent
Total Injection efficiency	91.8%	92.9%			
SQZ to OMC mismatch	N/A		(0.1, 8) %	0.1-10 %	Independent
SQZ to OMC mismatch phase	N/A	0°			
Phase noise (RMS)	$<$ 20 mrad		(20, 30) mrad	10-60 mrad	Independent

The prior probability is Gaussian with 16th-84th percentile shown in the Prior column for each parameter. The initial walkers are distributed with a flat probability in the range shown in the initial walker column. The fixed parameter is not touched by MCMC, and the parameter we used in O4 squeezing paper is also listed for comparison. The independent parameters inferred by MCMC for each individual FIS are plotted against the squeezing angles of each measurement.

The residual plots of each FIS DARM difference are shown below.

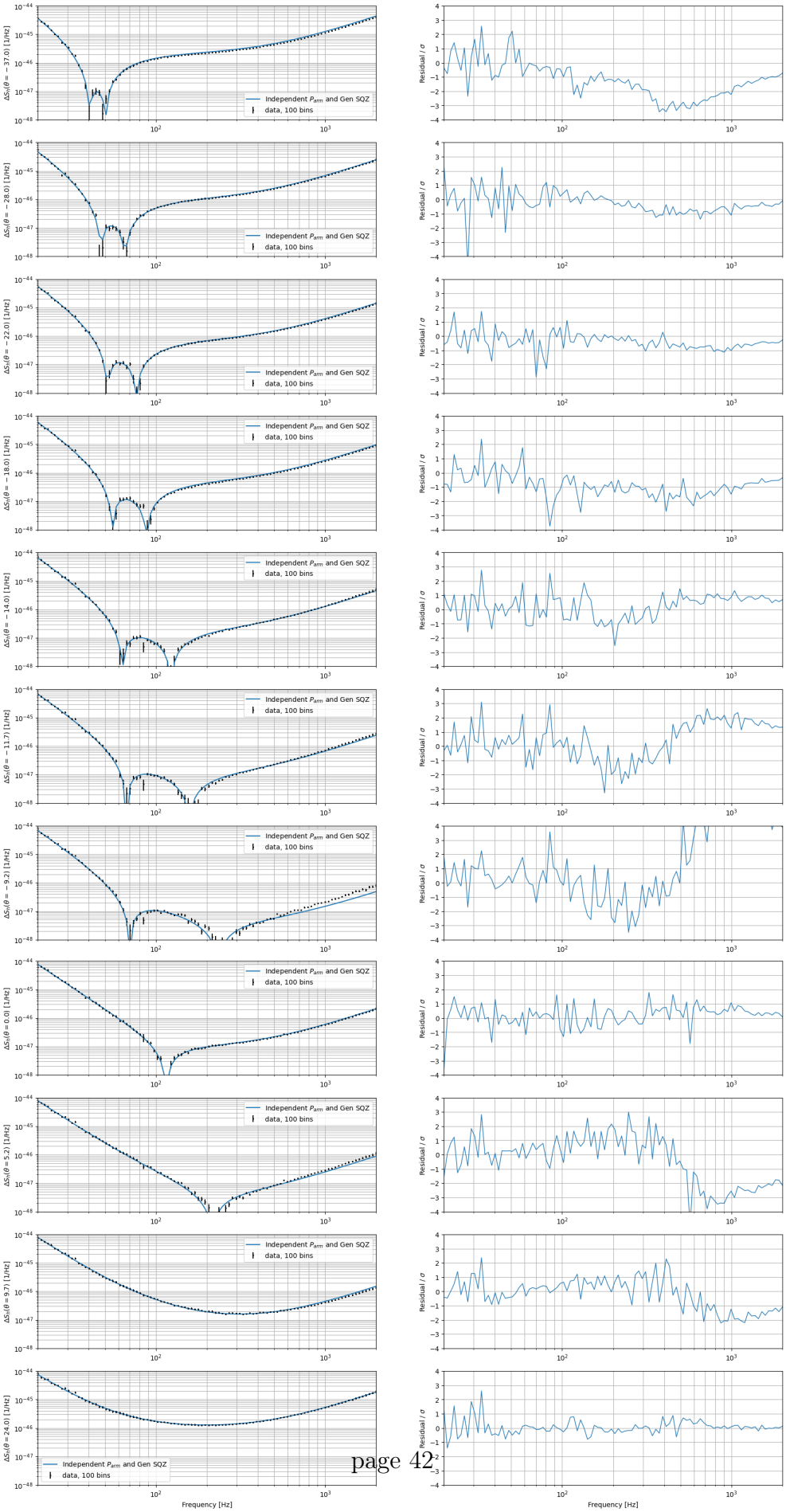
Independent P_{arm} and Gen SQZ
data, 100 bins
Residual / σ
Frequency [Hz]

The left plots show the measurement and model at different squeezing angles labeled in the yaxis. The right plots show the residual normalized by the 1-sigma error of the measured data at each frequency. The model fits all of the FIS measurements successfully.

The result of the MCMC parameters are plotted against the squeezing angle of each data below.

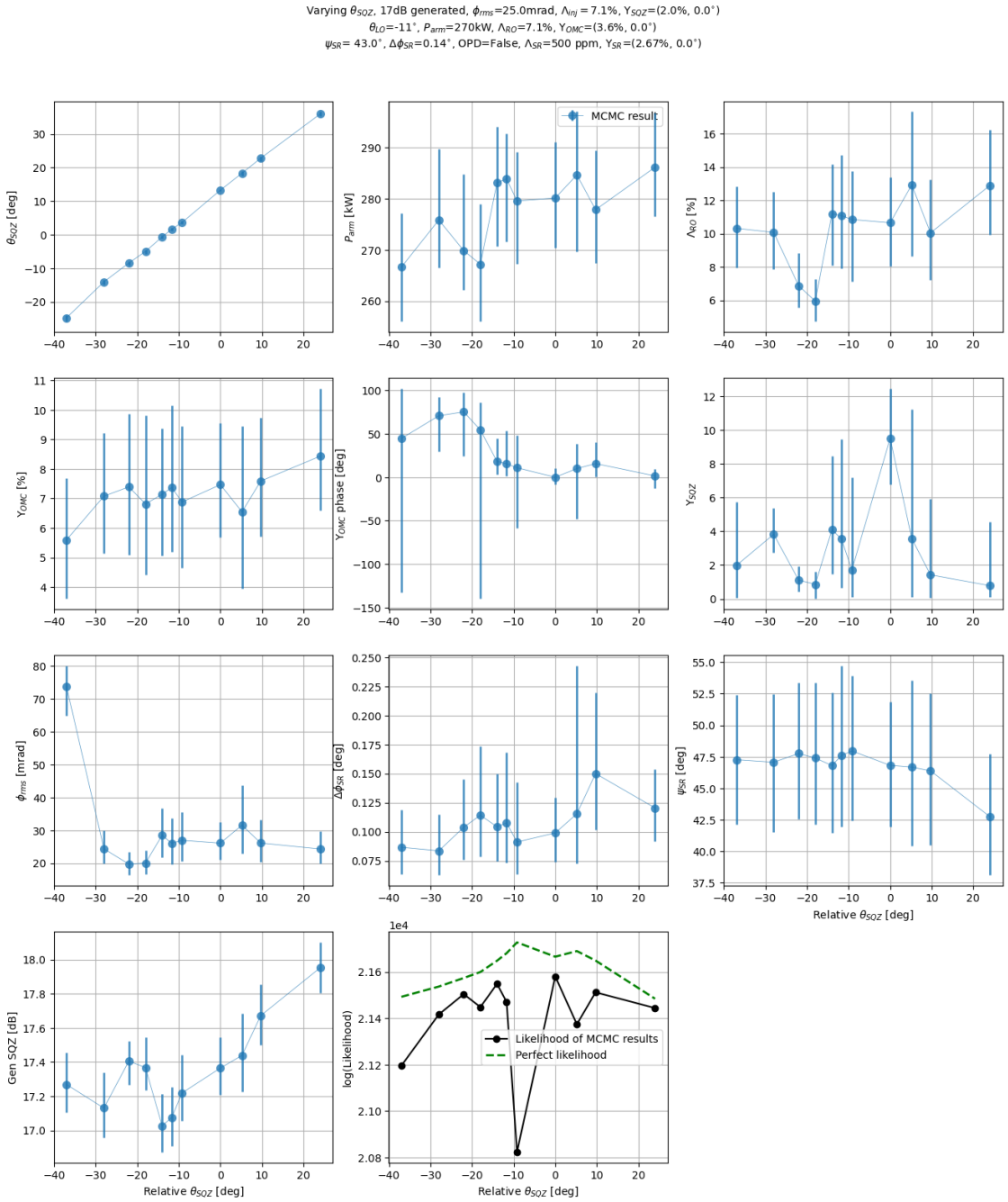

The inferred squeezing angle is shown to be linearly correlated with input squeezing angle, which makes sense because it is the parameter that we actively change to get various FIS data. There is a DC difference between two angles, namely $\theta_{SQZ} = 0$ (phase squeezing) corresponds to ~12 degree in gwinc model. This is due to the non-zero LO angle and other phasing degradations.

Other parameters shouldn't depend on the relative θ_{SQZ} because they are not actively changed. In this trial, we can see Λ_{RO} covaries with arm power P_{arm}. This is because these dual parameters are constrained by the NULL spectra. The readout loss follows arm power that is changed to fit DARM difference. As discussed previously, the arm power has an upper bound of 280-300 kW from studying the FIS DARM difference with max squeezing on high-f shot noise. We also see that the arm power is around 270-280 kW from MCMC inferrence.

The last subplot shows how good the MCMC result is at each squeezing angle. The green is perfect likelihood where the residuals are zero. The MCMC likelihood is pretty close to the theroretically maximum likelihood, proving that the MCMC fitting is reasonably good.

The IFO to OMC mismatch and SQZ to OMC mismatch vary slightly with squeezing angle. Their errorbars are very large because we probably have redundant parameters in this trial. Same conclusion for SRC detuning and Gouy phase. We need to fix some independent parameters to remove some redundancies.

Here we fix the arm power, SRC detuning, and generated squeezing to repeat the same analysis. The MCMC set-up, residual, and inferred parameters are shown below.

	PRX	MCMC			
			Set-up		Inferred
		Fixed/	Prior	Initial walker	Common/
		Chosen	Gaussian $(-\sigma, \sigma)$	Flat probability	Independent
Interferometer parameters					
Arm power	300 kW	270 kW			
Arm to SEC mismatch	N/A	2.7%			
SEC detuning (round-trip phase)	0.1°	0.14°			
SEC Gouy phase	N/A		(20, 50) °	10-80 °	Independent
Readout angle	-14°	-11°			
Readout efficiency					
Optical throughput (SEC to OMC)	97.5%				
OMC transmission	98%				
Photodiode quantum efficiency	98 %				
Total readout loss	6%		(8, 10) %	1-15 %	Independent
IFO to OMC mismatch	N/A		(4, 12) %	1-15 %	Independent
IFO to OMC mismatch phase	N/A		(-40, -10) °	-60-20 °	Independent
Squeezing parameters					
Generated squeezing	17 dB	17.4 dB			
Measured squeezing	-5.8 dB				
Measured anti-squeezing	15.8 dB				
OPO throughput	98.7%				
Squeezing angle	0°		$(\phi - 1, \phi + 1)°$	$(\phi - 2) - (\phi + 2)°$	Independent
Total Injection efficiency	91.8%	93.6%			
SQZ to OMC mismatch	N/A		(1, 8) %	1-12 %	Independent
Phase noise (RMS)	$<$ 20 mrad		(20, 30) mrad	10-70 mrad	Independent
Total expected throughput	86%				
Inferred throughput	$>$ 77%				

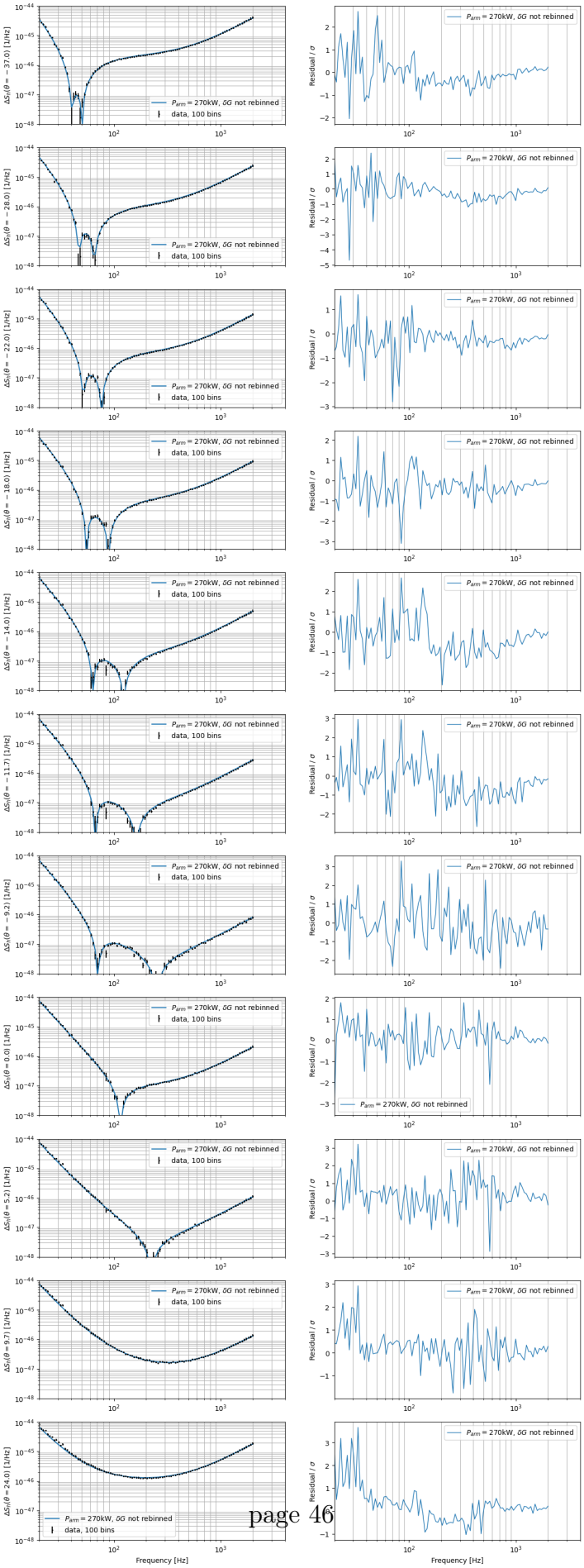
P_{arm} = 270kW, δG not rebinned
data, 100 bins
Residual / σ
Frequency [Hz]

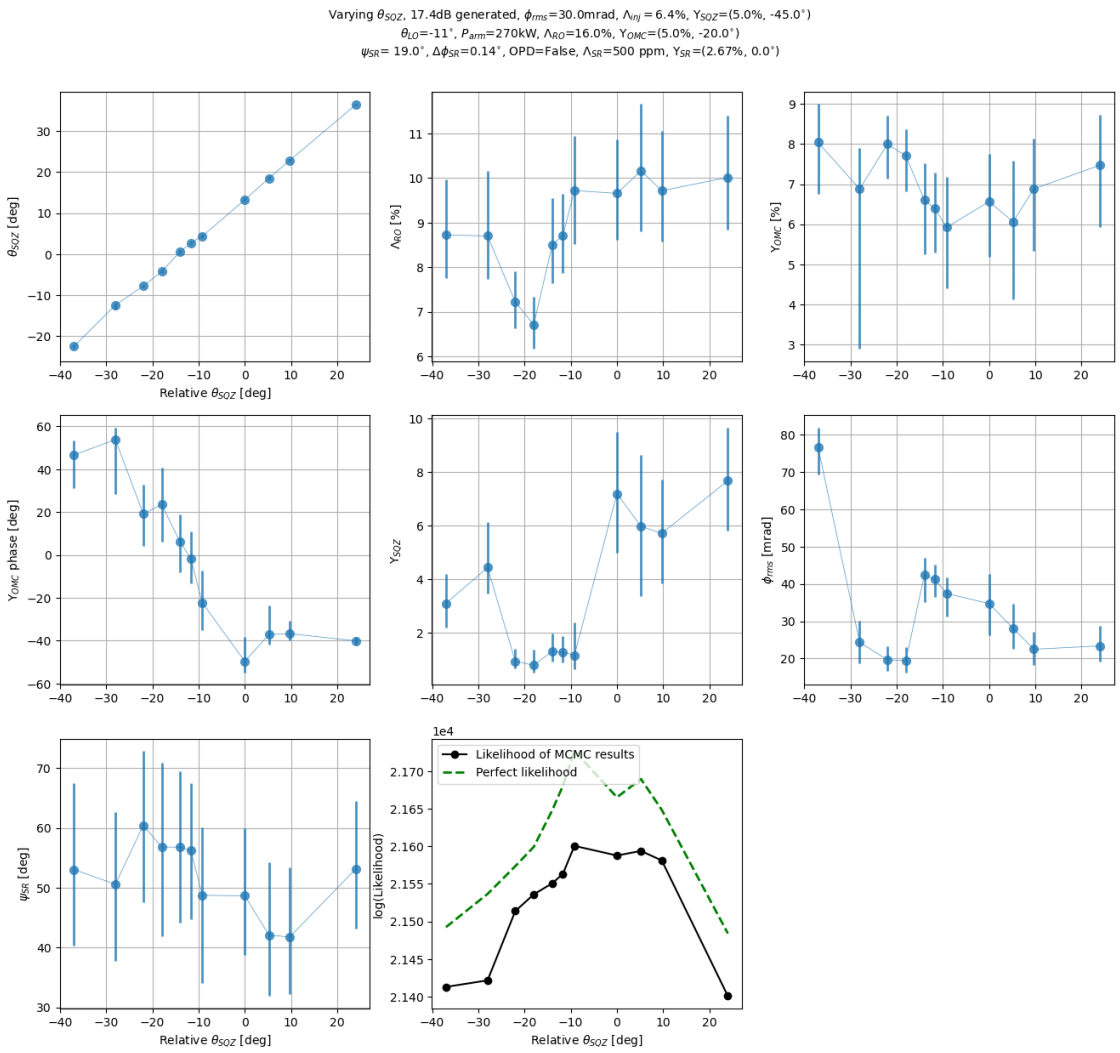

The readout loss has less dependencies with squeezing angle after we fix the arm power. The IFO parameters like Υ_{OMC} and ψ_{SR} vary a little bit to the squeezing angle, which is promising to us after we set them to be common parameters.

The parameters that change with squeezing angles are Υ_{OMC} phase, Υ_{SQZ}, and ϕ_{rms}. Phase noise is known to change with different squeezing angle (different locking point changes the control loop). The Υ_{OMC} phase is changed probably because it tries to mimic the change of the phase of squeezed vacuum due to X/Y arm cavity mode-mismatch or differential loss, which leads to the non-zero LO angle and is not modeled in the current version of gwinc (superQK branch). The Υ_{SQZ} is also drifting because SQZ ASC was not engaged during the data taking. Keep in mind that we are actually "over-fitting" the individual FIS in some sense, since we allow parameters that shouldn't change over time to be a variable that fits

the individual DARM difference. Our goal is to find a set of common parameters that fit all of the FIS simultaneously. This would be the physical case close to the reality.

More trials of the MCMC on individual FIS with various settings are collected in the Appendix D.

4.7 MCMC on all FIS simultaneously

4.7.1 MCMC setup

Knowing that it's possible to fit individual FIS, we now try to fit all of the FIS simutaneously. The initialized parameters are categorized as:

- Fixed: parameter is fixed and used for all FIS. E.g. LO angle
- Chosen: paramter is fixed but different for each measurement. E.g. squeezing angle
- Common: parameter is not fixed but a degree of freedom for MCMC. The common parameter is common to all FIS measurement. E.g. arm power
- Independent: parameter is not fixed but a degree of freedom for MCMC. The common parameter is common to all FIS measurement. E.g. IFO to OMC mismatch phase

	PRX		MCMC		
			Set-up		Inferred
		Fixed/	Prior	Initial walker	Common/
		Chosen	Gaussian $(-\sigma, \sigma)$	Flat probability	Independent
Interferometer parameters					
Arm power	300 kW		(270, 320) kW	270-310 kW	$257^{+3.9}_{-1.6}$ kW
Arm to SEC mismatch	N/A	2.7%			
Arm to SEC mismatch phase	N/A	0°			
SEC detuning (round-trip phase)	0.1°	0.14°			
SEC Gouy phase	N/A		(20, 50) °	20-70 °	$43.0^{+4.5}_{-5.2}$ °
Readout angle	-14°	-11°			
Readout efficiency					
Optical throughput (SEC to OMC)	97.5%				
OMC transmission	98%				
Photodiode quantum efficiency	98 %				
Total readout loss	6%		(8, 10) %	6-10 %	$92.0^{+0.5}_{-1.2}$ %
IFO to OMC mismatch	N/A		(6, 8) %	4-10 %	$3.6^{+0.5}_{-0.5}$ %
IFO to OMC mismatch phase	N/A				Independent
Squeezing parameters					
Generated squeezing	17 dB	17.4 dB			
Measured squeezing	-5.8 dB				
Measured anti-squeezing	15.8 dB				
OPO throughput	98.7%				
Squeezing angle	0°	Chosen			
Total Injection efficiency	91.8%	93.6%			
SQZ to OMC mismatch	N/A		(1, 8) %	1-8 %	$1.1^{+1.3}_{-0.2}$ %
SQZ to OMC mismatch phase	N/A	-45°			
Phase noise (RMS)	< 20 mrad	Chosen			
Total expected throughput	86%				
Inferred throughput	> 77%				

We can only allow one kind of independent parameters because of time constraint. To fit all ~10 FIS curves simultaenously, we have ~10 more parameters for MCMC for each of the squeezing angle. The model also has to extend to all FIS curves, so we need to calculate 1 unsqz and ~10 FIS. The time to run it with 10000 steps per walker is $0.025 * 17 * 10000 * 34/3600 = 40$ hours. If we have 2 independent parameters, the iteration time is doubled and becomes too long.

4.7.2 MCMC result

Result of MCMC using common Υ_{SR} and phase instead of SRC Gouy phase. The squeezing angle is fixed from individual MCMC FIS results.

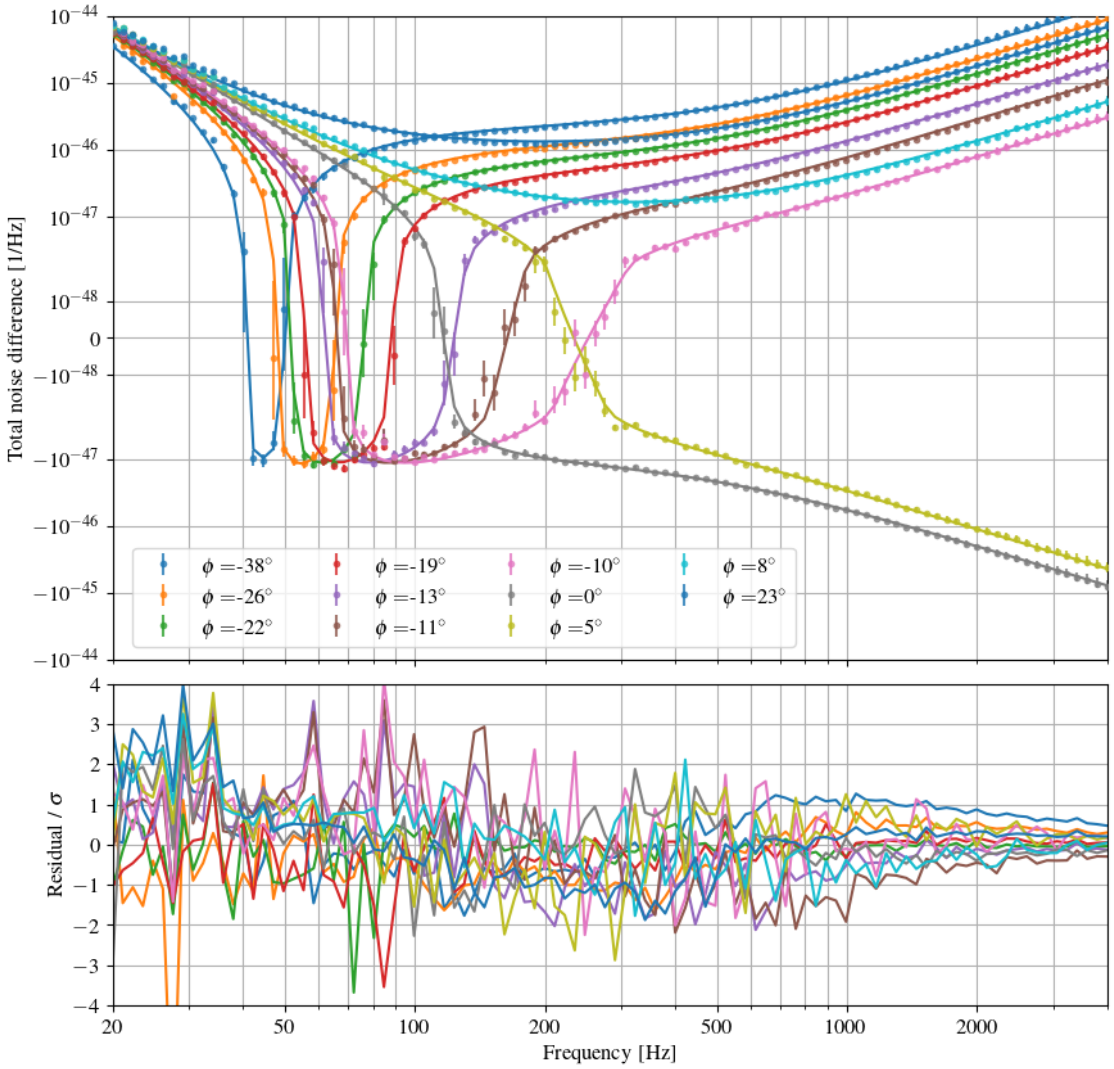

This is our best model that is able to minimize residuals for all FIS. The inferred results are also summarized in the table above. Notably, the arm power is inferred to be around 260 kW instead of 300 kW calculated from PRG. Since we don't have other data that directly measures arm power yet, we will use 260 kW.

The residuals of the NULL spectra that are fit simultaneously are shown below

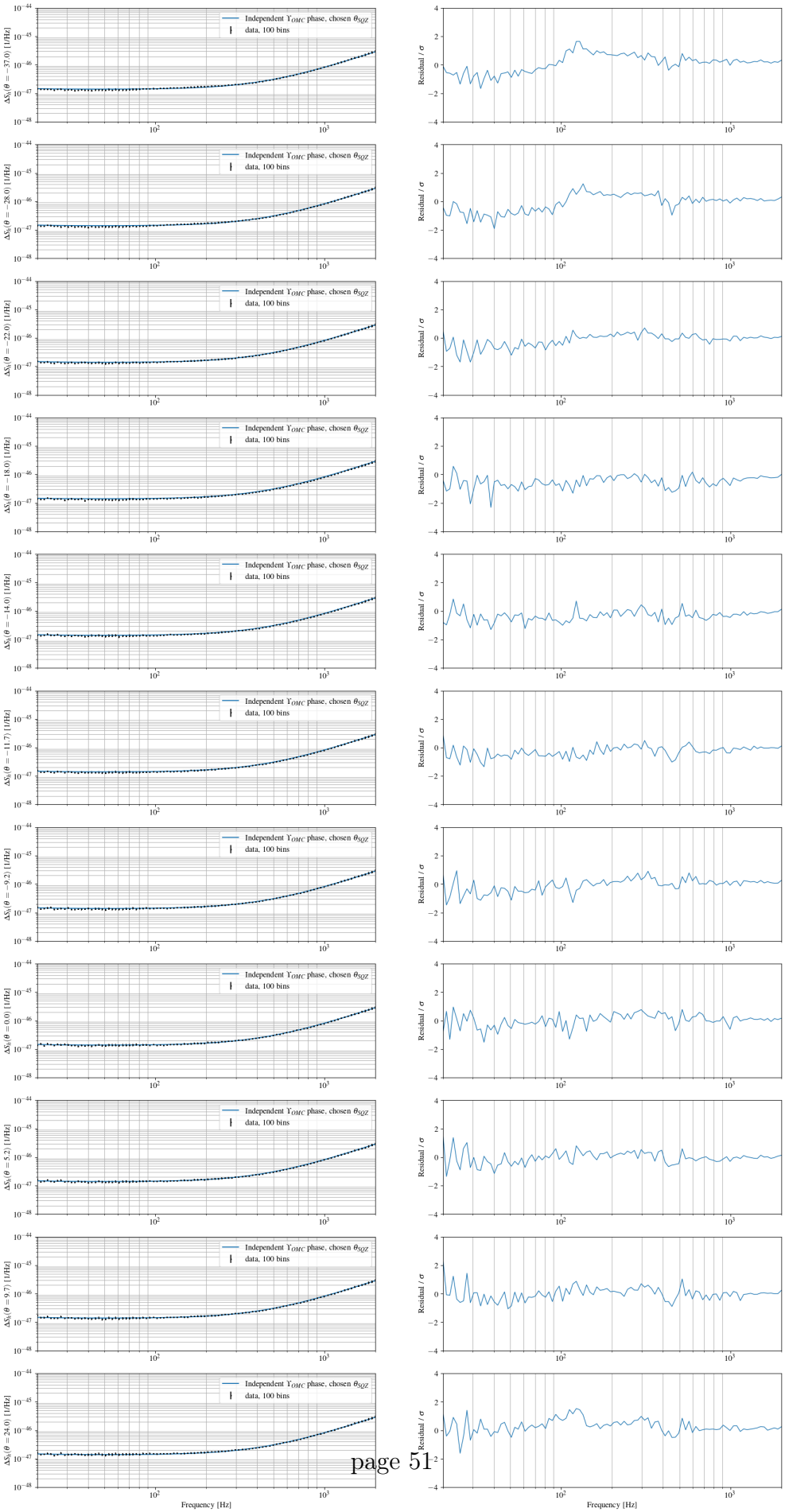
Independent Y_{OMC} phase, chosen θ_{SQZ}
data, 100 bins
$\Delta S_h(\theta = -37.0)$ [1/Hz]
$\Delta S_h(\theta = -28.0)$ [1/Hz]
$\Delta S_h(\theta = -22.0)$ [1/Hz]
$\Delta S_h(\theta = -18.0)$ [1/Hz]
$\Delta S_h(\theta = -14.0)$ [1/Hz]
$\Delta S_h(\theta = -11.7)$ [1/Hz]
$\Delta S_h(\theta = -9.2)$ [1/Hz]
$\Delta S_h(\theta = 0.0)$ [1/Hz]
$\Delta S_h(\theta = 5.2)$ [1/Hz]
$\Delta S_h(\theta = 9.7)$ [1/Hz]
$\Delta S_h(\theta = 24.0)$ [1/Hz]
Residual / σ
Frequency [Hz]

The parameters inferred by MCMC are mostly reasonable, except for arm power and SQZ to OMC mismatch Υ_{SQZ}. The model suggests that the arm power is around 260 kW, compared to ~300 kW calculated from PRG. We tried to tighten prior probability on arm power to penalize if arm power is too low or too high (decreasing the 1-sigma of prior), but the MCMC still moves arm power to low 270 kW regardless of the prior because the likelihood is still higher at low power to compensate lower prior (posterior is maximal at the end). We couldn't find a parameter set with 300 kW that is as optimal (low residual) as what we have now. As for the SQZ to OMC mismatch, it is the product of SQZ to IFO and IFO to OMC mismatch chain. A small SQZ to OMC mismatch doesn't mean the SQZ to IFO is well mode-matched. In fact, we can have zero SQZ to OMC Υ_{SQZ} mismatch with nonzero SQZ to IFO mismatch.

5 Analysis of Frequency-Dependent Squeezing

Frequency-dependent squeezing (FDS) can be observed when we have a filter cavity (FC).

These parameters that affect FIS are ranked by impact:

- FC1 Transmission T_{FC1} (from Vendor's report)
- FC detuning ω_{FC}
- FC loss Λ_{FC} (inferred from LLO62683)
- FC mismatch + phase Υ_{FC}
- FC Gouy phase ψ_{FC}
- FC length RMS noise L_{FCRMS}

Since we are only fitting FC and SQZ parameters, we are not touching any IFO parameters so the unsqueezed quantum noise model is not changing. Therefore, we can fit the FDS quantum noise directly in our familiar ASD unit without taking DARM difference. Specifically, we subtract the measured unsqueezed DARM with unsqueezed quantum noise model to get classical noise, which doesn't vary when we are fitting with FC parameters. Then we subtract classical noise from measured FDS DARM to get measured FDS quantum noise, which we can directly fit with FDS quantum noise model.

5.1 Getting all FDS spectra

These FDS spectra were taken with FC nominally locked and FC ASC engaged. The SQZ ASC was not necessarily engaged. The FIS parameters we inferred should also hold for FDS case.

We took 13 measurements at three different days (we have more during observing mode)

- 0514_0, 21, 22
- 0515_01, 02, 03, 04, 3
- 0523_1, 10, 11, 12, 13

Notice that we changed FC detuning from 107 Hz to 113 Hz on 05/17. The FDS data taken on 05/23 is

- 0523_5, FDS at angle 1
- 0523_6, FDS at angle 2
- 0523_7, FDS at angle 3

5.2 Cross-check NULL

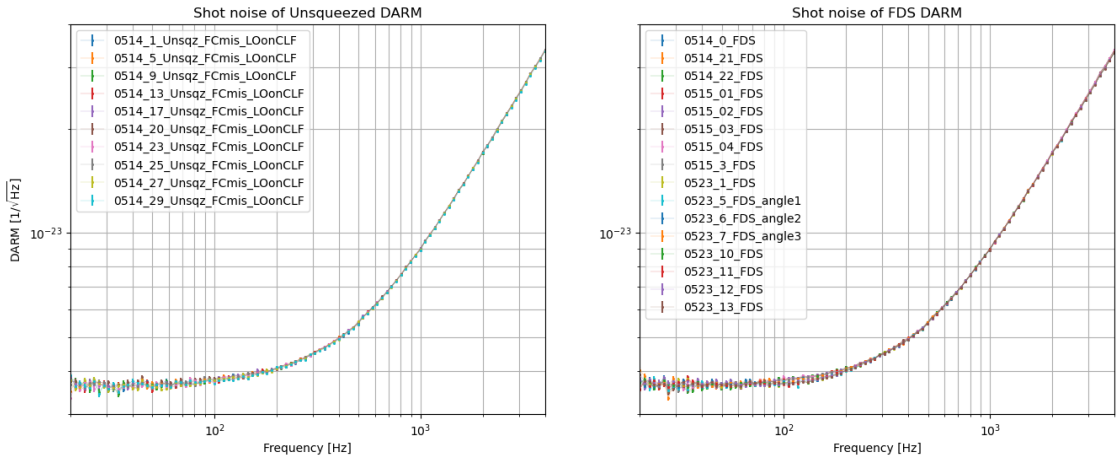

Both NULL from unsqueezed and FDS DARM are equivalent, which is good.

5.3 Preliminary fitting

As mentioned above, the inferred frequency-dependent squeezed quantum noise Q is

$$Q = D_s - (D_r - M)$$

The total error of Q is

$$\Delta Q^2 = Q^2 \delta G_{cal}^2 + \left[\Delta D_s^2 + \Delta D_r^2 + \Delta M_r^2 + C^2(\delta N_t^2 + \delta N_m^2)\right]$$

or in relative error

$$\delta Q^2 = \delta G_{cal}^2 + \frac{1}{Q^2}\left[\Delta D_s^2 + \Delta D_r^2 + \Delta M_r^2 + C^2(\delta N_t^2 + \delta N_m^2)\right]$$

or in ASD

$$\delta q = \frac{1}{2}\delta Q = \sqrt{\frac{\delta G_{cal}^2}{4} + \frac{1}{4Q^2}\left[\Delta D_s^2 + \Delta D_r^2 + \Delta M_r^2 + C^2(\delta N_t^2 + \delta N_m^2)\right]}$$

where

- δG_{cal} is the quoted combined calibration error and uncertainty estimate ($|R^{(\mathrm{sample})}/R^{(\mathrm{MAP})}| - 1$).

- ΔD is the statistical uncertainty due to PSD estimation of measured DARM ($D/\sqrt{\Delta T \Delta f}$).
- ΔM_r is the uncertainty in inferred gwinc model on unsqueezed quantum noise.
- δN is the non-stationary changes in the classical noise contributions, where δN_t is time-stationarity and δN_m is the operating mode stationarity between unsqueezed and squeezed interferometer.

We can manually find a set of preliminary parameters that is not too far away from the truth.

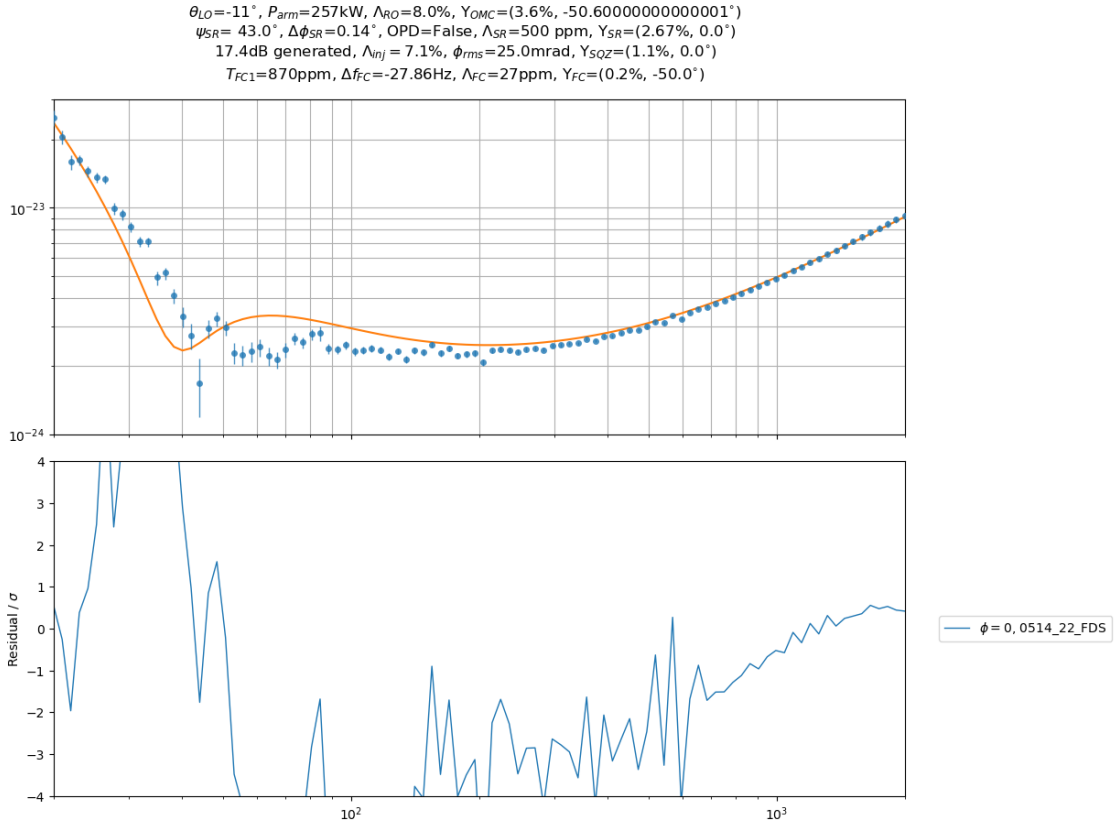

5.4 Parametric study

We perturb parameters around the canonical setting and see how each one affects the DARM differences. We will do the max squeezing of shot noise first.

θ_{LO}=-11°, P_{arm}=257kW, Λ_{RO}=8.0%, Y_{OMC}=(3.6%, -50.60000000000001°)
ψ_{SR}= 43.0°, $\Delta\phi_{SR}$=0.14°, OPD=False, Λ_{SR}=500 ppm, Y_{SR}=(2.67%, 0.0°)
17.4dB generated, Λ_{inj}=6.4%, ϕ_{rms}=34.727000000000004mrad, Y_{SQZ}=(1.1%, 0.0°)
T_{FC1}=919ppm, Δf_{FC}=-26Hz, Λ_{FC}=36ppm, Y_{FC}=(1.0%, -8.4°)

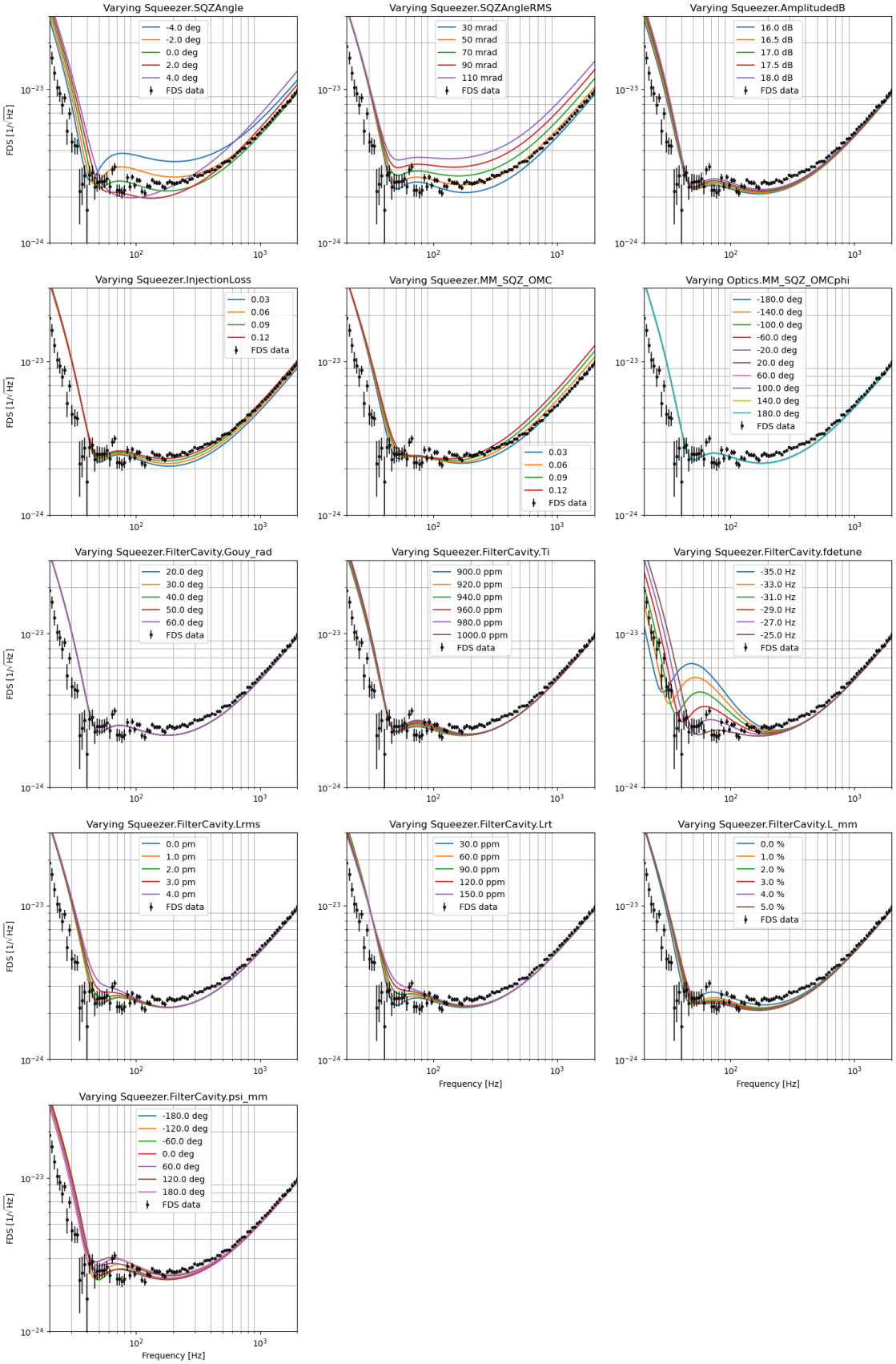

These parameters above are only affecting the squeezing system, and not IFO. We only want to change these to not affect the inferred FDS data.

The phase noise, generated squeezing, and injection loss act similarly on the FDS DARM. It's a broadband effect. The SQZ to OMC mismatch also affects the spectrum at all frequencies, but the combination of mismatch would produce frequency-dependent losses.

Filter cavity parameters such as the input coupler transmission, detuning, residual length fluctuation, round-trip loss, mode-mismatch and mismatch phase only affect spectrum inside the filter cavity full linewidth. The input transmission and frequency detuning changes pair has similar effects. This degeneracy also exists for parameter pairs of FC RTL, residual motion, and SQZ to FC mismatch and mismatch phase. It's difficult to attribute unique frequency-dependent degradations to specific parameters. So we still use MCMC to find the best inferrence.

The two parameters that affect the spectrum negligibly are SQZ to OMC mismatch phase and FC Gouy phase. The reason is that the amount of scattered squeezed fields are too small, and the scattered back squeezed fields are even less so their actual phase doesn't matter. The scattered back fields scales with the product of all mismatches along the path. Even 10% mismatches along the path would contribute to 1%. The FC Gouy phase shouldn't change because there are no thermal effects in the filter cavity (only RLF sideband and low-frequency squeezed vacuum are circulating within the cavity).

5.5 MCMC result

We first attempt to fit the FDS quantum noise with $T_{FC1} = 919$ ppm from vendor's report.

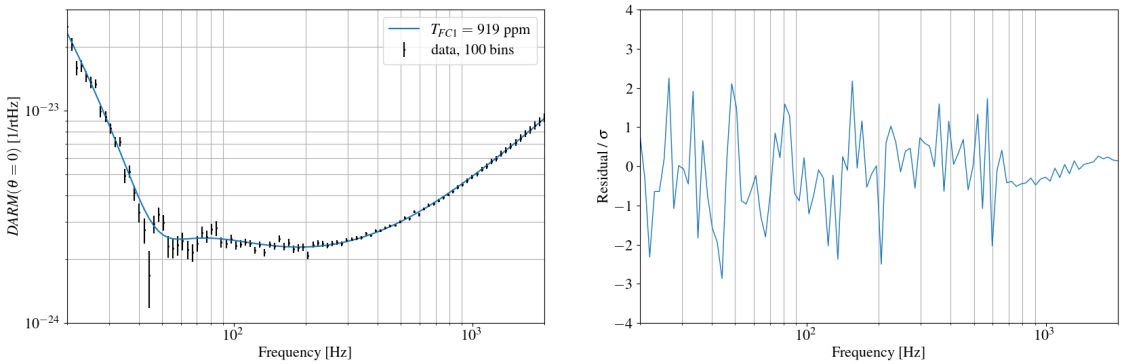


```
'Squeezer.SQZAngle': 9.745779,
'Squeezer.MM_SQZ_OMC': 1.9042481,
'Squeezer.FilterCavity.fdetune': -28.193434,
```

```
'Squeezer.FilterCavity.Lrt': 13.317217,
'Squeezer.FilterCavity.L_mm': 14.08929,
'Squeezer.FilterCavity.psi_mm': -25.345737,
'Squeezer.FilterCavity.Lrms': 0.18205652
```

The inferred parameters are printed above with sensible units (phases are in degree, mismatch in percent, FC loss in ppm, and FC residual RMS length in pm). The MCMC fit and residual plot look good, but we have one inferred parameters that deviate away from what we measured otherwise. The SQZ to FC mismatch inferred is 14%, compared to 0.2% we measured from LLO63093. The reason for a large mismatch implies that the model prefers less amount of squeezed vacuum to experience the frequency-dependent phase shift imparted by filter cavity. The finesse of FC from inferred parameter is around 6700, which is not high enough to give the cavity linewidth that matches with the SQL frequency (37 Hz coresponding to 260 kW). Besides, the round-trip loss of 13 ppm is also doubtful.

We then attempted another MCMC inferrence that fix the FC finesse instead of input coupler transmission. We used three different methods to measure FC finesse LLO62683 with the results of 5700 - 7000. Therefore, we fix the FC finesse to 7000 and do another MCMC inferrence.

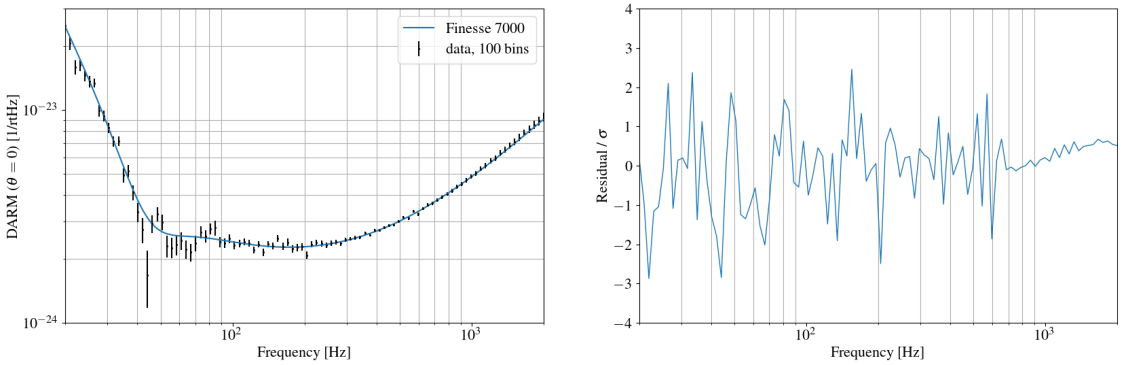


```
'Squeezer.SQZAngle': 10.220849,
'Squeezer.FilterCavity.fdetune': -25.582218,
'Squeezer.FilterCavity.psi_mm': -65.48146,
'Squeezer.FilterCavity.Lrms': 0.1729011,
'Squeezer.FilterCavity.Ti': 797.02527
```

The MCMC fitting result with FC finesse of 7000 is also good. The inferred input transmission is 800 ppm, which is 11% smaller than what's measured by vendor's report. The FC loss calculated from finesse and input transmission is 100 ppm, which is larger than what we would expect. In the end, we could only measure finesse in-situ instead of transmission or FC loss. In addition, the inferred SQZ to FC mismatch is 0.17%, which is equal to our mode-scan measurement of 0.2%. Therefore, we will choose and use this MCMC result.

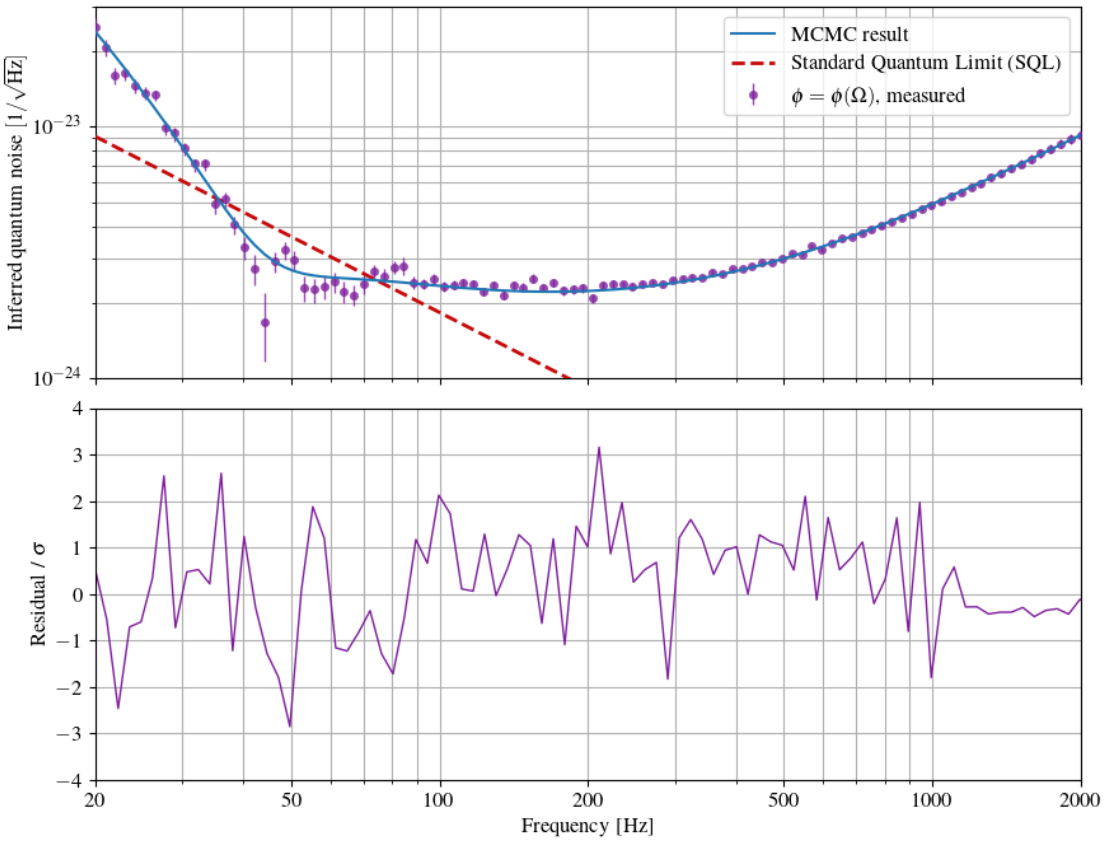

The total uncertainty of the FDS data is shown below. The error sources have been explained in the previous sections. The FDS quantum noise is seen below standard quantum limit by up to 3 dB at 50 Hz, while maintaining squeezing at high-frequencies. This marks LIGO as a quantum nondemolition gravitational-wave detector (KLMTV).

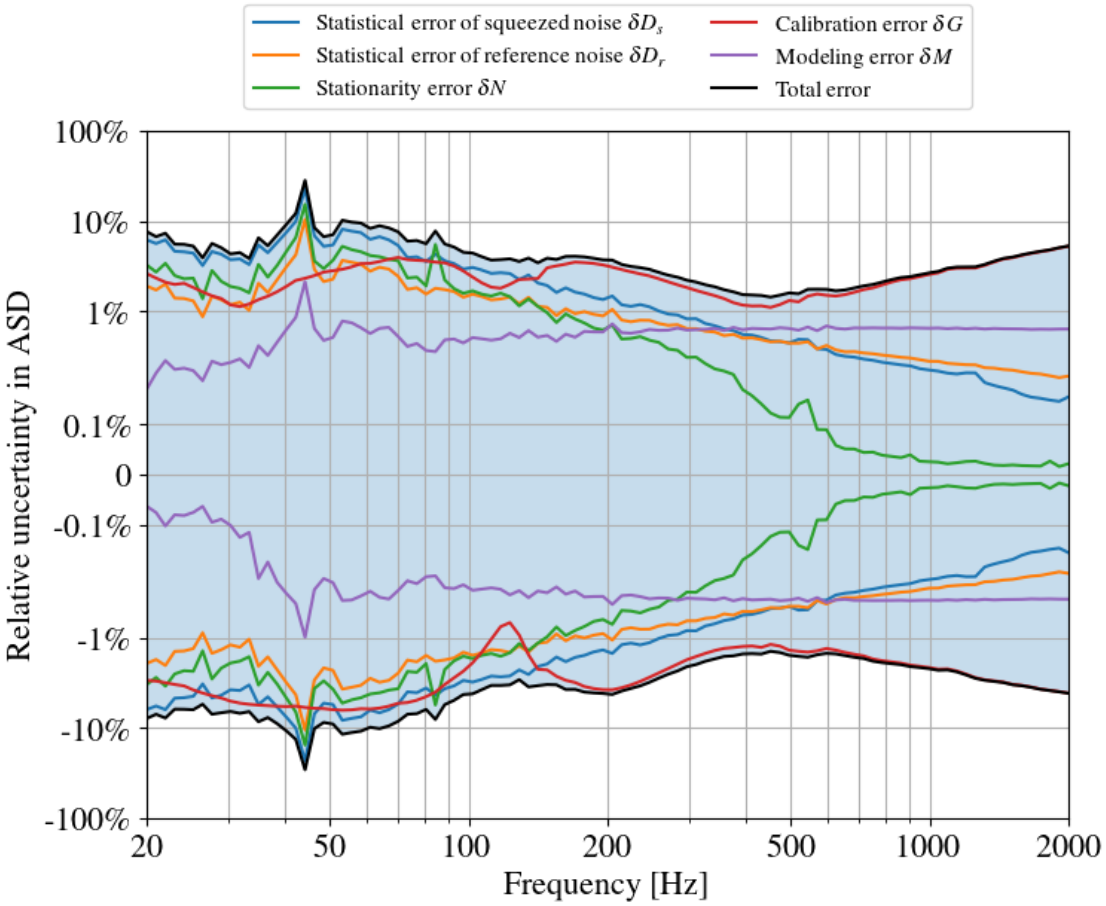
Statistical error of squeezed noise δD_s
Statistical error of reference noise δD_r
Stationarity error δN
Calibration error δG
Modeling error δM
Total error
100%
10%
1%
0.1%
0
-0.1%
-1%
-10%
-100%
Relative uncertainty in ASD
20
50
100
200
500
1000
2000
Frequency [Hz]

6 Conclusion

In this report, we successfully find a set of parameters that are able to fit all measured frequency-independent squeezing DARM measurement at various squeezing angles, and frequency-dependent squeezing that is nominal to LIGO Livingston O4 operation. It is the best estimation of the quantum noise. The full parameters at nominal configuration are presented in the table below:

L1 parameters	
Arm power	$257^{+3.9}_{-1.6}$ kW
Arm to SEC mismatch	2.7%
Arm to SEC mismatch phase	0°
SEC detuning (round-trip phase)	0.14°
SEC Gouy phase	$43.0^{+4.5}_{-5.2}$ °
Readout angle	-11°
Total readout loss	$8.0^{+1.2}_{-0.5}$ %
IFO to OMC mismatch	$3.6^{+0.5}_{-0.5}$ %
IFO to OMC mismatch phase	-51 °
Squeezing parameters	
Generated squeezing	17.4 dB
Squeezing angle	10.5 °
Injection loss	7.1%
SQZ to OMC mismatch	$1.1^{+1.3}_{-0.2}$ %
SQZ to OMC mismatch phase	-45°
Phase noise (RMS)	27 mrad
Filter cavity parameters	
Length	300 m
Detuning	−25.6 Hz
Finesse	7000
Full-linewidth	71 Hz
Input coupler transmission	797 ppm
Derived round-trip loss	100 ppm
Squeezer to FC mismatch	0.2%
Squeezer to FC mismatch phase	−65°
Length noise (RMS)	0.2 pm

The parameters are also saved in the .yaml file attached with this report.

Appendix A: DARM PSD estimation

We discuss some technical details on how to properly estimate power spectral density (PSD) of DARM. Various methods are used and compared to find the best estimation methods.

A.1 Mean vs. Median

Welch's method estimates the power spectral density by collecting statistics from each data segment δt. The default statistics is the mean. However, median is better in terms of being less affected by glitches that inject lots of spectral energies in the data segment that contains it. Here we compare mean vs. median in a clean data stream and one with known glitches.

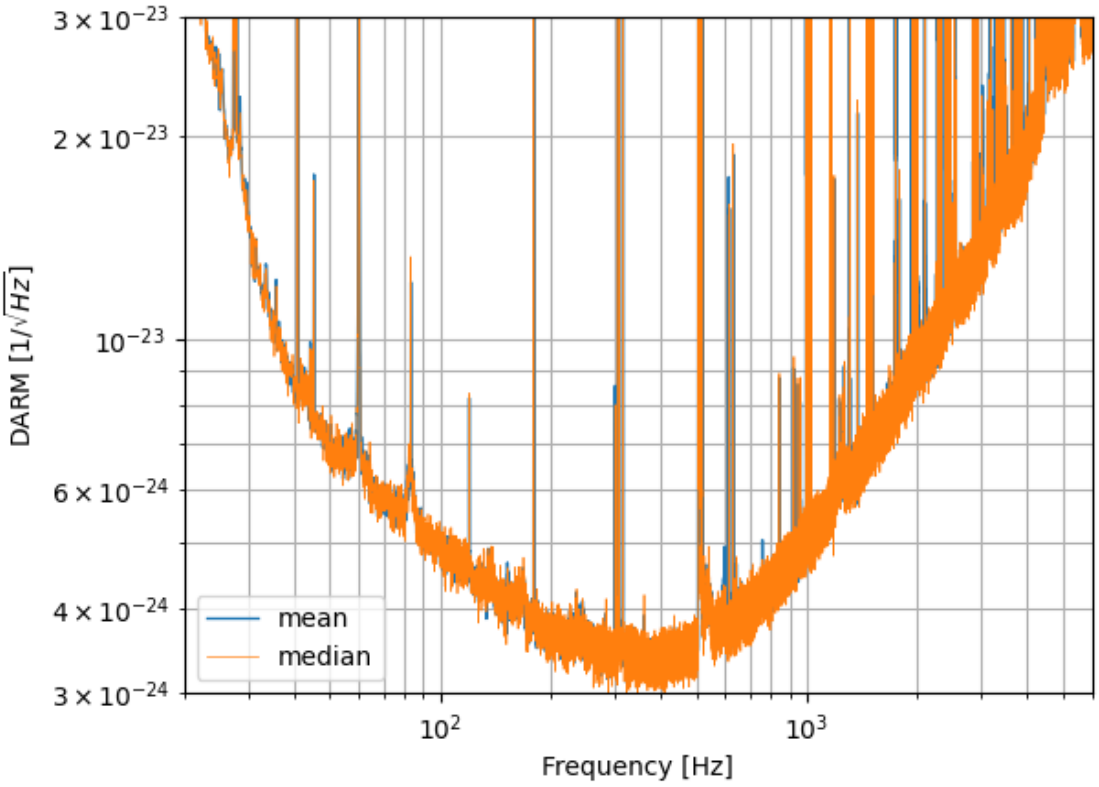

The two spectra are nearly identical to each other, no log(2) factor that is probably taken care of in scipy.welch.

Now we compare both statistics that is used on a time-series known to have glitches.

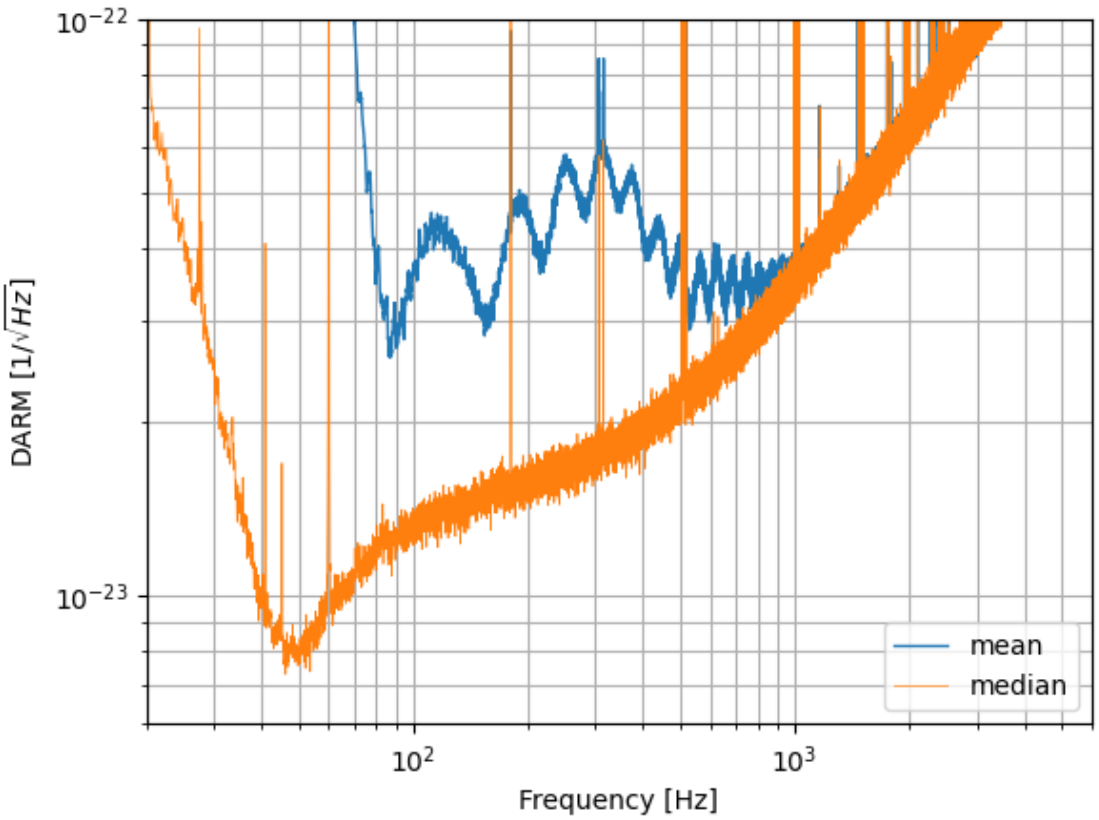

As seen in the plot, the mean statistics is heavily affected by the glitch whereas median is less affected and captures the sub-SQL dip at 50 Hz.

A.2 Statistical Uncertainty

There are a few ways to estimate the error of PSD calculation. Craig Cahillane's thesis talks about the uncertainty of PSD in its Appendix D.

$$\sigma^2 = \frac{\lambda^2}{N} \qquad \text{(D.12)}$$

Eq. (D.12) says the variance is the square of average divided by the number of sample. (PRD 104, 062006) also talks about how to get uncertainty in the caption of Figure.2

$$\sigma \propto \frac{1}{\sqrt{\Delta T \Delta f}}$$

where the total time ΔT consists of N individual segments Δt (up to the overlapping ratio)

$$\Delta T \propto N \Delta t$$

and the frequency resolution bandwidth depends on the duration of each segment (window size)

$$\Delta f = \frac{f_s}{n} = \frac{f_s}{\Delta t/(1/f_s)} = \frac{1}{\Delta t}$$

where n is the number of sampled data points in each segment. Therefore, the final results agree with each other

$$\sigma \propto \frac{1}{\sqrt{N}}$$

This actually makes sense because calculating PSD involves with measuring each segment's DFT one-by-one, which is similar to a Poisson process of measuring the photon power one-by-one. More measurements (longer data so more segments) gives better estimation with lowered uncertainty. For example, a 25-min data with window size $2^3 * f_s$ gives $N = 25*60/2^3 = 187$. Making the overlapping to 50% doubles $N = 375$, and the relative uncertainty of the PSD $1/\sqrt{N} = 5$, reasonable. We'll need to fine tune the window size and fractional overlap to get the best uncertainty.

The ASD is sometimes what we want, which has relative error

$$\sqrt{1 + \frac{1}{\sqrt{N}}} - 1 \approx \frac{1}{2\sqrt{N}}$$

A.3 Subtraction

Given the total squeezed darm PSD S and inferred classical noise PSD C, one can infer the quantum noise by subtracting these PSD. You can choose either PSD or ASD as the random variable, because their error propagations are the same. If we choose the PSD as random variable, we have

$$Q(\Omega) = S(\Omega) - C(\Omega)$$

where Q is the subtracted quantum noise. The error of Q is

$$\Delta Q^2 = \Delta S^2 + \Delta C^2 = S^2 \delta S^2 + C^2 \delta C^2$$

If we want to plot ASD $q = \sqrt{Q}$ and its error bars, we have

$$\Delta q^2 = \left(\frac{1}{2\sqrt{Q}}\right)^2 \Delta Q^2 = \frac{1}{4Q}(S^2 \delta S^2 + C^2 \delta C)$$

The relative error of q is

$$\delta q = \frac{\Delta q}{q} = \left(\frac{1}{2\sqrt{Q}}\right)\Delta Q \frac{1}{\sqrt{Q}} = \frac{1}{2}\delta Q$$

If we observe ASD q as the random variable, we have

$$q(\Omega) = \sqrt{s^2(\Omega) - c^2(\Omega)}$$

Its error is

$$\Delta q^2 = \left(\frac{1}{2q}2s\right)^2 \Delta s^2 + \left(\frac{1}{2q}2c\right)^2 \Delta c^2 = \frac{1}{q^2}(s^2\Delta s^2 + c^2\Delta c^2) = \frac{1}{q^2}(s^4\delta s^2 + c^4\delta c^2)$$

The relative error is

$$\delta q = \frac{1}{q}\sqrt{s^4\delta s^2 + c^4\delta c^2}\frac{1}{q} = \frac{1}{Q}\sqrt{S^2\delta S^2/4 + C^2\delta C^2/4} = \frac{1}{2}\delta Q$$

Same result recovered. Therefore, it doesn't matter which convention to choose, so long as it's consistent over analysis. We will use PSD as our random variable throughout this analysis because its relative error is from central limit theorem

$$\delta S = \frac{1}{\sqrt{N}} = \frac{1}{\sqrt{\Delta T_{total}\Delta f_{resolution}}}$$

Note that the Δ in the last term means duration instead of uncertainty.

A.4 Rebinning

The linear-binned ASD from FFT can be rebinned into log-scale frequency bins. The total spectral energy has to be conserved. For the new frequency bin $(f'_{k+1} - f'_k)$ that contains n old bins $(f_{j+1} - f_j)$ with amplitudes A_i, we have

$$A' = \sqrt{\frac{1}{(f'_{k+1} - f'_k)}\sum_i A_i^2(f_i - f_{i-1})} = \sqrt{\frac{1}{n}\sum_i A_i^2}$$

Propagate uncertainty:

$$\Delta A'^2 = \sum_i \left(\frac{\partial A'}{\partial A_i}\right)^2 \Delta A_i^2 = \frac{1}{n^2 A'^2}\sum_i A_i^2 \Delta A_i^2$$

If we write in relative uncertainty $\delta A' = \Delta A'/A'$

$$\delta A' = \frac{1}{nA'^2}\sqrt{\sum_i A_i^4 \delta A_i^2} = \frac{\sqrt{\sum_i A_i^4 \delta A_i^2}}{\sum_i A_i^2}$$

In a simple case where $A_i = A$ and $\delta A_i = \delta A$:

$$\delta A' = \frac{1}{\sqrt{n}}\delta A$$

Central limit theorem is taking effect. Another sanity test is that the rebinned ASD still follows the rule:

$$\delta A' = \frac{1}{\sqrt{n}}\delta A = \frac{1}{\sqrt{n}}\frac{1}{2\sqrt{\Delta T \Delta f}} = \frac{1}{\sqrt{\Delta T \Delta f'}}$$

Rebinning PSD takes similar form. The total spectral energy has to be conserved. For the new frequency bin $(f'_{k+1} - f'_k)$ that contains n old bins $(f_{j+1} - f_j)$ with amplitudes $S_i = A_i^2$, we have

$$S' = \frac{1}{(f'_{k+1} - f'_k)}\sum_i S_i (f_i - f_{i-1}) = \frac{1}{n}\sum_i S_i$$

Propagate uncertainty:

$$\Delta S'^2 = \sum_i \left(\frac{\partial S'}{\partial S_i}\right)^2 \Delta S_i^2 = \frac{1}{n^2}\sum_i \Delta S_i^2$$

If we write in relative uncertainty $\delta S' = \Delta S'/S'$

$$\delta S' = \frac{\sqrt{\sum_i S_i^2 \delta S_i^2}}{\sum_i S_i} = \frac{\sqrt{\sum_i A_i^4 \delta A_i^2}}{\sum_i A_i^2}$$

The same result is recovered.

The PSD at each frequency represents the resolution bandwidth around each frequency. So there is no ambiguity of integration when we rebin spectral densities to a different resolution bandwidth. See the comparison below when there's an ambiguity, for example, whether $S(f)$ stands for the energy between $[f - \Delta f, f]$ or $[f, f + \Delta f]$

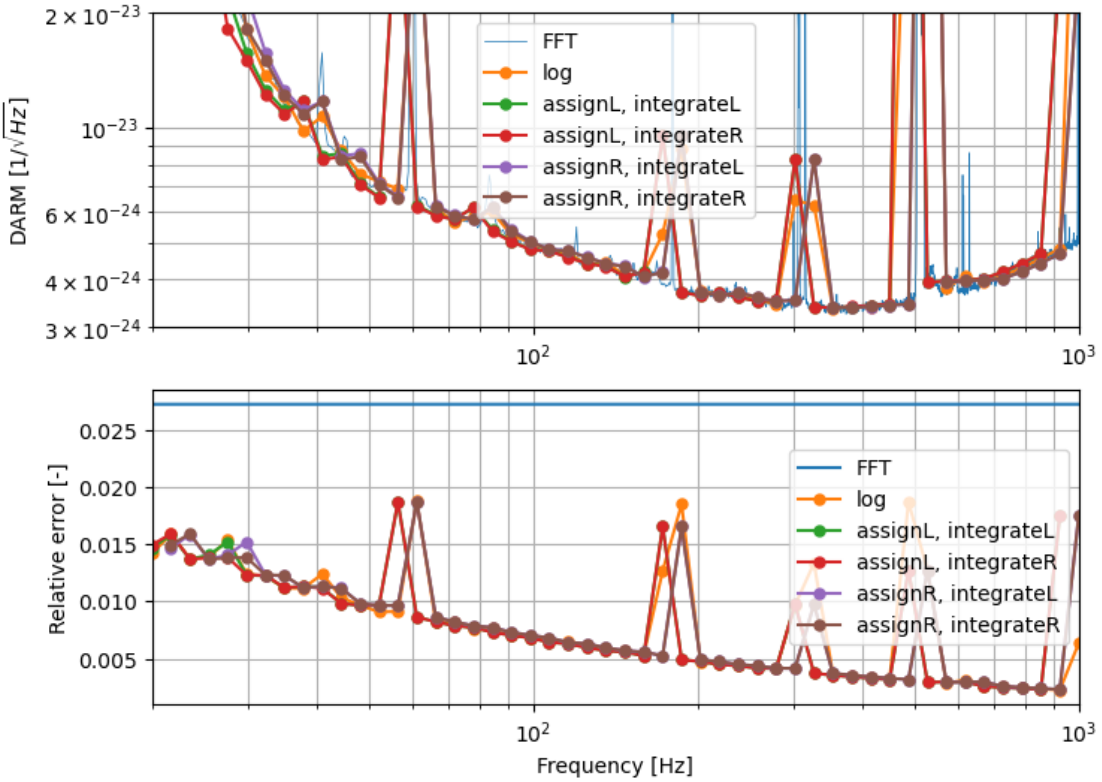

Comparison of various FFT resolution and the rebinned results. The $\Delta f = 2^{-4}$ Hz is minimally required to correctly estimate PSD at low frequency. However, the spectral resolution affects the accuracy of low-frequency PSD and especially the subtracted noises.

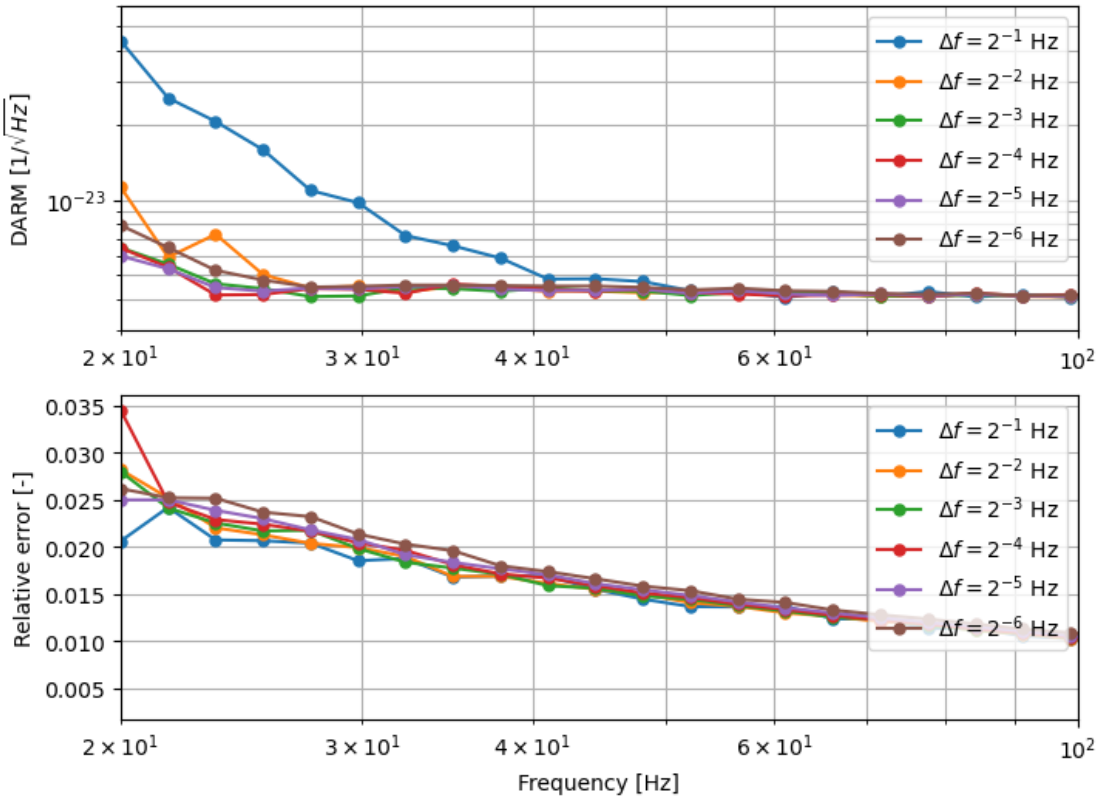

The relative error is set to the PSD error before rebinning. The rebinned relative error doesn't depend on the spectral resolution, which makes sense. As we increase the spectral resolution, we have less averaging so the statistics are not enough. There's a trade-off in the resolution selection, and we pick 2^{-4} Hz to balance the trade-off.

A.5 Line removal

The DARM spectra contain a lot of narrow lines due to various causes. There are two ways to remove lines. One is to hardcode all lines inside the frequency band of interest. The other is to use a filter, for example, median filter to remove all spikes.

The median filter is easier to implement, but it also removes transient noises like scatter noise. This is not we want so we need to hardcode all lines within linewidth of 2 Hz.

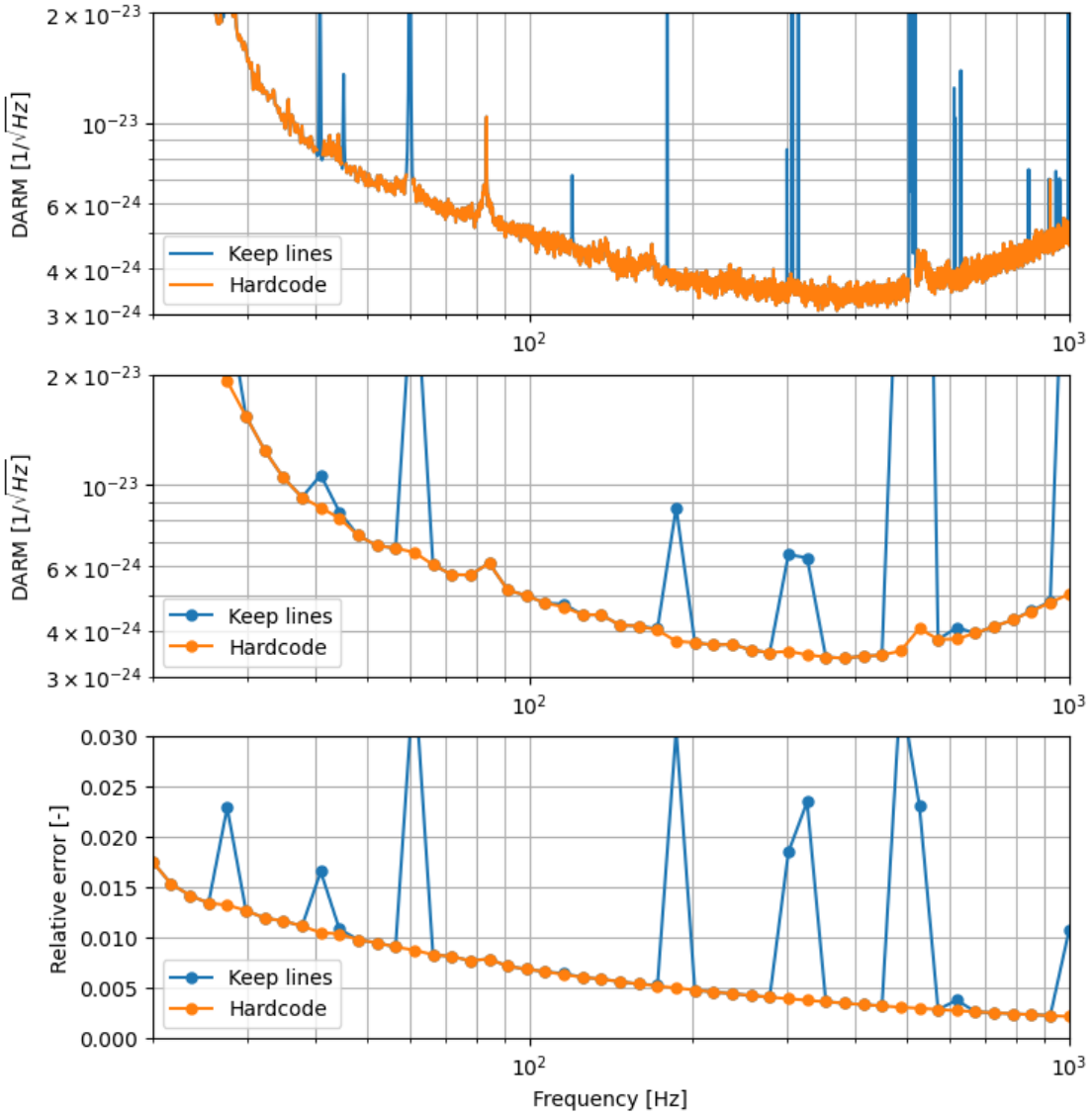

A.6 Systematic error

There is a known systematic error from calibration group (see Vladimir Bossikov's llo66431). The estimated calibration uncertainty envelope fails to capture the uncertainties in the monitoring Pcal injections.

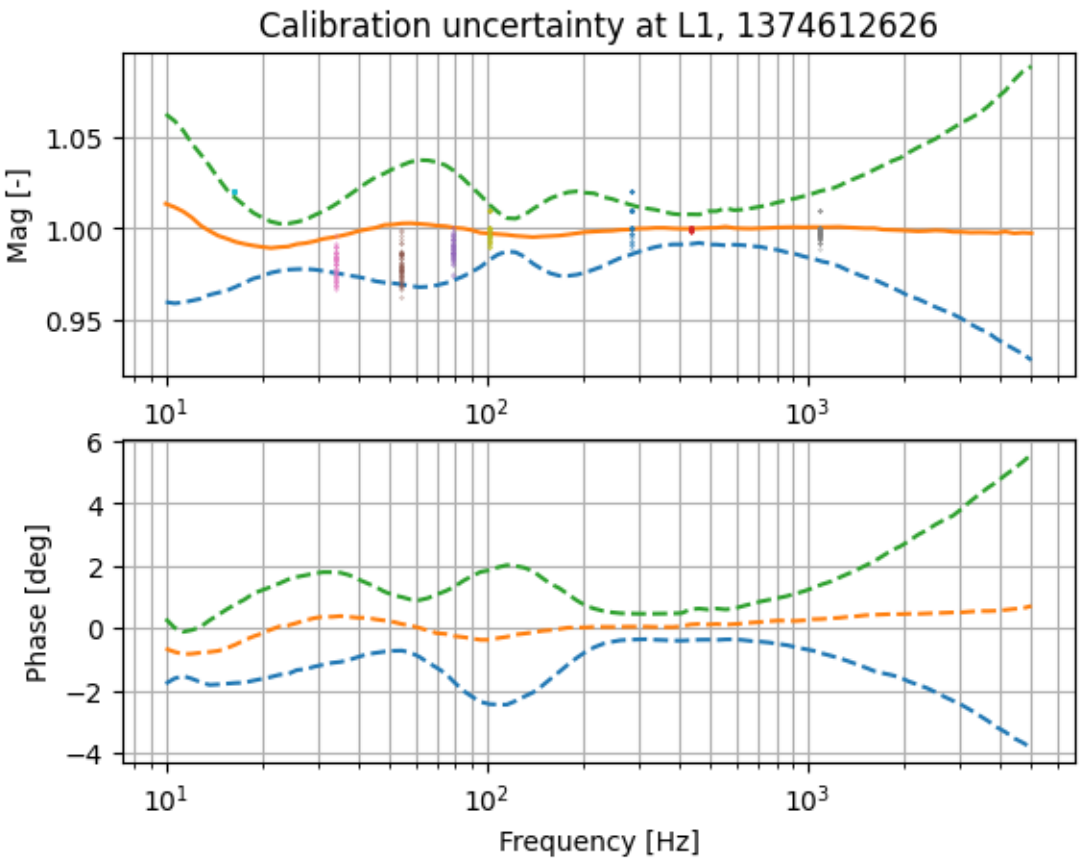

The monitor lines are lower than medians by 2% at 33.93, 54.17, and 78.23 Hz. When we multiply the median curve with the correction, the new envelope is correct and contains the uncertainty of monitors (see Ling Sun's comment).

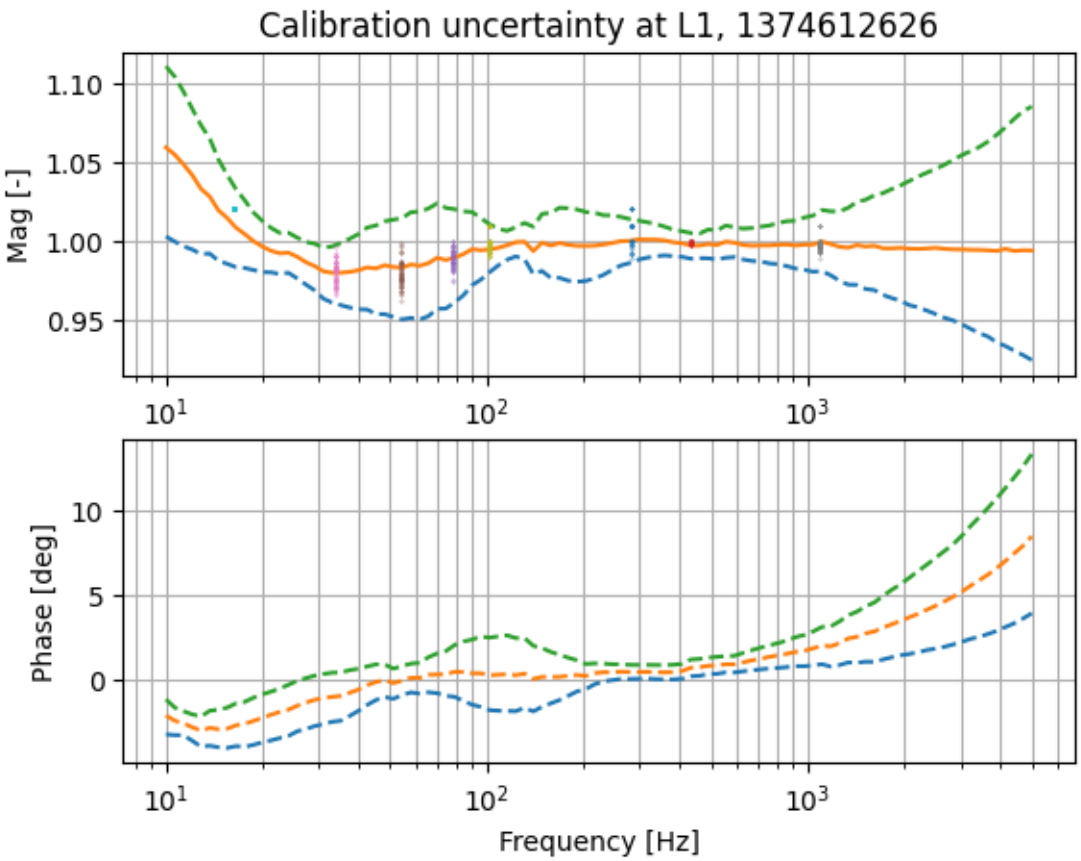

The correction transfer function is here. We mostly care about the magnitude and not the phase.

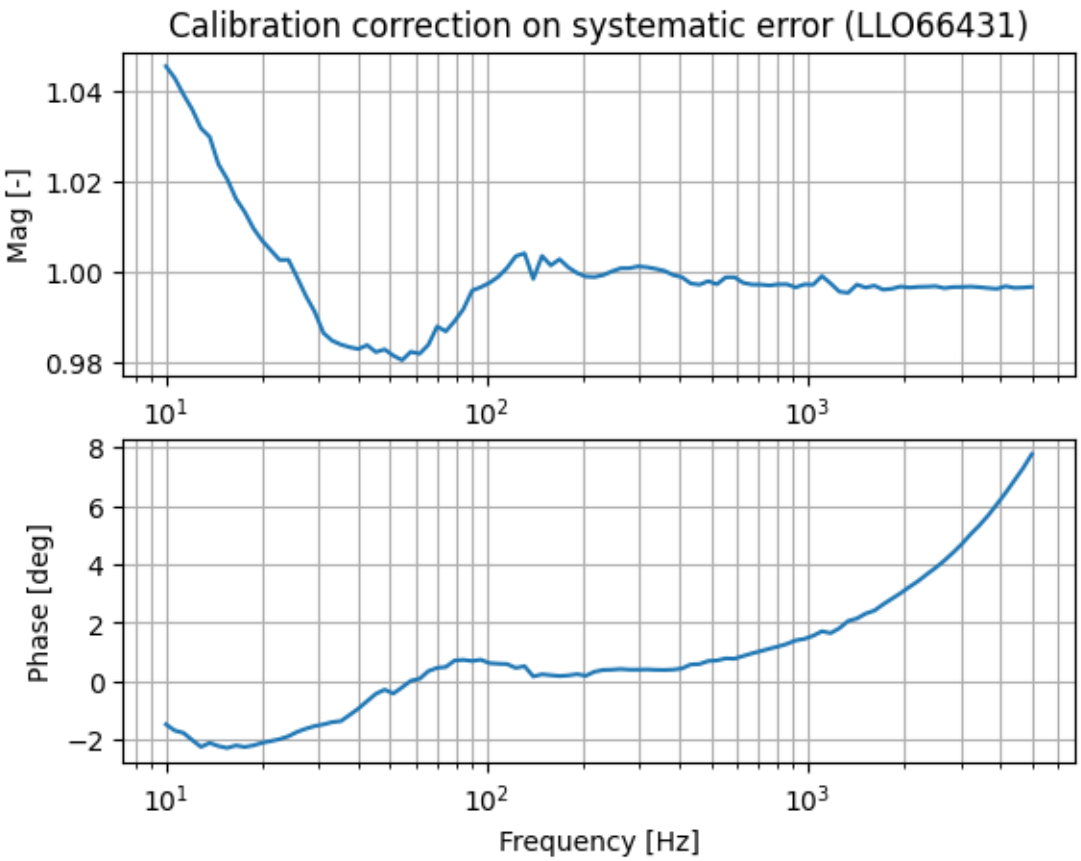
Calibration correction on systematic error (LLO66431)
Mag [-]
1.04
1.02
1.00
0.98
10^1
10^2
10^3
Phase [deg]
8
6
4
2
0
−2
10^1
10^2
10^3
Frequency [Hz]

Appendix B: Cross power spectral density estimation

For a quick sanity check, we compare two different methods to calculate cross power spectral density given two time series: Python-based scipy.signal.csd and MATLAB-based LPSD (Trobs & Heinzel, Measurement 39 (2006) 120–129).

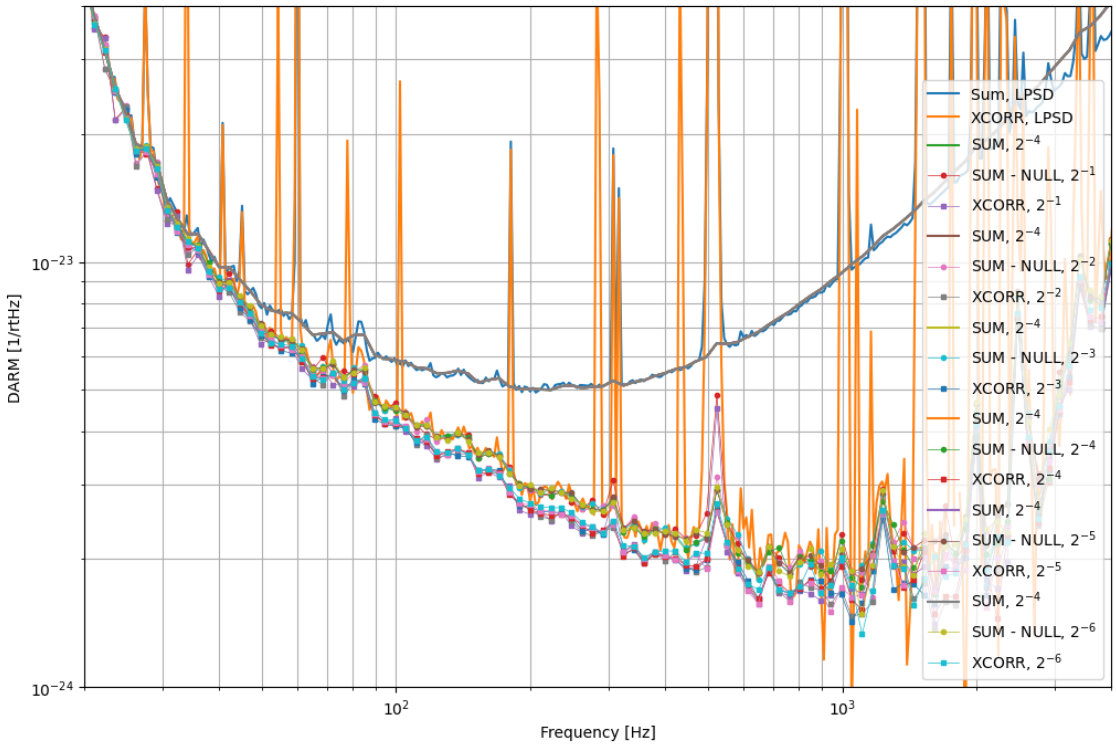

As shown in the plot above, the rebinned SUM - NULL traces are consistent with LPSD results, but the rebinned scipy.signal.csd traces don't follow. This problem doesn't improve when we increase the spectral resolution. It's a systematic error introduced during the rebinning of the xcorr spectra. The difference between the SUM and Sum, LPSD at high frequencies are due to the known cailbration problem in PD time series. It doesn't affect the discrepancy at low frequency.

This discrepancy due to systematic error can be removed if we take the mean statistics of the xcorr instead of median. This is perhaps due to the trouble when scipy.signal.csd samples median from the complex values. If we take mean, the xcorr is equal to LPSD, and sum - null, which are all consistent.

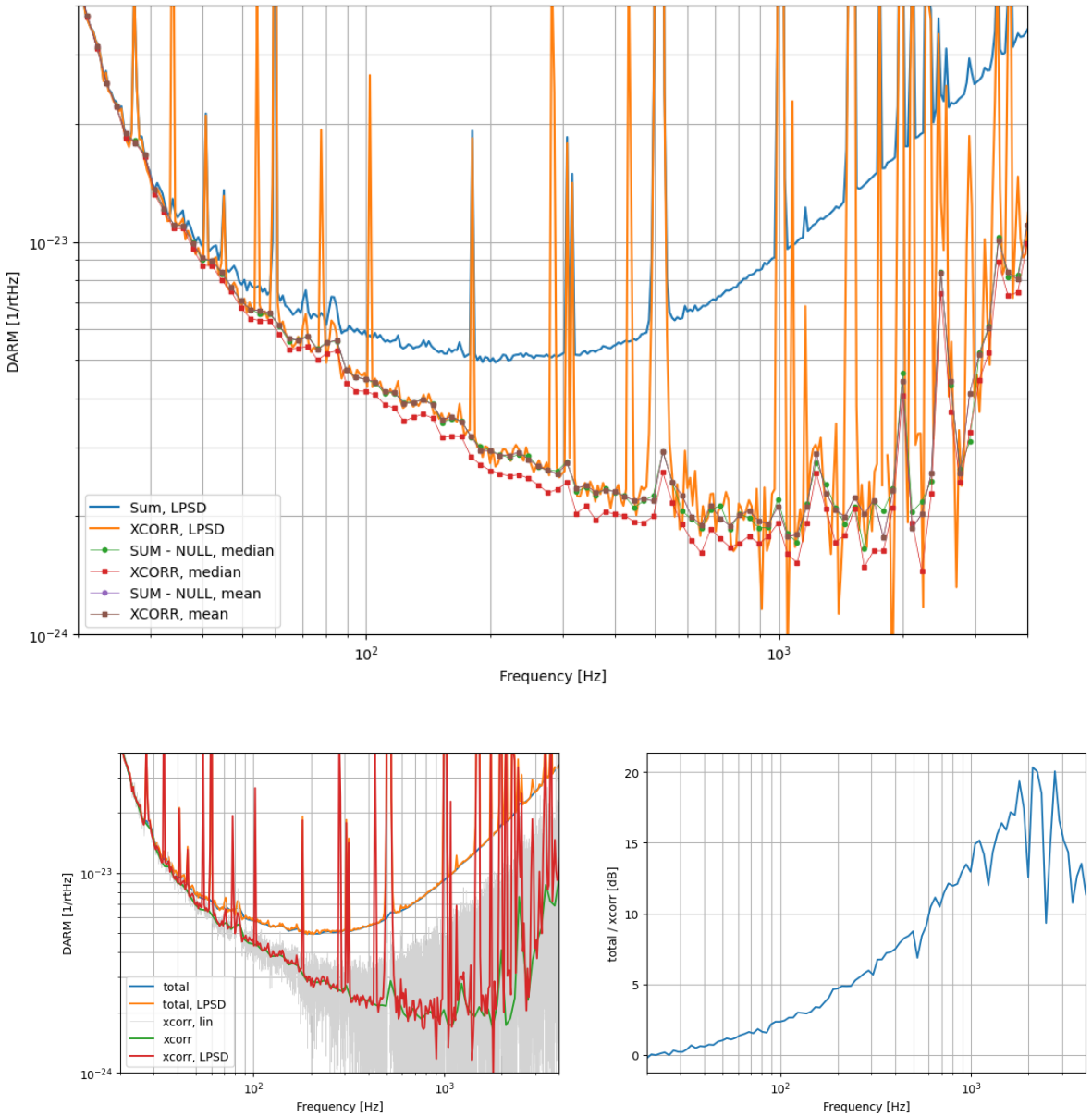

Both scipy.signal.csd and LPSD are consistent. The classical noise at 1 kHz are around 15 dB (5.6) lower than total noise.

Appendix C: Coating thermal noise study

The L1 noise budget presented in LVK 2023 Sep meeting is shown below. This is DARM with frequency-dependent squeezing.

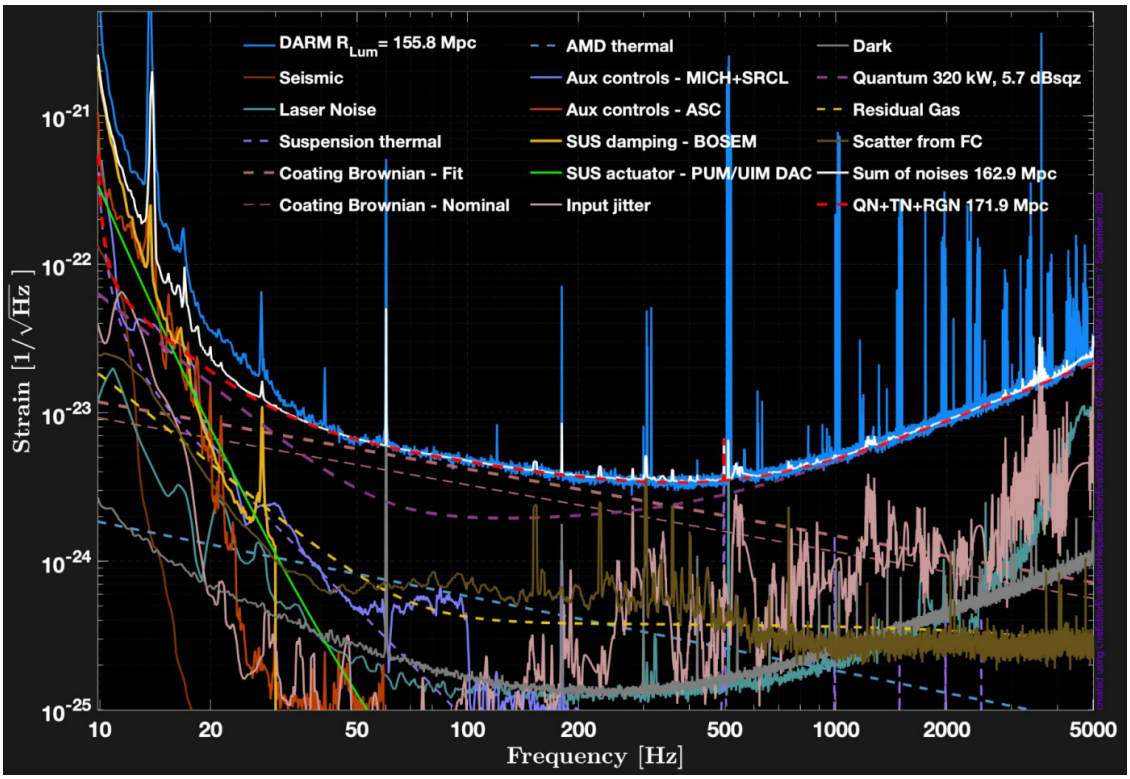

In the band 40 - 200 Hz, all the noises that are not quantum nor Brownian are at the level of 1e-24. They are 3 times less than Brownian noise, so our over-estimation of Brownian noise is maximum 10% at 200 Hz and less at lower frequencies. Knowing the shot noise, we can have a band of possible QRPN:

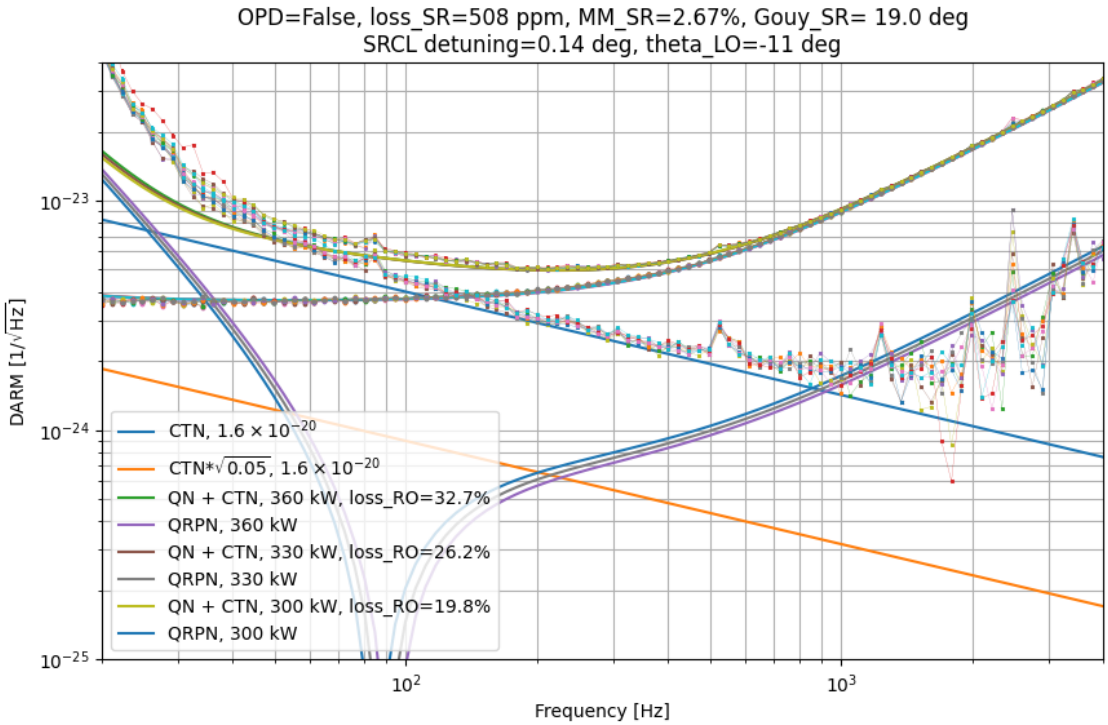

As we can see here, the QRPN is below 5% of coating Brownian noise PSD between 60 - 200 Hz, even with the highest arm power possible of 360 kW. Besides QRPN and shot noise, there is also other classical noise there, for example, scatter noise at 80 Hz and FC backscatter noise with the magnitude of 7e-25. Therefore, we can safely infer CTN with the frequency band of 100 - 200 Hz. The other classical noise there will not lead to more than 5% overestimation of the coefficient.

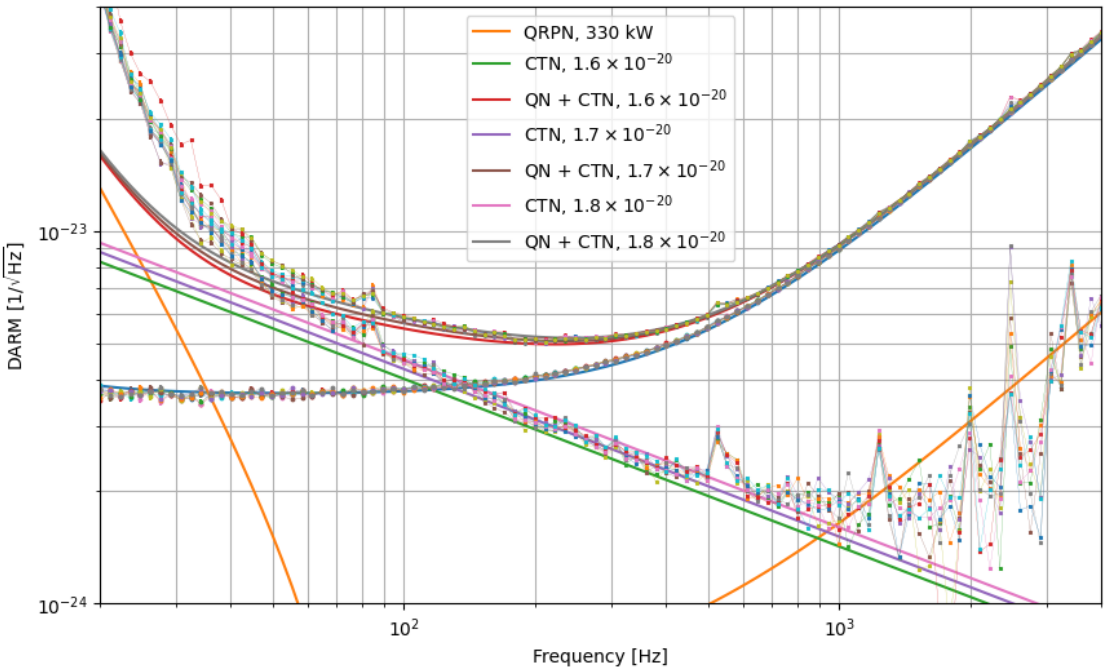

The real CTN is more likely to be larger than 1.6e-20 given the plot above.

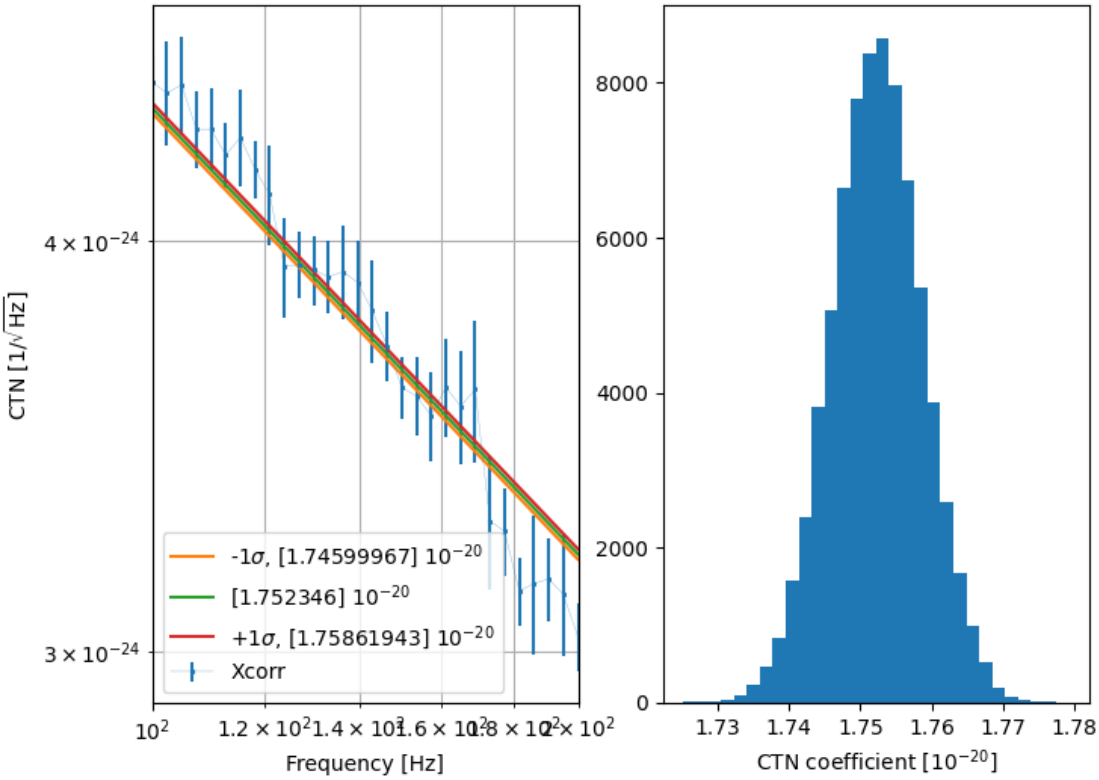

This is the MCMC where we infer the magnitude of CTN coefficient. The distribution of the result is pretty Gaussian which is good. However, the slope doesn't look correct. We can also fit it with slope as another free parameter.

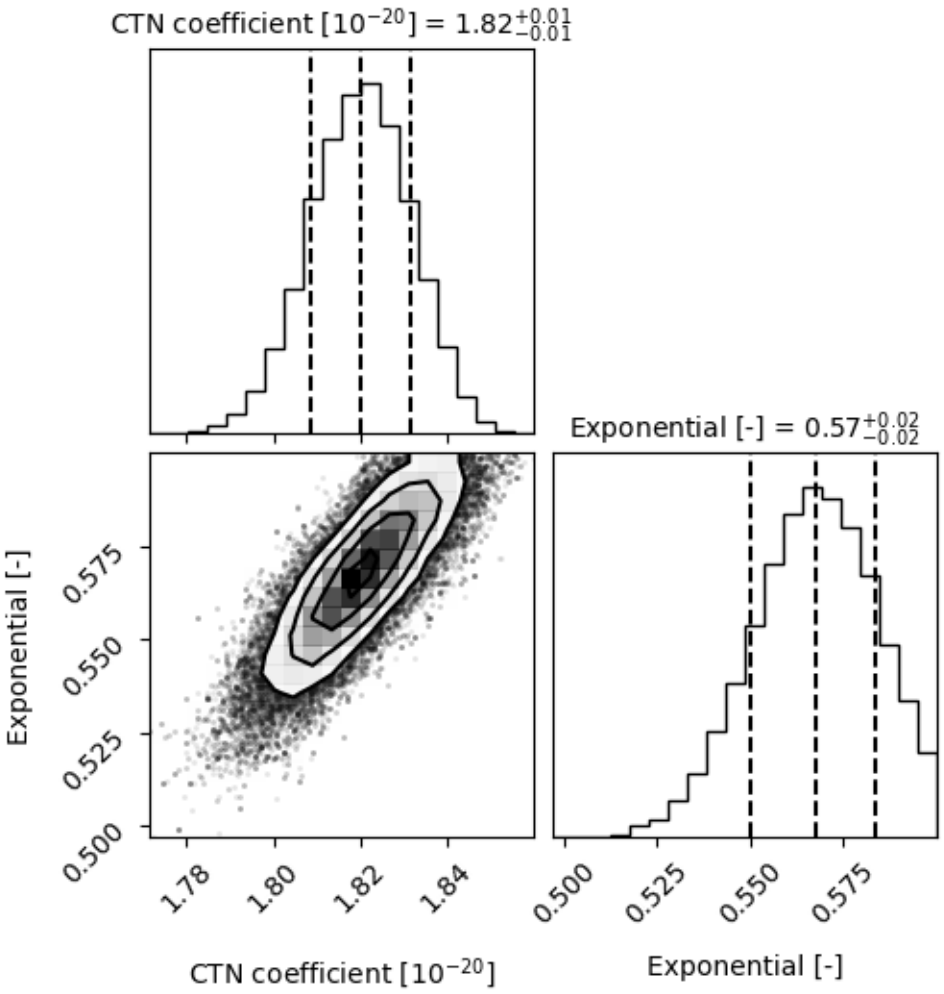
CTN coefficient [10^{-20}] = $1.82^{+0.01}_{-0.01}$
Exponential [-] = $0.57^{+0.02}_{-0.02}$
Exponential [-]
0.500
0.525
0.550
0.575
1.78
1.80
1.82
1.84
CTN coefficient [10^{-20}]

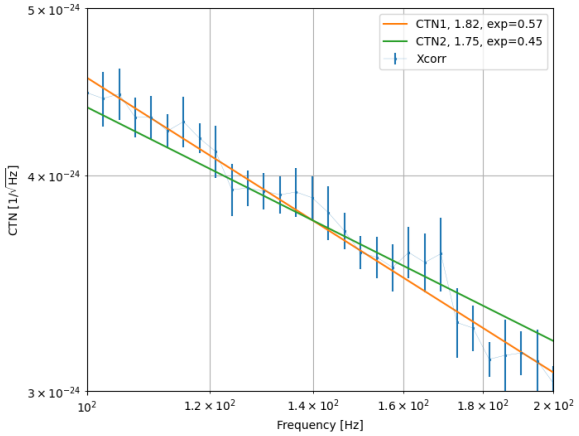
CTN1, 1.82, exp=0.57
CTN2, 1.75, exp=0.45
Xcorr
CTN [1/√Hz]
Frequency [Hz]

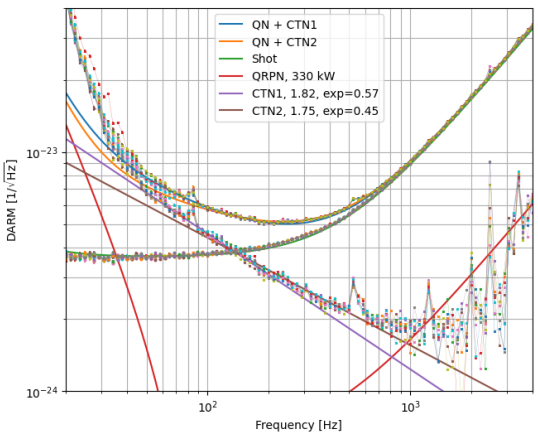
QN + CTN1
QN + CTN2
Shot
QRPN, 330 kW
CTN1, 1.82, exp=0.57
CTN2, 1.75, exp=0.45
DARM [1/√Hz]
Frequency [Hz]

The MCMC curve with slope as a free parameter gives a better fit to the data. However, it predicts an exponential of 0.57, which is more than 0.45 ± 0.02 used in PRD 103, 072001.

One other possible classical noise that contributes in this bandwidth and gives a steeper curve is the AMD thermal noise. We could also add that and do MCMC.

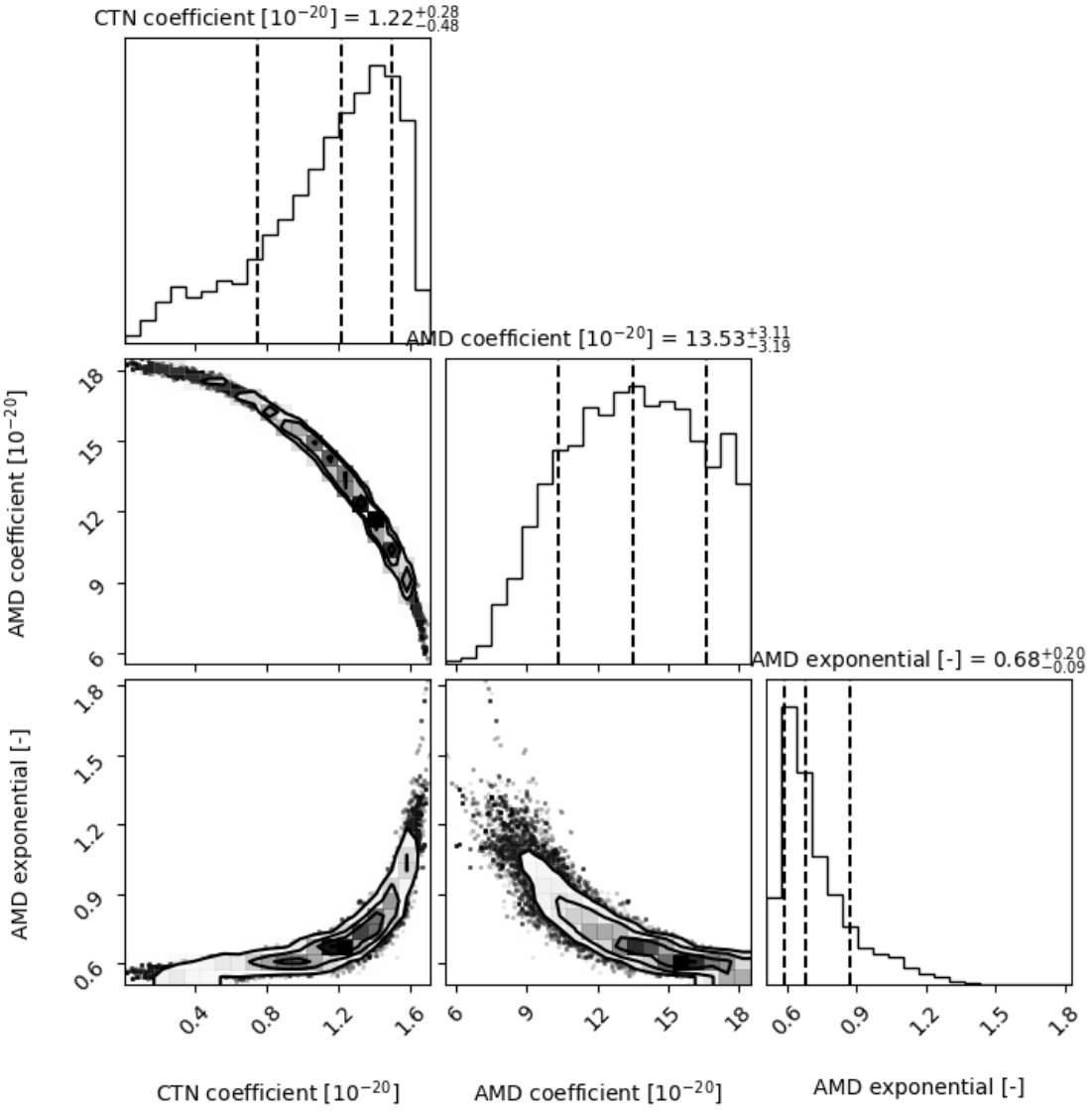

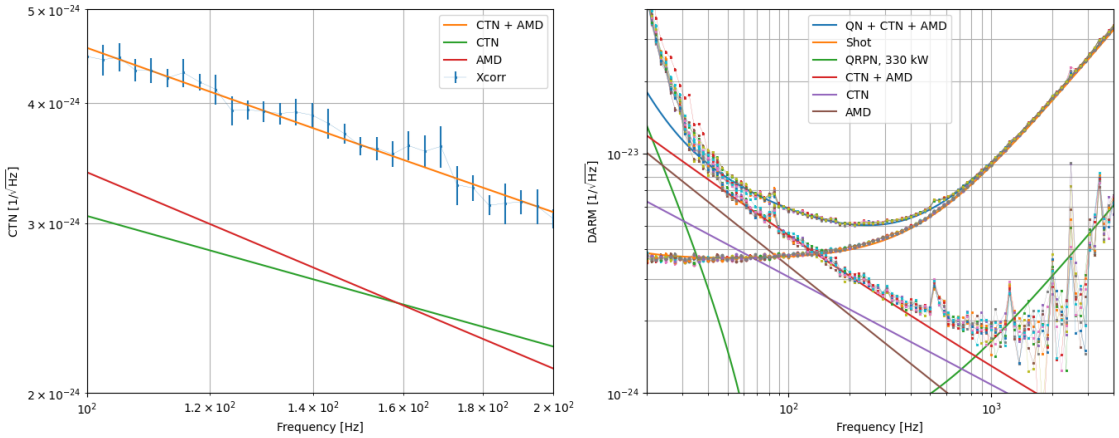

The difference between measured DARM and total noise budget is also smaller with the addition of AMD.

Another possible source of noise that gives a steeper curve is residual gas damping noise. It roughly falls as a $1/f^2$ noise in ASD.

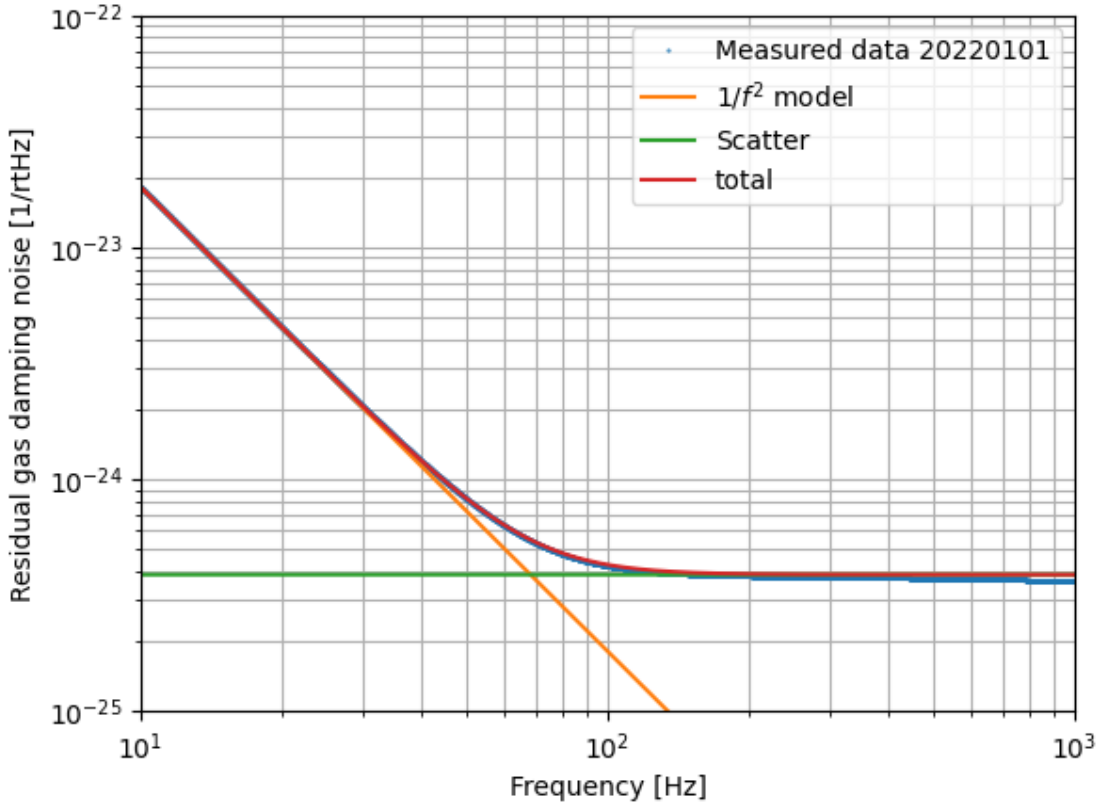

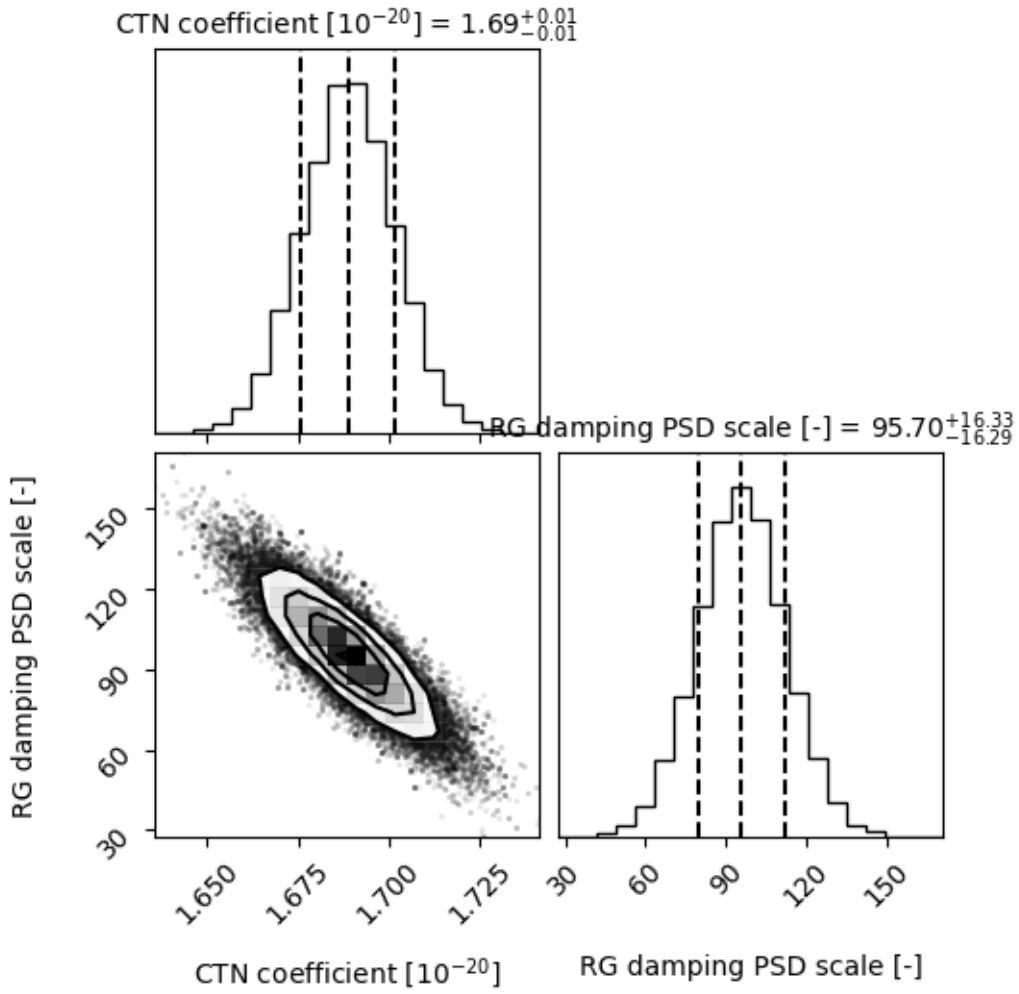
CTN coefficient [10^{-20}] = $1.69^{+0.01}_{-0.01}$
RG damping PSD scale [-] = $95.70^{+16.33}_{-16.29}$
RG damping PSD scale [-]
CTN coefficient [10^{-20}]
RG damping PSD scale [-]

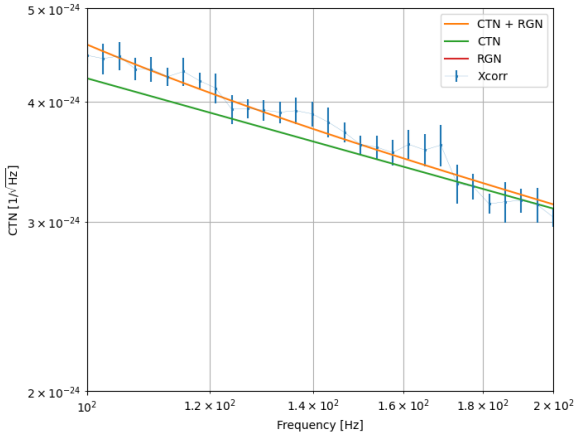
CTN + RGN
CTN
RGN
Xcorr
CTN [1/√Hz]
Frequency [Hz]

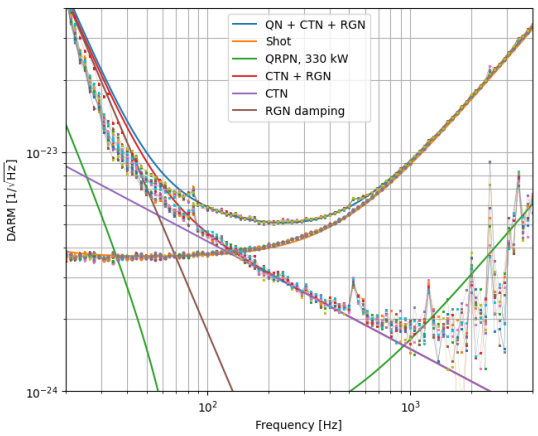
QN + CTN + RGN
Shot
QRPN, 330 kW
CTN + RGN
CTN
RGN damping
DARM [1/√Hz]
Frequency [Hz]

The residual gas damping noise can be elevated to fit the measured DARM at 100-200 Hz, but it doesn't make sense at low frequencies. We can't fudge the excessive residual gas noise to explain the steeper slope of the xcorr noise there.

Therefore, the only two options of classical noise model for xcorr is either CTN with a 0.57 exponential or normal CTN plus excessive AMD:

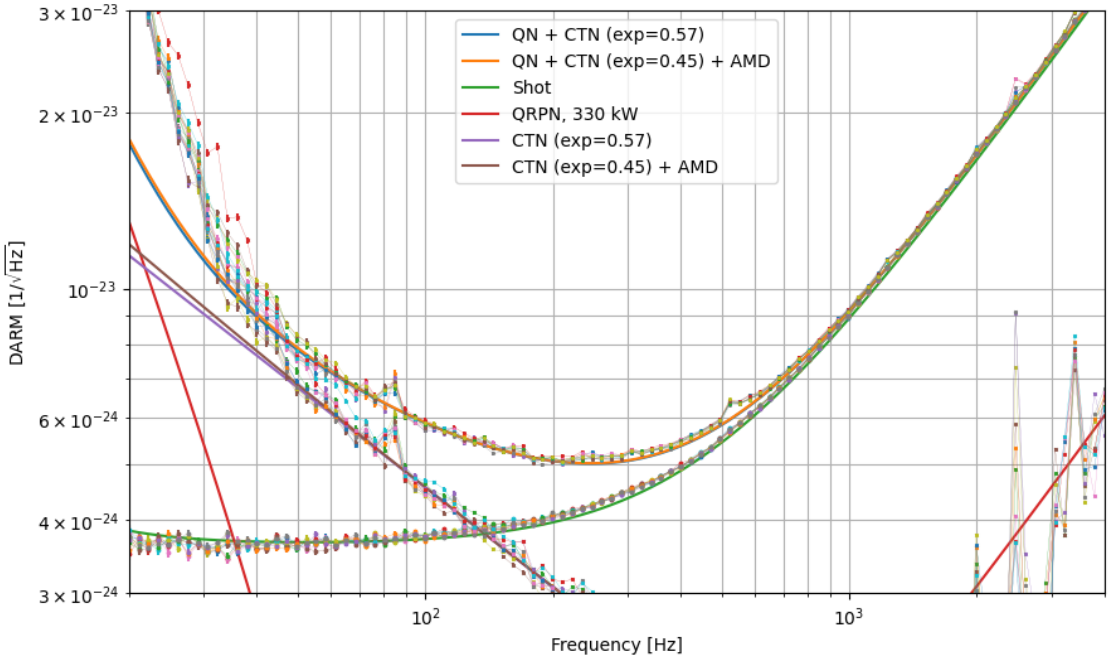

Since the xcorr contains QRPN and all classical noise in addition to thermal

$$S_{xcorr} = S_{rad} + S_{CTN} + S_{clasmc}$$

where S_{clasmc} is classical noises minus effective CTN. We can get total quantum noise by

$$S_{QN} + S_{clasmc} = S_{SUM} - S_{CTN} - S_{dark}$$

We can compare it with two effective CTN models

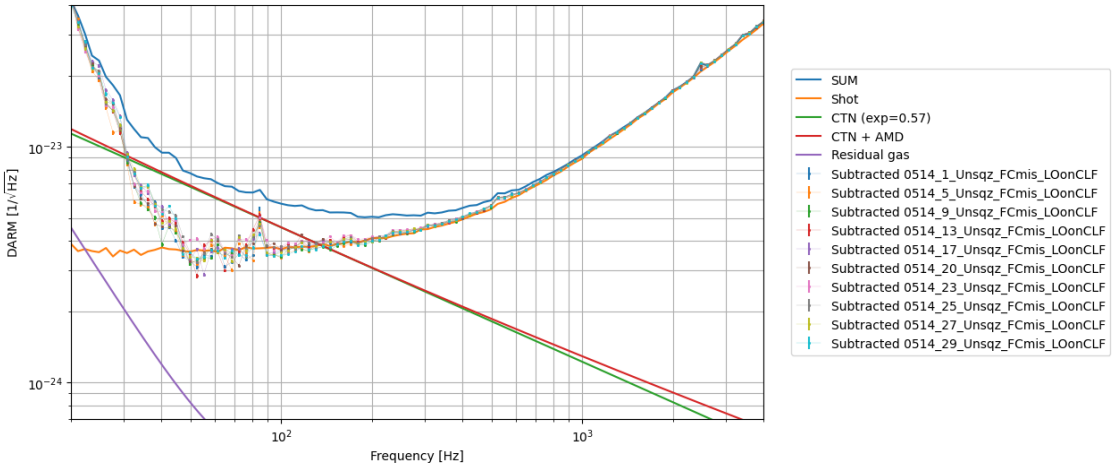

The subtracted DARM contains quantum noise plus classical noises that are not CTN. The difference between two CTN models are less than 8%. We will use the CTN model with AMD correction.

Although the classical noise is dominant below 40 Hz, we can still quantify QRPN above 40 Hz. The same L1 FDS noise budget at low frequencies are shown below. Any other noises that leads to over-estimation of QRPN are MICH+SRCL coupling, FC backscatter, and other scatter noise like the 80-Hz bump.

The self-fluctuation of the subtracted noise at 40 Hz is due to classical noises. We can't disentangle the classical noise over there with QRPN, but we can still give a upper bound on QRPN. We took out the locks on 05/16 that showed a lot higher classical noise at 40 Hz than those taken on 05/14.

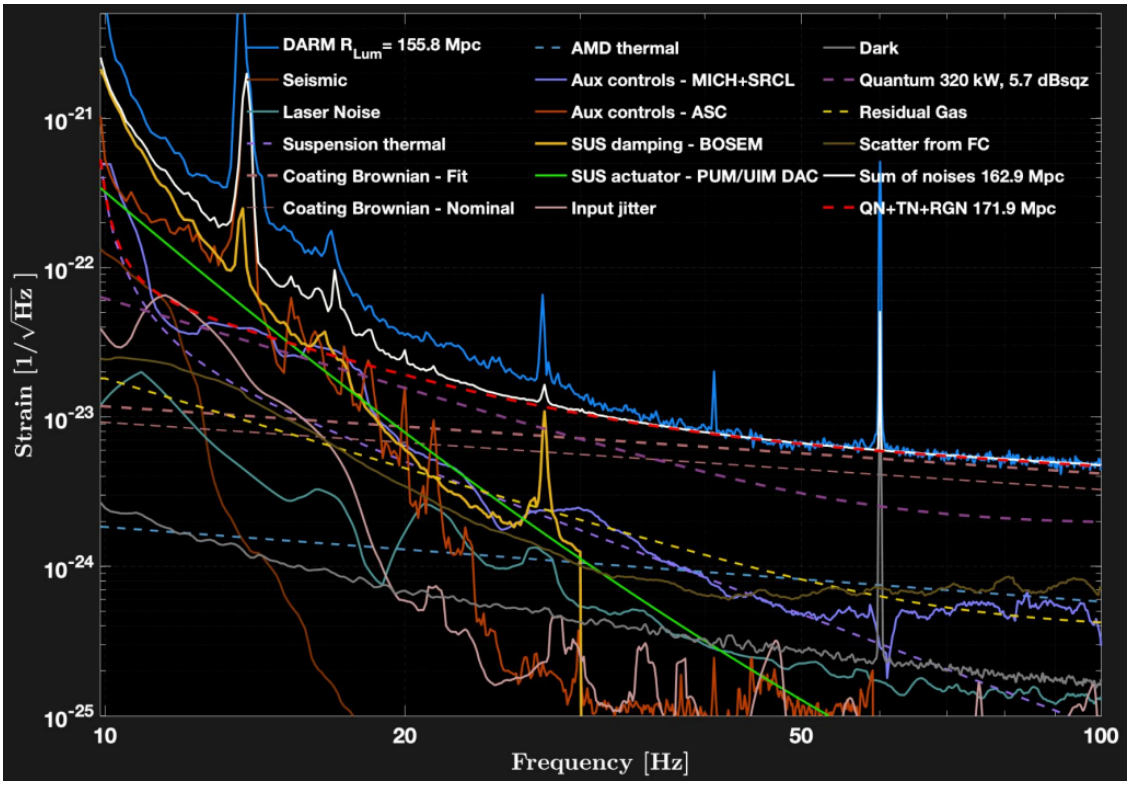
DARM R_Lum = 155.8 Mpc
Seismic
Laser Noise
Suspension thermal
Coating Brownian - Fit
Coating Brownian - Nominal
AMD thermal
Aux controls - MICH+SRCL
Aux controls - ASC
SUS damping - BOSEM
SUS actuator - PUM/UIM DAC
Input jitter
Dark
Quantum 320 kW, 5.7 dBsqz
Residual Gas
Scatter from FC
Sum of noises 162.9 Mpc
QN+TN+RGN 171.9 Mpc
Strain [1/√Hz]
10^-21
10^-22
10^-23
10^-24
10^-25
10
20
50
100
Frequency [Hz]

Appendix D: Comparison of distributions of initial walkers

The initial walkers are randomly distributed around the guess point in the parameter space. We can initialize the walker distribution with prior distribution, which is a Gaussian. Or we can initialize with a flat distribution to explore more parameter space.

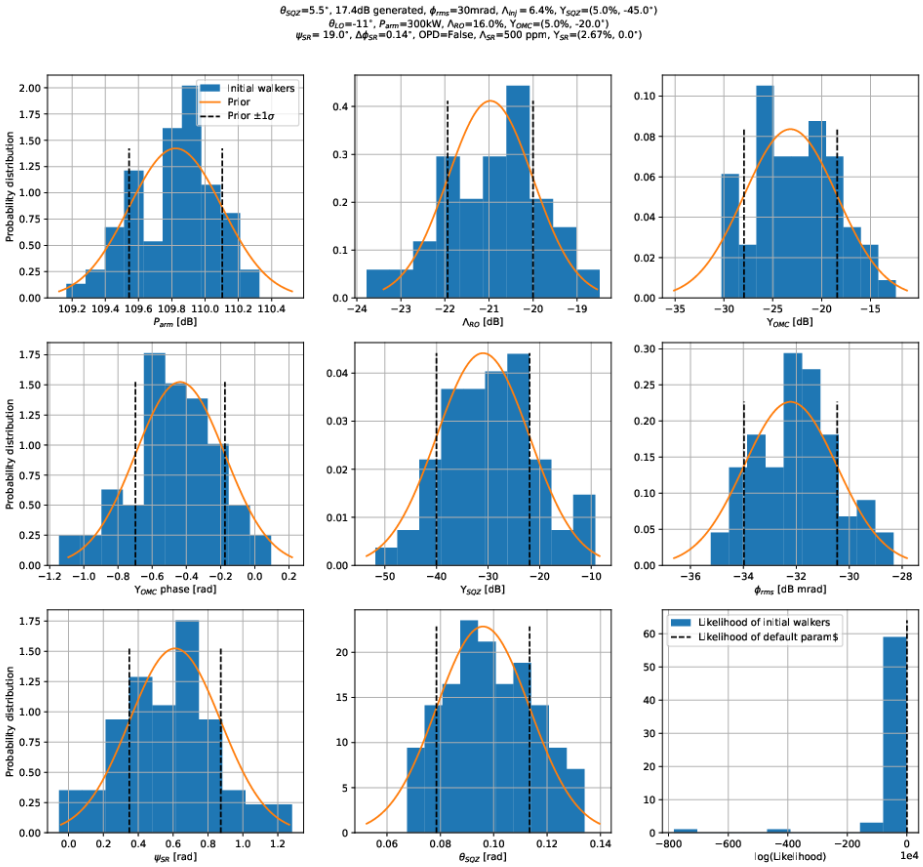

The prior distribution has bad units so see below plot where the unit is fixed. The arm power has distribution of 300-320 kW. The MCMC result is here

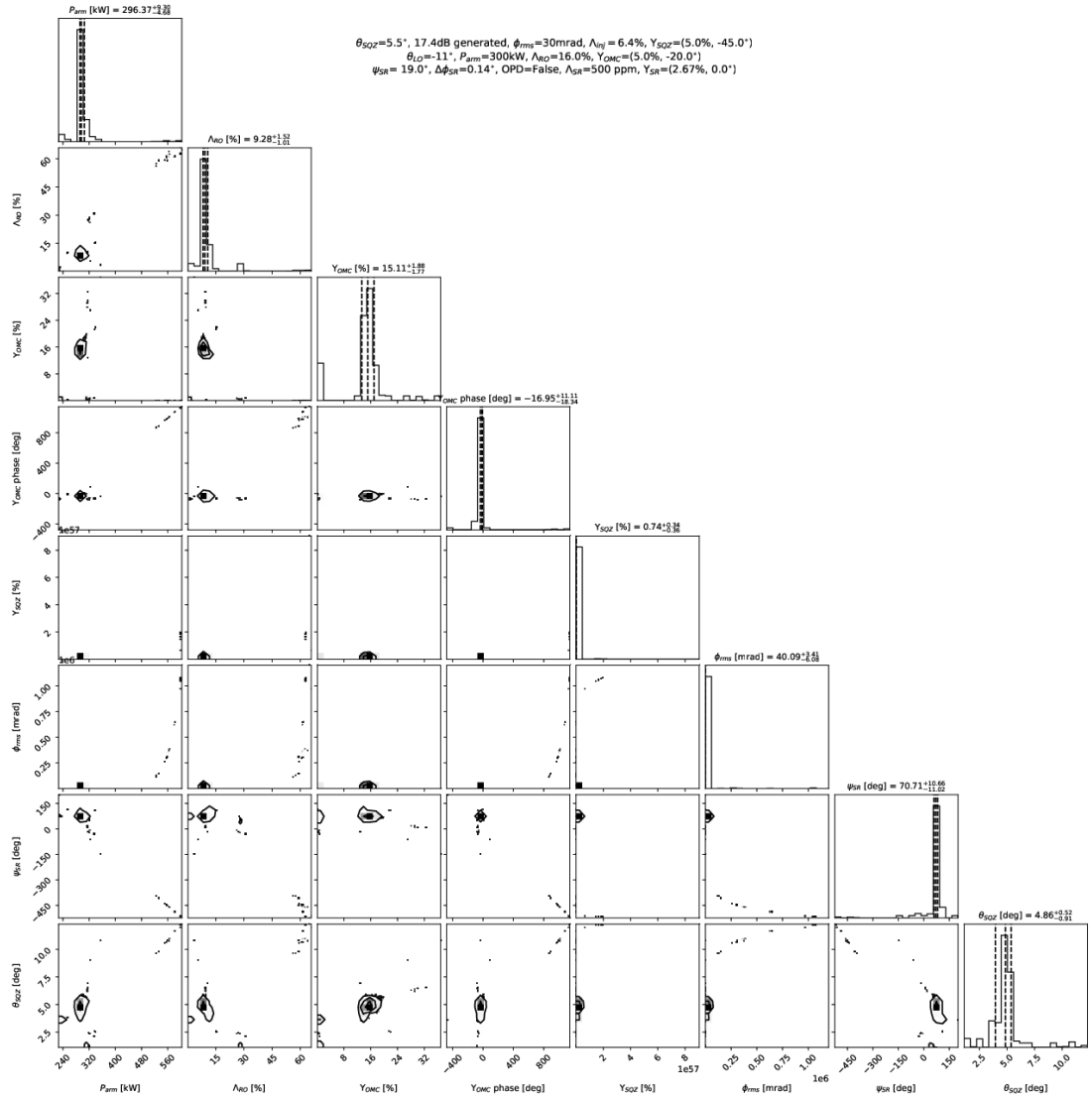

The MCMC result ends up at a place of 296 kW of arm power with final likelihood of 9954 (max 11020, default is 3814). It's pretty good. However, the walkers are distributed with prior so they are only exploring regions near 300 kW. We can distribute walkers flatly instead of following prior.

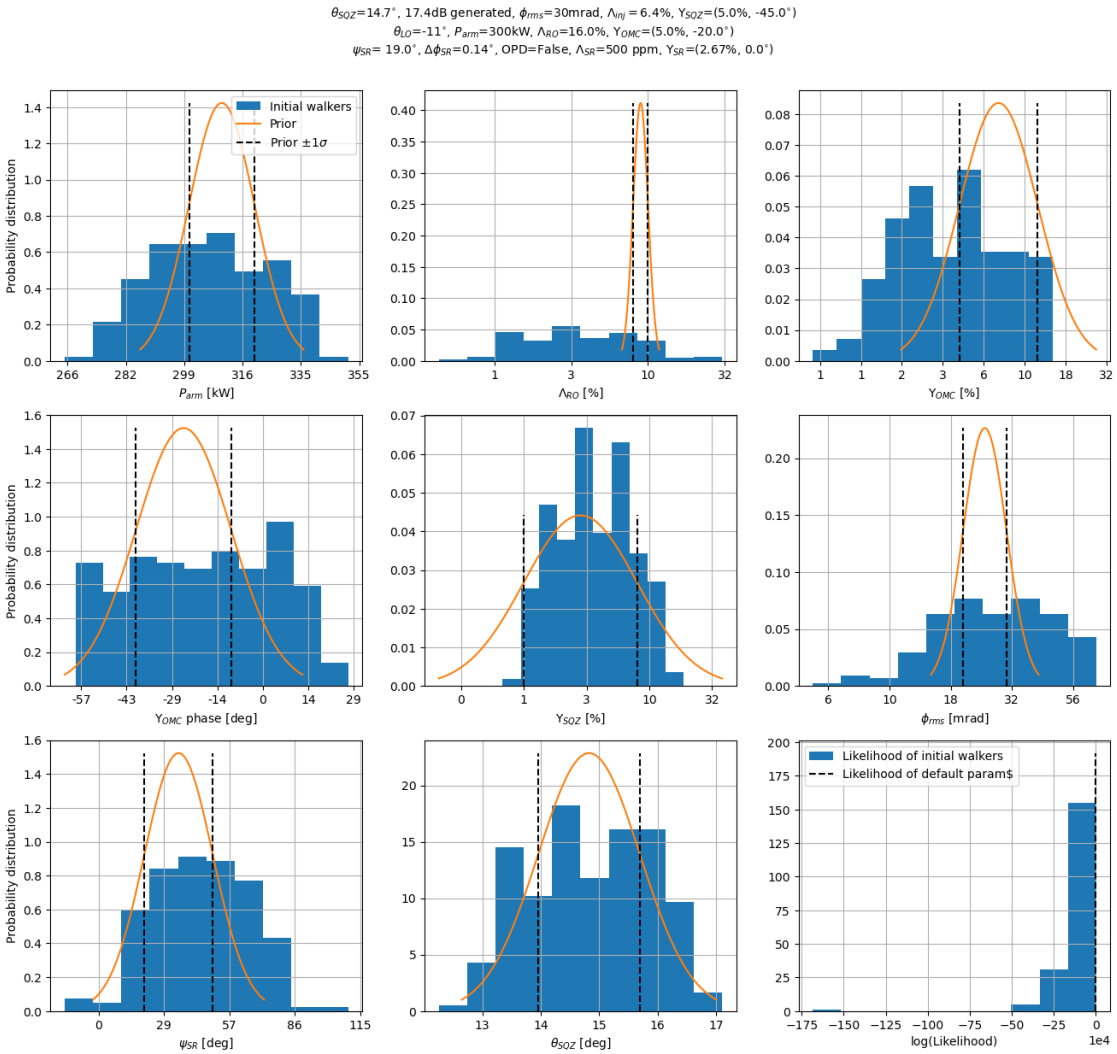

I manually paralleled the job by distributing it on multiple computers and stack all the chains together. The distribution of initial walkers looks Gaussian, but it's due to central limit theorem of many flat-distributed walkers.

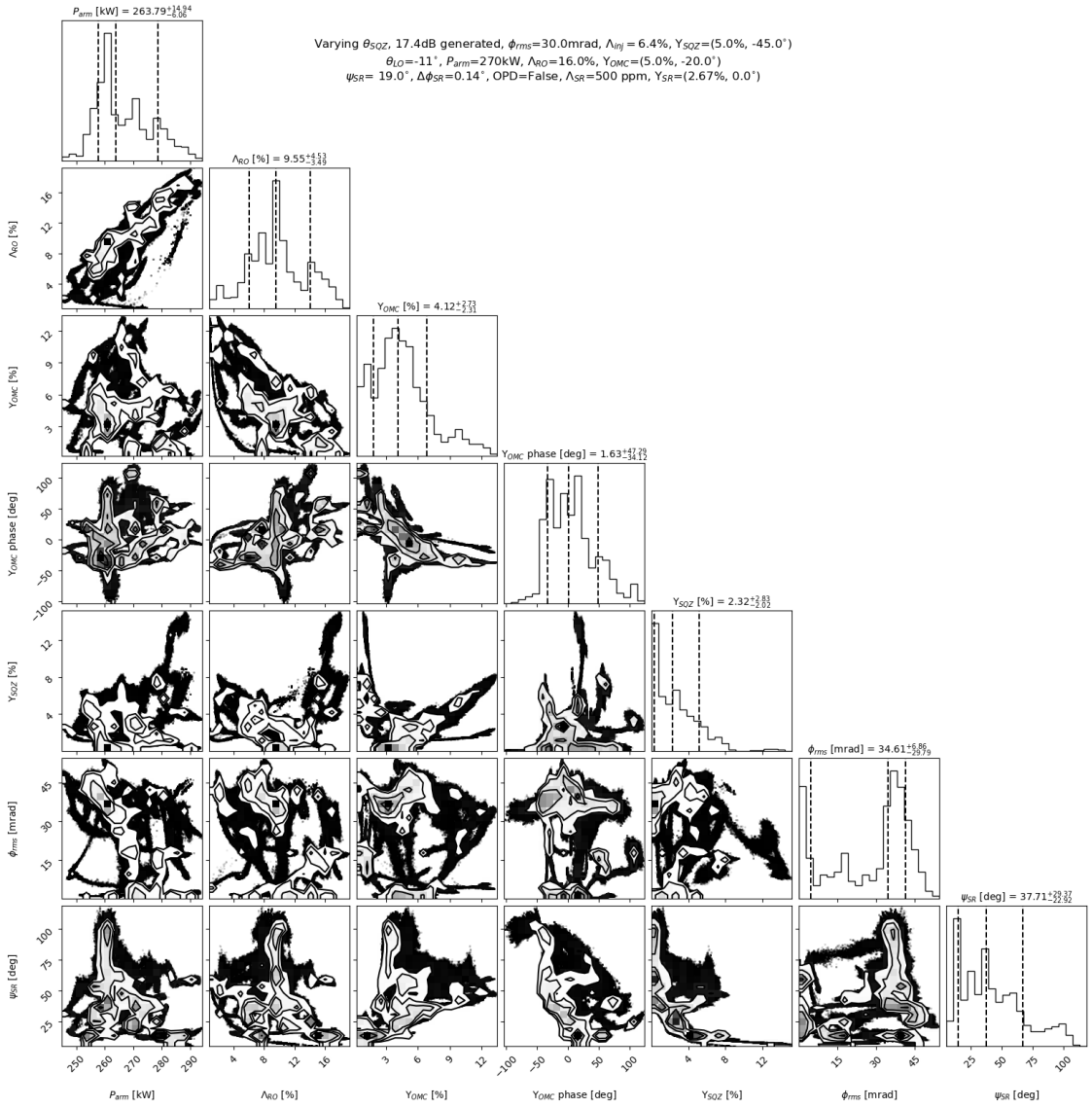

The final likelihood is 10144, slightly higher than Gaussian-distributed walkers. We should use a flat-distributed walkers for more explorations.

Appendix E: Additional results of MCMC on individual FIS

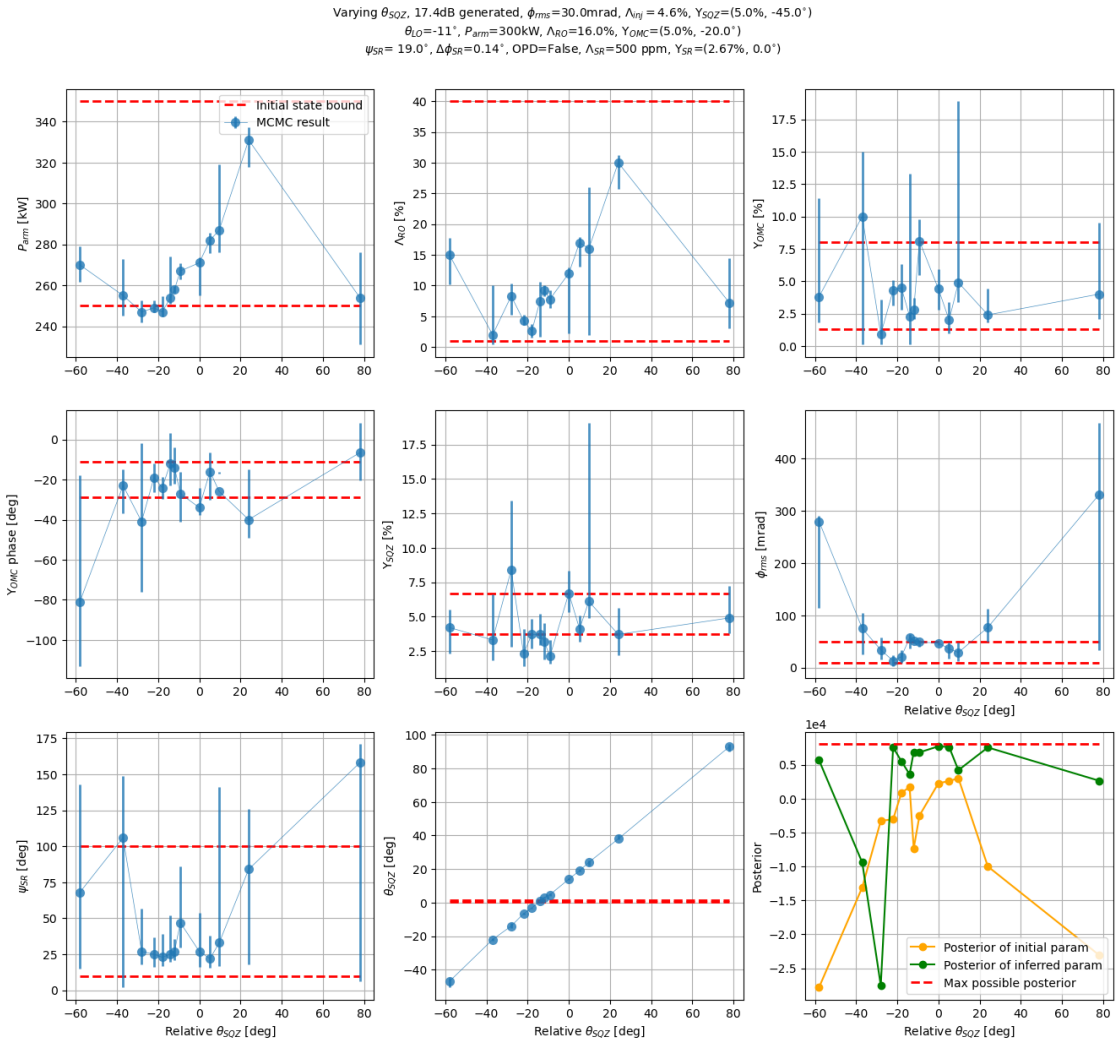

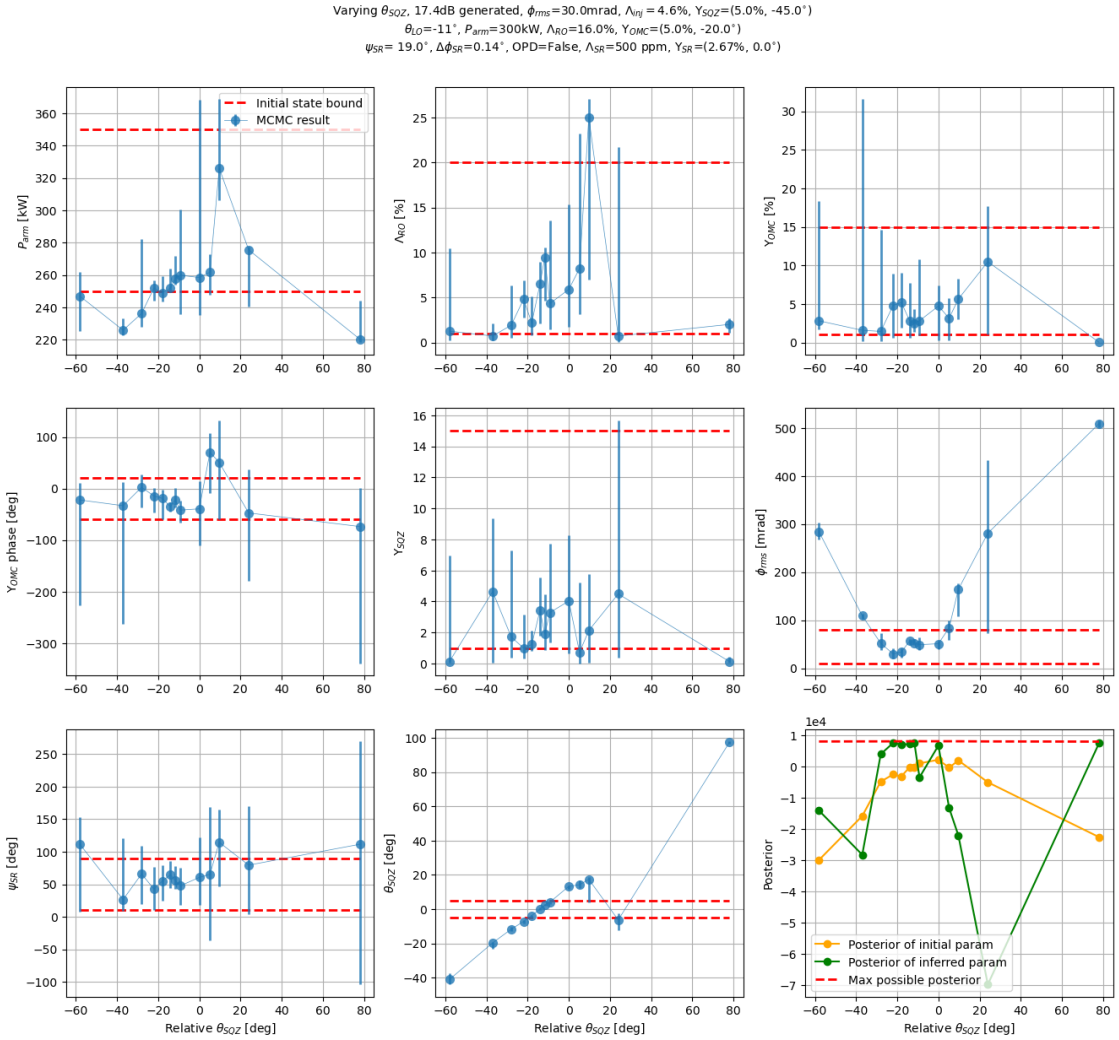
Varying θ_{SQZ}, 17.4dB generated, ϕ_{rms}=30.0mrad, Λ_{inj} = 4.6%, Y_{SQZ}=(5.0%, -45.0°)
θ_{LO}=-11°, P_{arm}=300kW, Λ_{RO}=16.0%, Y_{OMC}=(5.0%, -20.0°)
ψ_{SR}= 19.0°, $\Delta\phi_{SR}$=0.14°, OPD=False, Λ_{SR}=500 ppm, Y_{SR}=(2.67%, 0.0°)
Initial state bound
MCMC result
P_{arm} [kW]
Λ_{RO} [%]
Y_{OMC} [%]
Y_{OMC} phase [deg]
Y_{SQZ}
ϕ_{rms} [mrad]
ψ_{SR} [deg]
θ_{SQZ} [deg]
Posterior
1e4
Posterior of initial param
Posterior of inferred param
Max possible posterior
Relative θ_{SQZ} [deg]

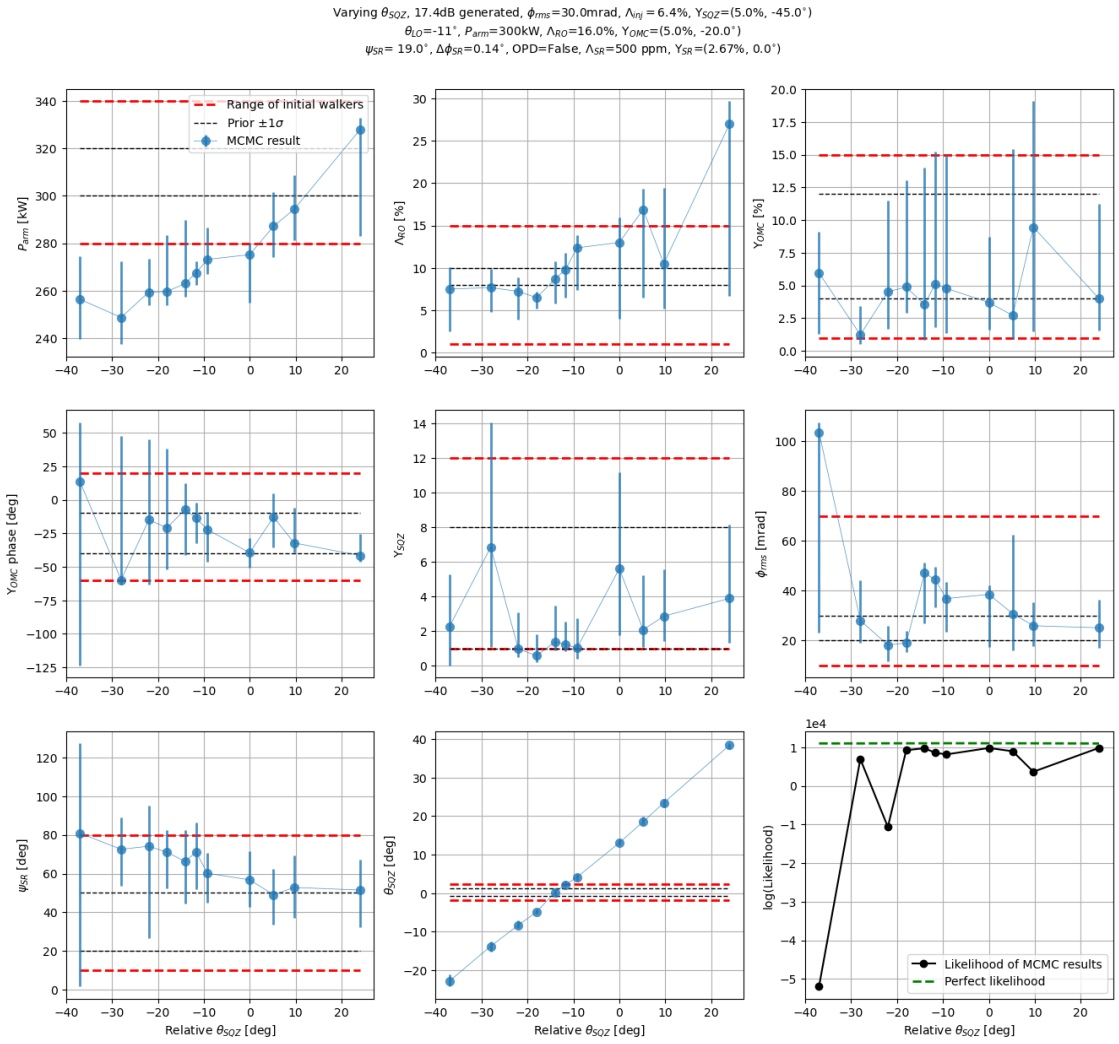

It's very interesting that we have an outlier of arm power at squeezing angle of 24 deg. Although the inferred arm power is much larger than other cases, the MCMC results give a better posterior than initial settings. It could be a case where the random starting points of all walkers are very bad so none of them converge. But I run a second MCMC and it gives the same result. Both of them yield much lower posterior than inputs.

The phase noise misbehaves near the anti-squeezing. We've already know that the low-frequency part of the DARM can't be squeezed as good as high frequency. When we anti-squeeze high frequency, we are reducing the QN of low frequency but we failed to observe it. Again, it might be a calibration failure or unknown frequency-dependent loss or phase noise.

We also saw a similar trend between arm power and readout loss. It's no surprise that they are correlated, but it's interesting that first, these powers don't agree, and second, no other parameters can break these degeneracies. We might need another parameter to fix that, for example, generated squeezing. We could also enlarge our bounds on initial positions and run MCMC with more walkers to sample more possibilities. We should also choose a larger

burn-in, like 2000. I'm not sure if each step MCMC takes is scaled by the range of initial states. For example, the initial states of P_{arm} has a range of 100e3, but the squeezing angle only has a range of 1. If P_{arm} takes a larger step than θ_{SQZ}, then the MCMC solution is inevitably biased.

Systematic error on arm power.

1. Transmon QPD sum power doesn't vary over 0.3% for X and 0.2% for Y, across and within locks on 05/14
2. The frequency bins are doubled to increase the uncertainty at low frequency. The calibration uncertainty is also taken out of rebinning.
3. We don't know how much arm power really is. PRG could be lower. C. Blair did radiation pressure measurement in O3, which agreed with PRG so PRG is trustworthy. This is not necessarily true in O4 because we haven't done radiation pressure test yet. We can also infer from IFO REFL, but it needs to subtract HOM, sideband, and don't give us any good error like a few %.

We can fix all other parameters except for SQZ angle and arm power. The other 6 parameters are obtained from the MCMC results above. We can combine the statistics of each measurements by putting all their chains together and sample a median from it.

We repeat MCMC with controlled arm power and controlled rest of parameters:

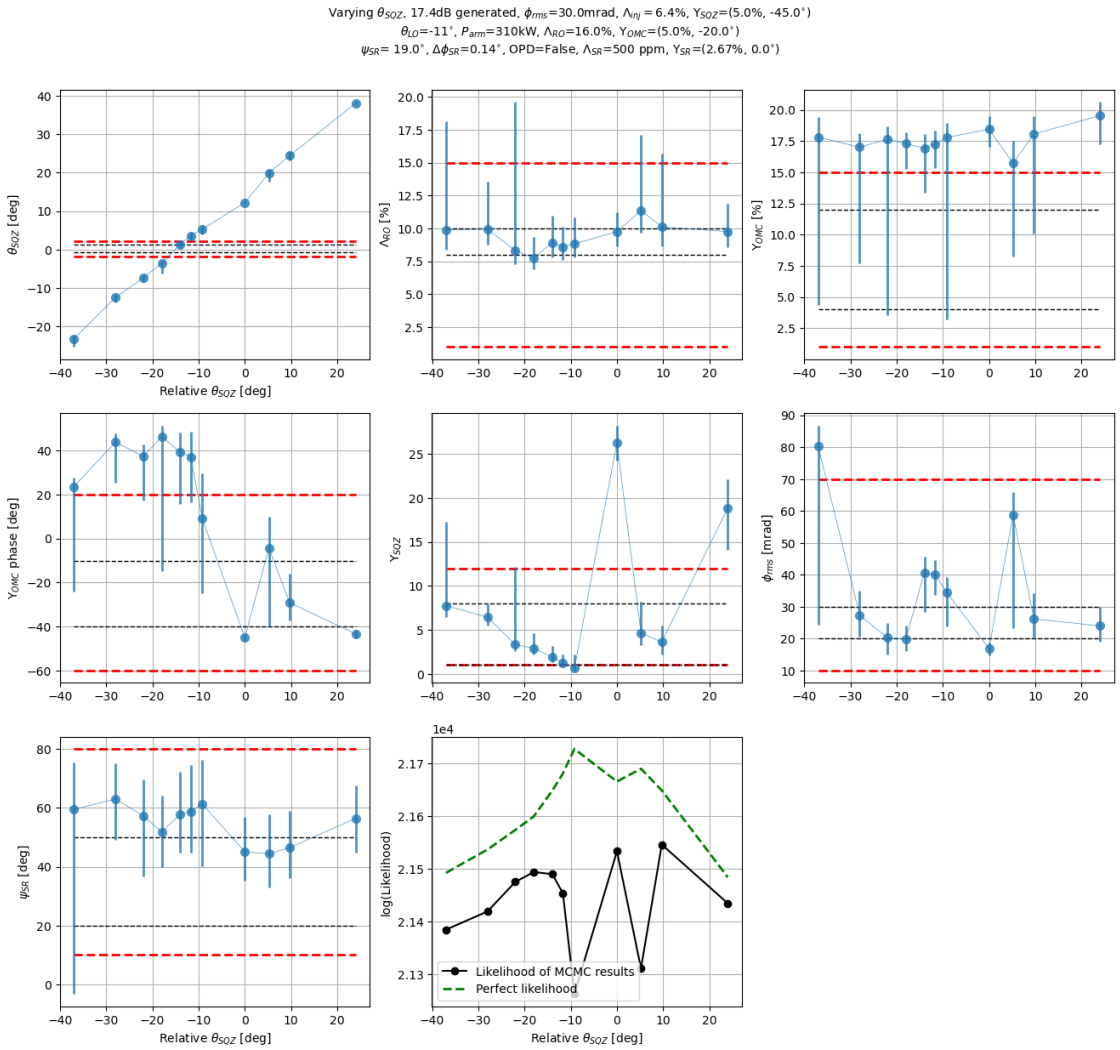

Leave calibration error out of rebinning and using more bins (100) increases the errorbar. In this case, the default parameter is already pretty good, and MCMC doesn't improve everything by too much. The calibration error is largest at high frequency, whereas we need it to be larger at low frequencies.

However, the calibration error is not an incoherent random uncertainty like statistical error, which can be rebinned. We can't rebin calibration error.

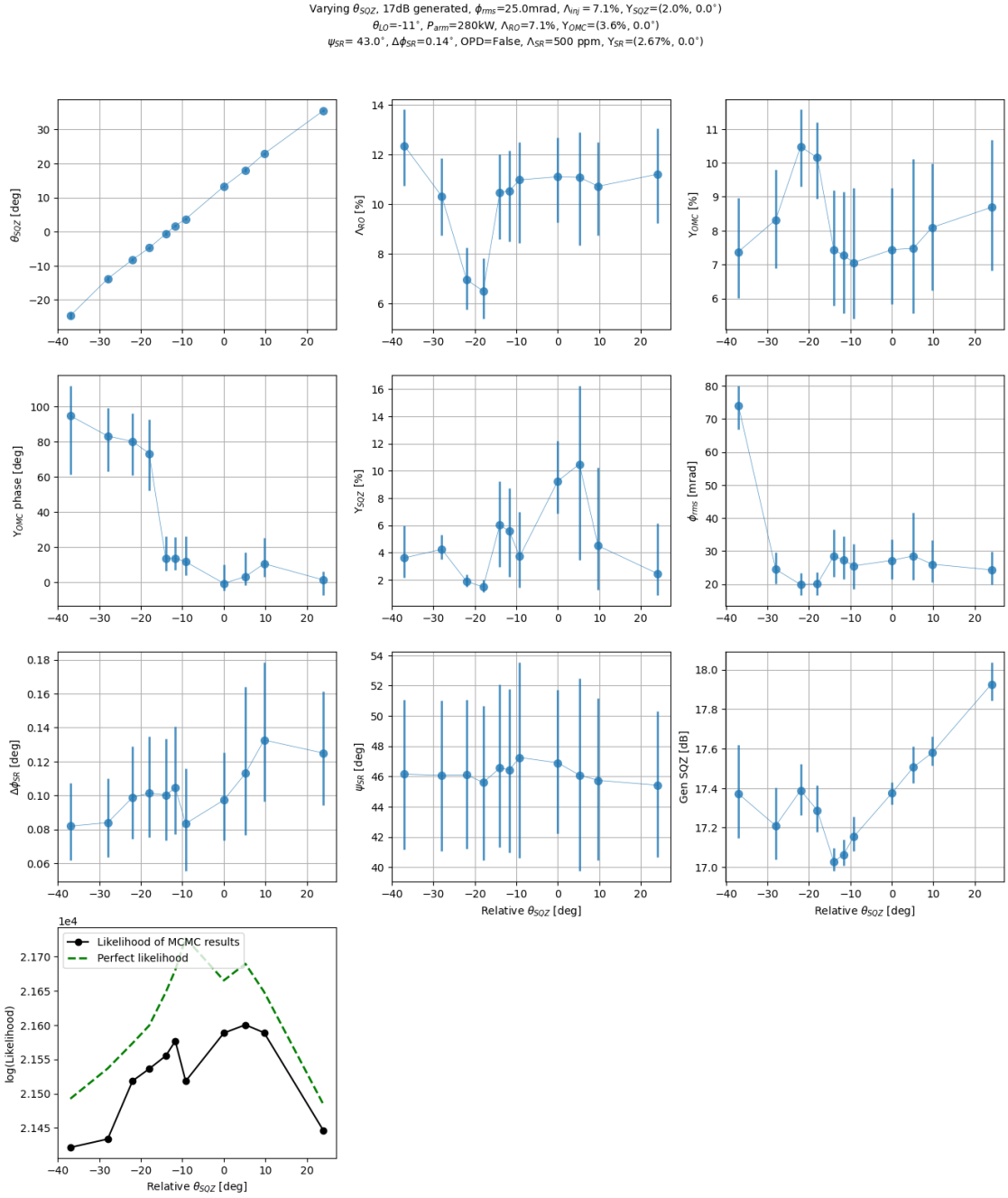
Varying θ_{SQZ}, 17dB generated, ϕ_{rms}=25.0mrad, Λ_{inj} = 7.1%, Y_{SQZ}=(2.0%, 0.0°)
θ_{LO}=-11°, P_{arm}=280kW, Λ_{RO}=7.1%, Y_{OMC}=(3.6%, 0.0°)
ψ_{SR}= 43.0°, $\Delta\phi_{SR}$=0.14°, OPD=False, Λ_{SR}=500 ppm, Y_{SR}=(2.67%, 0.0°)
θ_{SQZ} [deg]
Λ_{RO} [%]
Y_{OMC} [%]
Y_{OMC} phase [deg]
Y_{SQZ} [%]
ϕ_{rms} [mrad]
$\Delta\phi_{SR}$ [deg]
ψ_{SR} [deg]
Gen SQZ [dB]
Relative θ_{SQZ} [deg]
1e4
log(Likelihood)
Likelihood of MCMC results
Perfect likelihood

Appendix F: GPS times

GPS time	Task
LLO64872	
1367375000 - 1367404000	Sweep OM2 TSAMS
1367404000 - 1367413800	Sweep FC detuning, but interrupted by IFO lockloss
1367456000 - 1367470000	Sweep SR3 ring heater
1367474700 - 1367490000	Continue the unfinished FC detuning sweep
1367490200 - 1367526000	Sweep SRCL detuning
1367529000 - 1367533300	No SQZ, FC misaligned, OPO idle
1367534600 - 1367337500	No SQZ, FC aligned, single CLF (no ISS)
1367544500 - 1367550000	No SQZ, single CLF tests on DARM
1367635010	Power outage
1368077800 - 1368104350	Sweeping 10 different SQZ angles + reference
1368128000 - 1368138200	Continue SQZ angle sweeping
1368148280 - 1368164000	Sweeping 4 QND SQZ angles until lockloss
1368219200 - 1368242000	Taking FDS data in one lock
1368249000 - 1368261300	Taking No SQZ reference data
LLO64982	
1368810020 - 1368811350	Unsqz, FC aligned test 1
1368853400 - 1368855320	Unsqz, FC aligned test 2
1368855860 - 1368857150	Unsqz, FC aligned test 3
1368857200 - 1368858200	Unsqz, FC misaligned test 1
1368858260 - 1368859560	Unsqz, FC misaligned test 2
LLO65124	
1368916300 - 1368917700	5.7-5.8 dB FDS
1368921070 - 1368922580	5.7-5.8 dB FIS
1368923420 - 1368924820	FIAS
1368925880 - 1368926980	FDAS, SQZ angle a bit off
1368927030 - 1368927930	FDS angle 1
1368927960 - 1368928860	FDS angle 2
1368928900 - 1368929800	FDS angle 3
1368931950 - 1368932950	Unsqz